Program & Abstracts

9th OCARINA International Symposium

Joint mini-symposiums on Structural Biology and Catalysis

The OCU Advanced Research Institutefor Natural Science and Technology(OCARINA),
and the OCU Professional Development Program

6th - 7th March, 2018 Conference Room (10th Floor), Media Center and Library,
Osaka City University, 3-3-138 Sugimoto, 558-8585 Osaka, Japan
Organized by Osaka City University

9th OCARINA International Symposium

Joint mini-symposiums on Structural Biology and Catalysis

Preface

The OCU Advanced Research Institute for Natural Science and Technology (OCARINA) is organized to find solutions for global-level energy and environmental issues and complex and advanced research subjects, and contribute to the establishment of a sustainable society. Since its foundation in 2010, OCARINA has set up research projects across the graduate schools to promote multidisciplinary researches.

Currently, we have seven big projects from Graduate School of Science, Graduate School of Engineering, Graduate School of Human Life Science and Graduate School of Medicine in Osaka City University (OCU). To promote interdisciplinary discussions among those research projects, we will hold the 9th international symposium on March 6-7, 2018, at OCU Osaka, Japan.

This symposium organizes the annual reports of the research projects and invited lectures. We added two keynote subjects on the structural biology by using cryo-electron microscopy, which honored the 2017 Nobel Prize in chemistry, and catalysis, which is a crucial substrate to govern chemical reaction.

The symposium promotes the poster presentations for younger carrier researchers (age under 35) in order to increase opportunities for lively and informative exchange of views. Thanks for the promotions; we successfully received over 60 submissions. Approximately 20% of posters will be awarded the poster prize. It will be announced at the banquet.

On behalf of organizing committee, it is my great pleasure to welcome you to this symposium and I hope all of you to interact and enjoy with fruitfull discussions.

Chair organizer Michio MIYANO

Adviser to the President of OCU

Director of OCARINA

第９回 OCARINA 国際シンポジウム

ご挨拶

大阪市立大学・複合先端研究機構（OCARINA）は、地球規模でのエネルギー、資源、生態系など、環境を含めた全人類に係る複合的および先端的な研究課題に対して、プロジェクト制により研究科横断型で最先端科学・技術を融合して取り組むことにより、学術的・社会的提言並びに人材育成を行い、得られた成果を社会や地域へ効果的に還元することを目的とします。

現在、機構では理学研究科・工学研究科・生活科学研究科の３研究科を横断する研究組織を構築し、７つのプロジェクト研究を推進しています。これらのプロジェクト研究の相互理解を深める場として、「第９回OCARINA国際シンポジウム」を開催いたします。

今年度は、2017年ノーベル化学賞を受賞した「クライオ電子顕微鏡」と、化学反応をつかさどる極めて重要な物質である「触媒」に関する２つのトピックスについて、研究のトップランナーとしてご活躍の外国人研究者による講演を企画しました。

また、学内理系分野間の相互理解を深めることを目的として、本学「人材育成プロジェクト」と連携したポスターセッションを設けました。おかげさまで、60名を超える申し込みをいただきました。ポスターは英語によるショートプレゼンテーションとポスター発表により審査され、優秀ポスター賞が贈られます。 ポスター賞授与式は懇親会で行います。ご参加された皆様にはぜひ活発な異分野交流と議論を行っていただけますようお願い申し上げます。

2018年３月

複合先端研究機構・機構長

宮野　道雄

Date

6th March (Tue.) , 2018 (Registration:09:00-) 09:30-18:00

7th March (Wed) , 2018 (Registration:09:30-) 10:00-18:00

***Notice: Symposium Photo** at 10F (18:10-18:20)

Venue

Conference Room (10th Floor) , Media Center, OCU

Banquet

7th March (Wed.) , 2018 18:30-

at "Nonohana House" 1st Floor, Media Center, OCU

Organizer

The OCU Advanced Research Institute for Natural Science and Technology (OCARINA)

Organizing committee

- Dr. Michio MIYANO (Adviser to the President of OCU / Director of OCARINA/Professor, Graduate School of Human Life Science, OCU, Japan)
- Dr. Nobuo KAMIYA (Vice Director, OCARINA/Professor, OCARINA, Japan)
- Dr. Naoteru SHIGEKAWA (Vice Director, OCARINA/Professor, Division of Physical Electronics and Informatics (Applied Physics and Electronics), Graduate School of Engineering, OCU, Japan)
- Dr. Yutaka AMAO (Director, ReCAP/Professor, OCARINA, Japan)
- Dr. Tomoko YOSHIDA (Deputy Director, ReCAP/Professor, OCARINA, Japan)
- Dr. Ritsuko FUJII (Associate Professor, OCARINA, Japan)
- Dr. Keisuke KAWAKAMI (Specially Appointed Associate Professor, OCARINA, Japan)
- Dr. Tomoyasu NOJI (Specially Appointed Lecturer, OCARINA, Japan)
- Dr. Shusaku IKEYAMA (Specially Appointed Research Associate, OCARINA, Japan)
- Dr. Yoshihiro YAMAGUCHI (Tenure-track Specially Appointed Associate Professor, OCARINA, Japan)

Invited speakers

- Dr. Pu QIAN (Researcher, The Univ. of Sheffield, United Kingdom)
- Dr. Laurean ILIES (Associate Professor, Graduate School of Science, The Univ. of Tokyo, Japan)
- Dr. Xing Yi LING (Associate Professor, Nanyang Technological Univ., Singapore)
- Dr. Katsura SUGAWARA (Japan Tissue Engineering Co. Ltd.)
- Dr. Mitsuhiro TERAKAWA (Associate Professor, Faculty of Science and Technology, Keio Univ., Japan)
- Dr. Tasuku HAMAGUCHI (Researcher, RIKEN SPring-8, Japan)
- Dr. Sin-ichiro OZAWA (Specially appointed Research Associate, Research Institute for Interdisciplinary Science, Okayama Univ., Japan)
- Dr. Masahiro UEDA (Professor, Graduate School of Frontier Biosciences, Osaka Univ., Japan)

Speakers in OCARINA project team

- Dr. Taro NAKAMURA（Professor, Division of Biology and Geosciences(Functional Biosciences), Graduate School of Science,OCU, Japan）
- Dr. Soichi SAEKI (Associate Professor,Division of Mechanical and Physical Engineering (Mechanical Engineering), Graduate School of Engineering, OCU,Japan)
- Dr. Tatsuya SHOJI (Lecturer, Graduate School of Science, Division of Molecular Materials and Science(Inorganic Chemistry), OCU,Japan)
- Dr. Yasuhiro NAKASO (Special Researcher, OCARINA, OCU,Japan)
- Dr. Masaki NAKAO (Extraordinary Professor, OCARINA, OCU,Japan)
- Dr. Tomoko YOSHIDA (Deputy Director, ReCAP/Professor, OCARINA, Japan)
- Dr. Makoto MIYATA (Professor, Division of Biology and Geosciences(Functional Biosciences), Graduate School of Science, OCU, Japan)
- Dr. Akihisa TERAKITA (Professor, Division of Biology and Geosciences(Science of Biomolecules), Graduate School of Science, OCU, Japan)
- Dr. Tetsuya SATOH (Professor, Division of Molecular Materials and Science(Organic Chemistry), Graduate School of Science OCU, Japan)
- Dr. Naoteru SHIGEKAWA (Deputy Director, OCARINA/Professor, Division of Physical Electronics and Informatics (Applied Physics and Electronics), Graduate School of Engineering, OCU, Japan)

日　時

2018年3月6日（火）（受付9:00）　9:30－18:00

2018年3月7日（水）（受付9:30）　10:00－18:00

＊3月7日終了後、会場にて集合写真を撮りますのでご参集ください。

会　場

大阪市立大学（杉本キャンパス）学術情報総合センター 10階 大会議室 研究者交流室

大阪市住吉区杉本3丁目3番138号 Tel:06-6344-9560

懇親会

2018年3月7日（水）18:30～

学術情報総合センター1階　カフェレストラン「野のはなハウス 」

主　催

大阪市立大学複合先端研究機構

組織委員

●宮野 道雄（大阪市立大学・学長補佐／大阪市立大学・複合先端研究機構・機構長／生活科学研究科・教授）

●神谷 信夫（大阪市立大学・複合先端研究機構・副機構長／複合先端研究機構・教授）

●重川 直輝（大阪市立大学・複合先端研究機構・副機構長／工学研究科電子情報系専攻・教授）

●天尾　豊（大阪市立大学・人工光合成研究センター・所長／複合先端研究機構・教授）

●吉田 朋子（大阪市立大学・人工光合成研究センター・副所長／複合先端研究機構・教授）

●藤井 律子（大阪市立大学・人工光合成研究センター・分析装置運営部会会長／複合先端研究機構・准教授）

●川上 恵典（大阪市立大学・複合先端研究機構・特任准教授）

●野地 智康（大阪市立大学・複合先端研究機構・特任講師）

●池山 秀作（大阪市立大学・複合先端研究機構・特任助教）

●山口 良弘（大阪市立大学・複合先端研究機構・テニュアトラック特任准教授）

招待講演者

●Dr. 銭 朴（シェフィールド大学、イギリス）

●Dr. イリエシュ　ラウレアン（東京大学、日本）

●Dr. Xing Yi Ling （南洋理工大学、シンガポール）

●Dr. 菅原　桂（株式会社 ジャパンティッシュ・エンジニアリング・再生医療事業（軟骨領域）首席、自家培養軟骨ジャック プロダクトマネージャー）

●Dr. 寺川　光洋（慶應大学・理工学部）

●Dr. 浜口　祐（理化学研究所・研究員）

●Dr. 小澤　真一郎（岡山大学異分野基礎科学研究所・特任助教）

●Dr. 上田　昌宏（大阪大学 生命機能研究科・教授）

プロジェクトチーム講演者

●中村 太郎（大阪市立大学・理学研究科生物地球系専攻・教授）

●佐伯 壮一（大阪市立大学・工学研究科機械物理系専攻・准教授）

●東海林 竜也（大阪市立大学・理学研究科物質分子系専攻・講師）

●中曽 康壽（大阪市立大学・複合先端研究機構・特別研究員）

●中尾 正喜（大阪市立大学・複合先端研究機構・特命教授）

●吉田 朋子（大阪市立大学・複合先端研究機構・教授）

●宮田 真人（大阪市立大学・理学研究科生物地球系専攻・教授）

●寺北 明久（大阪市立大学・理学研究科生物地球系専攻・教授）

●佐藤 哲也（大阪市立大学・理学研究科物質分子系専攻・教授）

●重川 直輝 （大阪市立大学・複合先端研究機構・副機構長／ 工学研究科電子情報系専攻・教授）

The 9th OCARINA International Symposium

Joint mini-symposiums on Structural Biology and Catalysis

At 10th Floor, Media Center, Osaka City University, Osaka, Japan

March 6 (Tue)

09:00-09:30	Registration
09:30-09:40	**Opening**　荒川 哲男（大阪市立大学・学長兼理事長） Tetsuo ARAKAWA (President of OCU)
	Session 1: バイオリソース(Bio-Resource)
09:40-10:00 O1	中村　太郎　(理学研究科生物地球系専攻・教授)[日本語講演] ナショナルバイオリソースプロジェクト酵母 Taro NAKAMURA (Grad. School of Science, OCU)[Japanese lecture] National BioResource Project yeast
10:00-10:10	Break
	Session 2: バイオメディカル先端医療工学(Frontier Bio-Medical Engineering)
10:10-10:30 O2	佐伯 壮一（工学研究科機械物理系専攻・准教授）[日本語講演] 多機能 OCT を用いたマイクロ断層診断法～コスメおよび医療への応用～ Souichi SAEKI (Grad. School of Engineering, OCU) [Japanese lecture] Micro-tomographic Diagnosis of Cosmetic and Medical Application using Multi-functional OCT
10:30-11:20 I1	招待講演 1（座長：佐伯 壮一 准教授）[日本語講演] 菅原 桂（株式会社 ジャパンティッシュ・エンジニアリング・再生医療事業（軟骨領域）首席、自家培養軟骨ジャック プロダクトマネージャー） 自家培養軟骨ジャックの開発と製品化 ***Invited Lecture 1*** (Chair: Souichi SAEKI) [Japanese lecture] Katsura SUGAWARA (Japan Tissue Engineering Co. Ltd.) Research, Development and Commercialization of an Autologous Cultured Cartilage, JACC
11:20-11:30	Break
	Session 3: ナノマテリアル光制御(Optical Control of Nano-Material)
11:30-12:20 I2	招待講演 2（座長：坪井 泰之 教授） 寺川　光洋（慶応義塾大学理工学部・准教授）[日本語講演] フェムト秒レーザによる金属とソフトマテリアルの複合微細構造の作製 ***Invited Lecture 2*** (Chair: Yasuyuki TSUBOI) Mitsuhiro TERAKAWA (Keio Univ.) [Japanese lecture] Fabrication of microstructures composed of metal and soft material by using femtosecond laser
12:20-12:40 O3	東海林 竜也（理学研究科物質分子系専攻・講師）[日本語講演] シリコンナノ構造を用いた NASSCA 光ピンセット法の開発 Tatsuya SHOJI (Grad. School of Science, OCU) [Japanese lecture] Nano-structured semi-conductor-assisted (NASSCA) optical tweezers with black silicon
12:40-13:40	Lunch Break
	Session 4: 都市エネルギー・防災(Urban energy)
13:40-14:10 O4	中曽 康壽（複合先端研究機構・特別研究員）[日本語講演] 高性能井戸を用いた帯水層蓄熱システムの開発と今後の普及展開 Yasuhiro NAKASO (OCARINA, OCU) [Japanese lecture] Development of aquifer thermal energy storage system with high performance thermal well and future spread measures
14:10-14:40 O5	中尾 正喜（複合先端研究機構・特命教授）[日本語講演] 帯水層蓄熱空調システムの省エネルギー性能 Masaki NAKAO (OCARINA, OCU) [Japanese lecture] Energy saving performance of developed aquifer thermal energy storage system
14:40-14:50	Break
	Poster Session [Presentations in English]
14:50-16:20	Short Presentations [English presentations] ポスター発表者によるショートプレゼンテーション[英語講演]
16:20-16:30	Break

16:30-17:10	Poster Viewing 1 (odd number) 奇数番号のポスター発表
17:10-17:20	Break
17:20-18:00	Poster Viewing 2 (even number) 偶数番号のポスター発表

March 7 (Wed)

09:30-10:00	Registration
	Mini Symposium on Structural Biology (Photosynthesis and Artificial Photosynthesis) （構造生物学ミニシンポジウム〜光合成・人工光合成）
10:00-10:40 I3	***Invited Lecture 3*** (Chair: Keisuke KAWAKAMI) Tasuku HAMAGUCHI (RIKEN SPring-8) [Japanese lecture] Visualization and structures of membrane proteins by cryo-electron microscopy 招待講演 3（座長：川上 恵典 特任准教授） 浜口 祐（理化学研究所 SPring-8・研究員）[日本語講演] クライオ電子顕微鏡法による膜タンパク質の構造
10:40-11:30 S1	***Special Lecture 1*** (Chair: Ritsuko FUJII) Pu QIAN (The Univ. of Sheffield) [English lecture] Cryo-EM structure of the *Blastochloris viridis* RC-LH1 complex at 2.87 Å 特別講演 1（座長：藤井 律子 准教授） 銭 朴（チェン プー）シェフィールド大学・研究員）[英語講演] クライオ電子顕微鏡法により分解能 2.87 Å で得られた紅色光合成細菌の RC-LH1 複合体の構造
11:30-11:40	Break
11:40-12:20 I4	***Invited Lecture 4*** (Chair: Keisuke KAWAKAMI) Sin-ichiro OZAWA (Okayama University) [English lecture] Configuration of antenna subunits in photosystem I complex 招待講演 4（座長：川上 恵典 特任准教授） 小澤 真一郎（岡山大学異分野基礎科学研究所・特任助教）[英語講演] 光化学系Ⅰ複合体におけるアンテナサブユニットの配置
12:20-12:40 O6	Tomoko YOSHIDA (OCARINA,OCU) [English lecture] XAFS/EELS analyses of nitrogen doped titanium oxide photocatalysts 吉田 朋子（複合先端研究機構・教授）[英語講演] 窒素添加チタニア光触媒の XAFS/EELS 解析
12:40-13:40	Lunch Break
	Session 5: Frontier Biology （先端バイオ）
13:40-13:50 O7	Makoto MIYATA (Grad. School of Science, OCU) [English lecture] Recommendation for quick freeze replica electron microscopy 宮田 真人（理学研究科生物地球系専攻・教授）[英語講演] 急速凍結レプリカ電子顕微鏡法の薦め
13:50-14:00 O8	Akihisa TERAKITA & Mitsumasa KOYANAGI (Grad. School of Science, OCU) [English lecture] Molecular physiology of diverse light-senor proteins and their optogenetic applications 寺北 明久（理学研究科生物地球系専攻・教授）、小柳 光正（同・准教授）[英語講演] 多様な光受容タンパク質の分子生理学とそれらの光遺伝学的利用
14:00-14:40 I5	***Invited Lecture 5*** (Chair: Akihisa TERAKITA) Masahiro UEDA (Grad. School of Frontier Bioscience, Osaka University) [English lecture] Automated single-molecule imaging analysis of cell signaling 招待講演 5（座長：寺北 明久 教授） 上田 昌宏（大阪大学生命機能研究科・教授）[英語講演] 細胞内シグナル伝達の自動１分子イメージング解析
14:40-14:50	Break
	Session 6: Frontier Materials （先端マテリアル）
14:50-15:20 O9	Tetsuya SATOH (Grad. School of Science, OCU) [English lecture] Synthesis of π-conjugated molecules via transition-metal-catalyzed C–H functionalization 佐藤 哲也（理学研究科物質分子系専攻・教授）[英語講演] 遷移金属触媒を用いる C–H 誘導体化を経るパイ共役分子合成

15:20-15:50 O10	Naoteru SHIGEKAWA (Grad. School of Engineering, OCU) [English lecture] Low-temperature direct bonding of dissimilar materials for advanced electronics 重川　直輝（工学研究科電子情報系専攻・教授）[英語講演] 次世代エレクトロニクスを拓く低温直接接合
15:50-16:00	Break
	Mini Symposium on Catalysis（触媒ミニシンポジウム[*注]）
16:00-16:50 S2	***Special Lecture 2*** (Chair: Tetsuya SATOH) Laurean ILIES (The Univ. of Tokyo) [English lecture] C-H Activation catalyzed by earth abundant metals 特別講演 2（座長：佐藤 哲也 教授） イリエシュ ラウレアン（東京大学理学研究科・准教授) [英語講演] 地球上に豊富に存在する鉄を触媒として用いる C-H 活性化
16:50-17:00	Break
17:00-17:50 S3	***Special Lecture 3*** (Chair: Yusuke YAMADA) Xing Yi LING (Nanyang Technological University, Singapore) [English lecture] Exploiting the nanoscale interface at metal nanoparticle and metal-organic framework for catalysis and sensing applications 特別講演 3（座長：山田 裕介 教授） Xing Yi LING（南洋理工大学・准教授）[英語講演] 金属ナノ粒子と金属有機構造体におけるナノスケールインターフェースの触媒およびセンシングへの応用
17:50-18:00	Break
18:00-18:10	**Closing**　Nobuo KAMIYA (OCARINA, OCU, Vice Director of OCARINA) 神谷 信夫（大阪市立大学複合先端研究機構・副機構長）
18:10-18:20	Symposium Photo at 10F (記念撮影)
18:30-20:30	Banquet & Celebration for Poster Prize (1F Nonohana House) 懇親会&ポスター賞授与式 (1F 野のはなハウス)

[*注] 後援：平成 29 年度大阪市立大学教育推進本部経費事業「研究科横断型大学院教育改革の推進と化学人材育成」

喫煙エリア

Guidelines for Poster Presentations

(1) Preparation for the poster

- The poster board provided is approximately 160 cm height x 110 cm width.
- Please limit the size of your entire poster or poster sections in it. (Recommended poster size is A0.)
- Please place your poster on the poster board numbered for you.
- Push pin will be available at the site.
- Poster viewing will be start from odd number, and then even number (40 min each). During your time, please stay around the poster.
- Display your poster during OCARINA symposium (6 March, 9:00 - 7 March, 18:00).

(2) Preparation for the short oral presentation

- All the poster presenters can present own short oral presentation.
- One separate file (pdf or power point format) is available to show during your presentation.
- No animation. Submit the file to the conference secretary.
- Gather and make a queue in front of the stage before starting of the short oral presentation. Allocated time is 1 minute including set up time. Please stand up nearby the microphone and be ready before finishing of the previous talk.

ポスター発表について

（1）添付ポスターについて（英語）

- ポスターサイズ　A0（ボードサイズは W110 x H160 cm 程度)
- 添　　付：自分のポスター番号（要旨集／ HP）の場所に添付してください。
- 会　　場：学術情報センター 10F　研究者交流室内
- 添付期間：3 月 6 日（火）9 時 ～ 3 月 7 日（水）18 時頃まで
- ポスター賞の審査を希望する方は、必ず最後まで貼付してください。
- ポスターの撤去は、ご自身でお願いします。放置されたポスターについてはこちらで処分いたします。
- ポスター発表：前半／奇数番号　後半／偶数番号
  ➢ 自分の発表の時間帯は、自身のポスターのそばにいてください。

（2）ポスターショートプレゼンテーションについて（英語、持ち時間 1 分（厳守））

上述赤字の注意事項を熟読のこと。

- ポスター賞審査方法　　招待講演者及び学内複合先端研究機構プロジェクトメンバー有志の審査員による審査。異分野の研究者に自身の研究を的確に伝えているかどうか。
  （研究の背景・目的・意義・狙いを理解してもらい、討論をする。）
- ポスター賞授与式3 月 7 日（水）18 時 30 分開始の懇親会場にて行います。皆様どうぞご参加ください。

Oral Presentations

March 6th (Tue), 2018

National BioResource Project yeast

Taro Nakamura

Graduate School of Science, Advanced Research Institute for Natural Science and Technology, Osaka City University, Sugimoto 3-3-138, Sumiyoshi-ku, Osaka

The National BioResource Project (NBRP) starts in FY 2002 to comprehensively promote life sciences. In the project, the systems of collection, preservation, and deposition have been established for bioresources, such as experimental animals, plants, and microbes (systems, groups, tissues, cells, and genetic materials of animals, plants, and microbes and their information as research and development materials) that are important for the nation to organize strategically.

Yeast is an important eukaryotic model organism. This is especially true of the fission yeast *Schizosaccharomyces pombe* and the budding yeast *Saccharomyces cerevisiae*, which are making significant contributions to research in a variety of areas within the life sciences. NBRP-Yeast has established a framework to collect, stock and distribute strain and DNA resources of mainly the two species. Through phases 1 and 3 (FY 2002 - 2016) of the NBRP, the NBRP-yeast has become one of the top international yeast resource centers. Here, I will introduce the activity of NBRP-yeast.

Micro-tomographic Diagnosis of Skin and Regenerative Tissue using Multi-functional OCT

Souichi SAEKI[1]

[1] *Graduate School of Engineering, Mechanical & Physical Engineering, Osaka City University. 3-3-138, Sugimoto, Sumiyoshi-ku, Osaka, 558-8585*

Abstract:

Water has significant influence on human body due to physiological carrier media. In addition, rheological behavior of interstitial fluid in epidermal and dermal tissue, including blood micro-circulation, can vary skin mechanics in micro scale, i.e. vis. Therefore, an in vivo measurement of moisture content and capillary blood flow velocity is necessary to clarify skin mechanics. This paper presents 2C-OCM (2-Color Optical Coherence Moisturegraphy), which was composed of two-band light sources having different optical absorption properties of water respectively. These are capable of tomographically *in vivo* diagnosing the moisture content. Furthermore, OCDV (Optical Coherence Doppler Velocigraphy) algorithm can visualize the tomographic flow velocity of red blood cell in capillaries of human epidermal skin. In this experiment, 2C-OCM & OCDV were *in vivo* applied to human skin and regenerative tissue. Consequently, it was concluded that 2C-OCM & OCDV can provide micro tomography of moisture content and capillary blood velocity inside skin tissue, which can be attributed to biomechanical properties.

References:

[1] Daisuke Furukawa, et al., “Accuracy Evaluation on Tomographic Micro-visualization of Flow Velocity using High Frequency Modulated Low Coherence Interferometer, J. JSEM, Vol.17, Issue 1, (2017), pp.52-56.

[2] Yusuke Hara, Toyonobu Yamashita, Kumiko Kikuchi, Yoshihide Kubo, Chika Katagiri, Kentaro Kajiya, Souichi Saeki, “Visualization of age-related vascular alterations in facial skin using optical coherence tomography-based angiography”, Journal of Dermatological Science, 2018, Jan. 8, S0923-1811(18).

[3] Yusuke Hara, Yuki Ogura, Toyonobu Yamashita, Daisuke Furukawa, Souichi Saeki, “Visualization of visco-elastic behavior in skin equivalent using optical coherence tomography straingraphy”, Skin Research and Technology, 2018, Jan, 24, 10.1111/srt.12435.

Research, Development and Commercialization of an Autologous Cultured Cartilage, JACC

Katsura SUGAWARA
Japan Tissue Engineering Co., Ltd., Gamagori, Aichi, Japan

Abstract: Recently, regenerative medicine has made remarkable progress and attracted attention worldwide. Articulat cartilage is a thin layer that covers the bones in knee joints and allowing them to move smoothly. However, since articular cartilage lacks blood vessels and nerves, once cartilage is damaged by trauma or overuse, it is not able to heal spontaneously. Brittberg and Peterson *et al.* performed autologous chondrocyte implantation (ACI) in patients with full- thickness cartilage defects in the knee [1]. In this procedure, cartilage pieces are taken from the unloaded resion of the knee and isolated chondrocytes are cultivated for two to three weeks. After the cultivation, chondrocytes are harvested and implanted into the cartilage defect of the patient in a cell suspension manner with a periosteum patch. This regenerative medicine for the cartilage repair was an epoc-making invention, however, some disadvantages were pointed out; 1) during the cultivation, chondrocytes lose their ECM producing activity 2) possible leakage of chondrocyte after implantation due to its formulation 3) an uneven distribution of chondrocytes because of gravity. To address these issues, Prof. Ochi at Hiroshima University developed three-dimensional cultivation of chondrocytes [2]. In the procedure, chondrocytes are embedded in atelocollagen gel and cultivated for three to four weeks. On the basis of basic and animal studies, clinical studies were conducted since 1996 at Shimane Medical University and Hiroshima University. This technology was transferrd to Japan Tissue Engineering Co., Ltd. (J-TEC) and a multi-center clinical trial was conducted in 2004 [3]. J-TEC obtained the approval for the three-dimensional cultured cartilage, named JACC, in 2012 as the first orthopaedic regenerative medicinal product in Japan and JACC was listed as an item covered by the National Health Insurance from 2013.
In this presentation, translational research, development and commercialization of JACC will be reviewed and discussed.

References:

[1] Brittberg, M.; Lindahl, A.; Peterson, L. *et al.*, *New Engl J Med* **1994**, 331, 889.
[2] Ochi, M.; Uchio, Y.; Kawasaki, K. *et al.*, *J Bone Joint Surg* **2002**, 84, 571.
[3] Tohyama, H.; Yasuda, K.; Ochi, M. *et al.*, *J Orthop Sci* **2009**, 14, 579.

Fabrication of Microstructures Composed of Metal and Soft Material by using Femtosecond Laser

Mitsuhiro Terakawa

Department of Electronics and Electrical Engineering, Keio University

3-14-1 Hiyoshi, Kohoku-ku, Yokohama 223-8522 Japan

Soft materials, including elastic polymers and hydrogels, are promising materials for implantable devices, wearable devices, and tissue engineering owing to their biocompatibility, flexibility, etc. The scope of use of such soft materials is expanding further in recent years because of their integration with metal micro- or nanostructures, which has increased the interest of researchers in the realization of novel flexible electrical, optical, and micro-mechanical devices. In this presentation, our study on the laser direct writing of metal microstructures inside a hydrogel will be described, followed by the fabrication of metal/polymer composite structures by using a femtosecond laser.

Hydrogel-based materials are emerging as promising biomaterials because of their attractive properties, such as permeability to tissue fluids, flexibility, high water retention, and biocompatibility. We have demonstrated the laser direct writing of silver microstructure inside a PEG-based hydrogel [1]. The optical diffraction pattern obtained with the silver grating inside a hydrogel showed spaced diffraction spots, which indicated that a regular periodic grating was formed [2]. Notably, the distance between the diffraction spots changed when the water content in the hydrogel was reduced. The grating period decreased when the hydrogel shrank owing to the loss of water, but the straight shapes of the line structures were preserved, which demonstrated the fabrication of the structure exhibiting tunable optical patten.

As for the electrical application, we have demonstrated the fabrication of silver/polydimethylsiloxane (PDMS) composite microstructures based on simultaneous induction of photoreduction of silver ions and photopolymerization by using femtosecond laser [3]. The metal component of the microstructures provides electrically conductive while the elastic PDMS contributes flexibility. Reproducable sensing of external mechanical forces was also demonstrated on the basis of the resistance increase of the line structure.

References:

[1] Terakawa, M.; Torres-Mapa, M. L.; Takami, A.; Heinemann, D; Nedyalkov, N. N.; Nakajima, Y.; Hördt, A.; Ripken, T.; Heisterkamp, A. *Optics Letters* **2016**, 41, 1392.

[2] Machida, M.; Nakajima, Y.; Torres-Mapa, M. L.; Heinemann, D.; Heisterkamp, A.; Terakawa, M.; *Scientific Reports* **2018**, 8, 187.

[3] Nakajima, Y.; Obata, K.; Machida, M.; Hohnholz, A.; Koch, J.; Suttmann, O.; Terakawa, M. *Optical Materials Express* **2017**, 7, 4203.

Nano-structured semi-conductor-assisted (NASSCA) optical tweezers with black silicon

Tatsuya Shoji

Graduate School of Science, Osaka City University

Abstract: We demonstrated a novel optical manipulation technique for nanoparticles with non-plasmonic semiconductor nanostructures; named nano-structured semi-conductor-assisted (NASSCA) optical tweezers[1]. A tightly focused laser beam exerts optical force on polarized microparitcles such as living cells, bacteria, and liquid droplets, leading to optical trapping and manipulation of them (optical tweezers). However, optical manipulation of smaller sized nanoparticles and molecules is a still challenging issue because of their quite small polarizability.

Instead of conventional optical trapping methods, we present an alternative and novel trapping method – NASCA optical tweezers – using metal-free black silicon (B-Si) whose surface has nano-needle structures. NASSCA optical tweezers have several advantages: (1) simple fabrication with high uniformity over wafer-sized areas (cm×cm), (2) free from thermal effects detrimental for trapping, (3) switchable trapping between one and two-dimensions, (4) tight trapping because of no detrimental thermal forces, and so on. We believe that NASSCA optical tweezers will become an indispensable tool for manipulating nanoparticles and molecules in the same way that conventional optical tweezers have been proven to be a valuable micromanipulation tool.

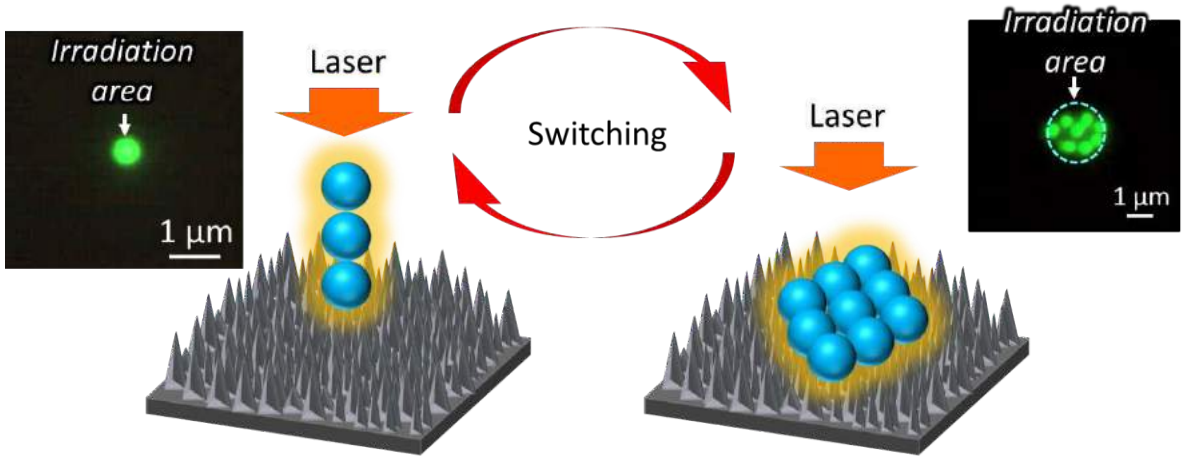

References:

[1] Shoji, T.; Mototsuji, A.; Balčytis, A.; Linklater, D.; Juodkazis, S.; Tsuboi, Y. Sci. Rep. **2017**, 7, 12298.

Development of Aquifer Thermal Energy Storage System with High Performance Thermal Well and future spread measures

Yasuhisa Nakaso

Reaserch Fellow, 3-9-11,Sugimoto,Sumiyoshi-ku,Osaka City, Japan

Abstract:

Large urban areas in high energy consuming density are required to applicable practical scale renewable energy technologies without damaging urban environment like global warming and heat island problem. In some Japanese urban area, renewable thermal energy utilization of sewage and river water has been realized as district heat and cool supply plant.

Now, we can realize direct groundwater heat source utilization under iron and salt ion rich location in the coastal urban area, that leads hard well clogging easily and so on which was difficult to use, and this technical development project is assisted by Japanese Ministry of the Environment.

We set up the well in the Umekita redevelopment area in the northern part of JR Osaka Station, and we tried pumping up a groundwater 100m^3 per hour from a well, getting a heat power and immediately rechrging the groundwater from another well to original same aquifer.

This is better way that reduce the influence of land subsidence problem in the urban area with keeping groundwater level in local area, and we confirmed it could be operated stably for a long period by using airtight structure.

In this paper, we introduce the background and the outline of this technology development including the preceding trial in Takasago area.

O-4

Osaka Umekita site

試験実施個所の概観

#1well (cold well)

#1well connection

Propaganda in Umekita site.

・Radiation panel through a ground water, fell cool in summer.

After pumping up, groundwater turns white. (including methane)

←After 1H it turns brown.

←It is no problem for drinking, but bad taste.

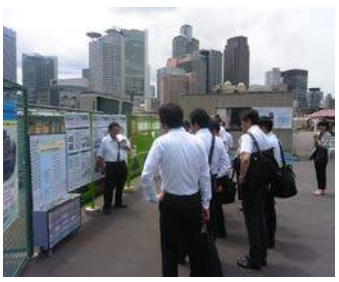

Site tour

Boring sample before 20,000 years

Measurement bar through the first aquifer

Criteria of drawdown vs. abstraction and injection volume

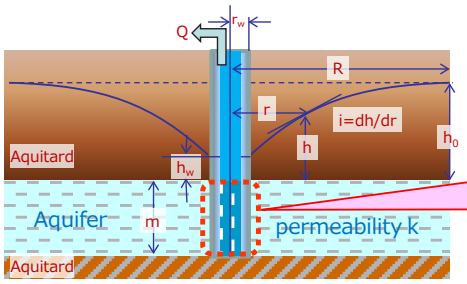

Abstraction volume Q, Permeability k, Drawdown h_w

$$h_0 - h_w = \frac{Q}{2\pi mk} ln \frac{R}{r_w}$$

→They have proportional relation

Clogging occurred near bore wall which have high water velocity

Same water vlume brings large drawdown

Takasago site operation report

Flow rate

Draw down

Draw down vs. flow rate

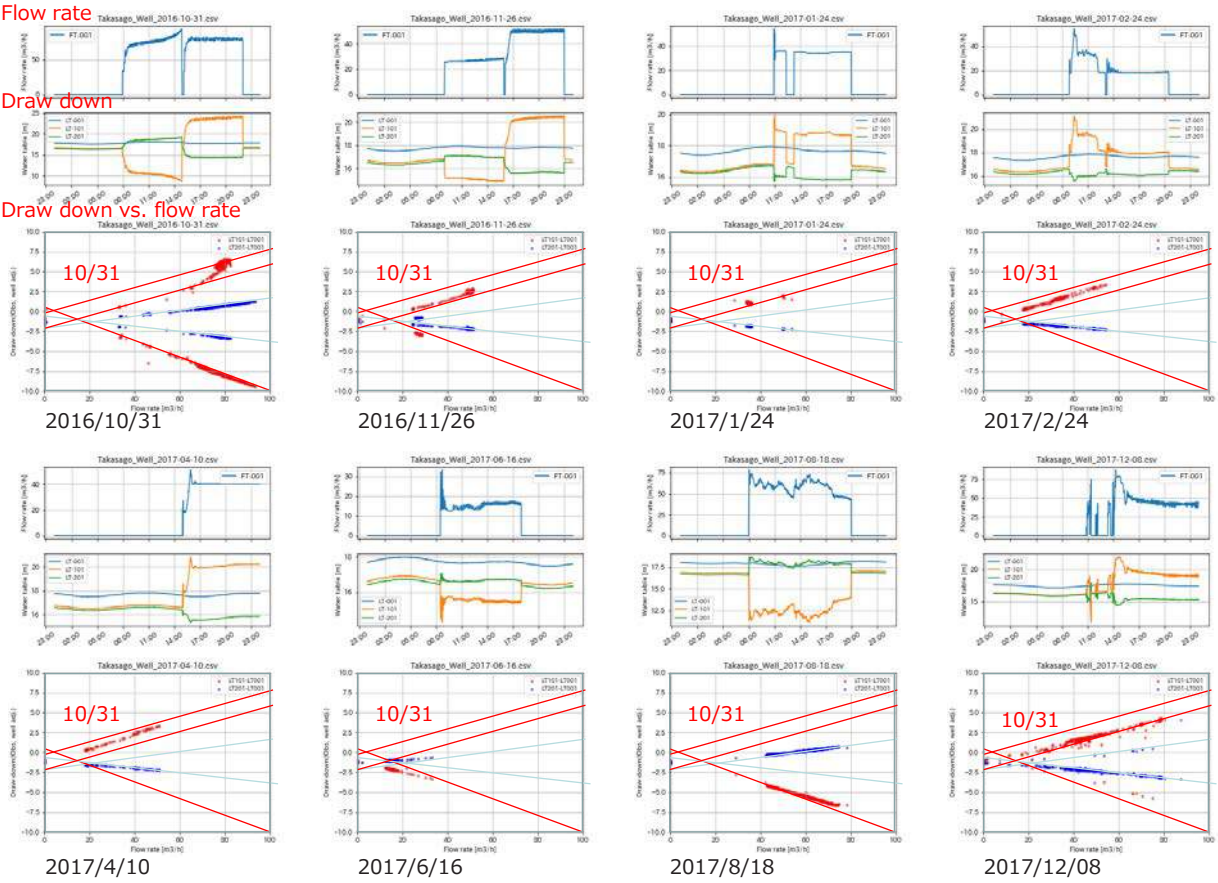

エネルギー消費密度の高い都市域において、地球温暖化防止やヒートアイランド問題など都市環境を損なうことなく、適用可能な実用規模の再生可能エネルギー技術の普及開発が求められている。わが国においても、地域熱供給事業として下水や河川水の熱利用が実用化されている。

この度、環境省の技術開発実証事業として始めた地下水の熱源利用研究において、臨海都市部で鉄分や塩分濃度が高く、これまで目詰まりを起こすなどして利用の難しかった熱源井の開発に成功した。

この井戸は JR 大阪駅北のうめきた地区の再開発エリアの一角に地下水を汲み上げるための井戸を設置し、実用規模レベルである毎時 100m3 で揚水を行い、熱利用後、直ちに元の帯水層に還元することで、地域の地下水レベルの低下を防止、都市域で問題となっている地盤沈下の影響を軽減すると共に、気密構造の徹底により、長期間、安定運用できることも確認した。本稿では、先行する高砂地区での事例も含め、この技術開発の背景と取り組み概要について紹介する。

Energy Saving Performance of Developed Aquifer Thermal Energy Storage System

Masaki Nakao

Professor, 3-9-11,Sugimoto,Sumiyoshi-ku,Osaka City, Japan

Abstract:

Aquifer Thermal Energy Storage System(ATES) is storage and recovery of thermal energy system which is achieved by extraction and injection of groundwater from aquifers using two groundwater wells.

ATES is a technology developed in the Netherlands, and it has already been installed in more than 1,000 facilities in the country.

In order to apply it to our country it is necessary to operate and control the thermal storage facility in consideration of the Japanese climate conditions, the cooling and heating load characteristics of the building, and the regional level of the aquifer temperature.

In this report, we show the test result and energy saving effect by introducing the ATES to the heating and cooling of the factory located in the coastal area. In addition, the verification results of the simulation model linking the aquifer and heating and cooling equipment is described. Furthermore, we show the effect of energy conservation when applying ATES to an office building in Osaka City using simulation model. In particular, it shows that it is effective to cool the aquifer of the low temperature well at low outside temperature in the winter season.

In order not to affect adjacent ATES, it is necessary to handle the heat transfer performance as a closed system. Further, it is necessary for the aquifer storage to perform stably for a long term. So, the following operation of ATES is discussed for long-term operation.

1) Prevent long-term aquifer temperature rise or decline.

2) The heat mass size of each well stabilizes

As a countermeasure, the spacial average temperature of the aquifer does not change over time. Moreover, the annual cumulative extraction of each well is equal to injection of groundwater amount.

In order to satisfy these two conditions, we devise an operation method of the ATES that changes the operation parameters of the following year from the results of the previous year.

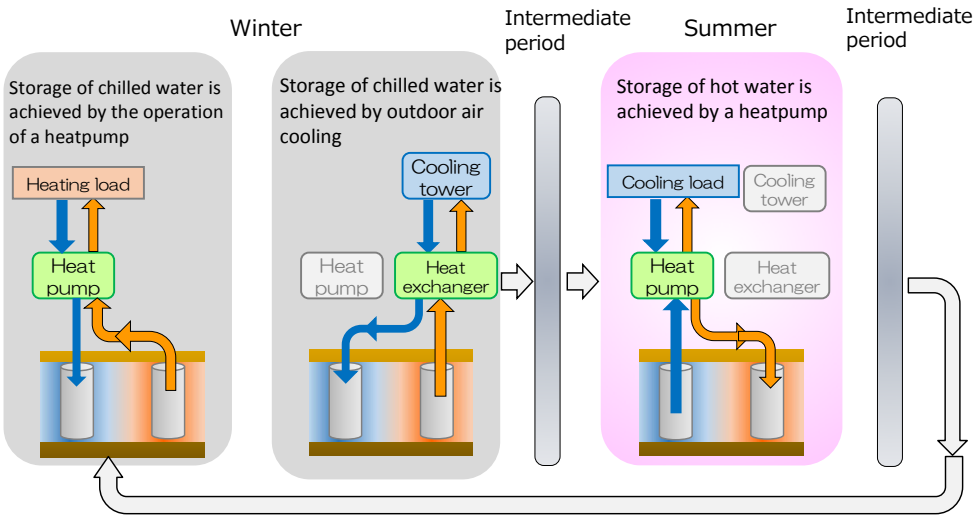

Annual cycle of ATES operation

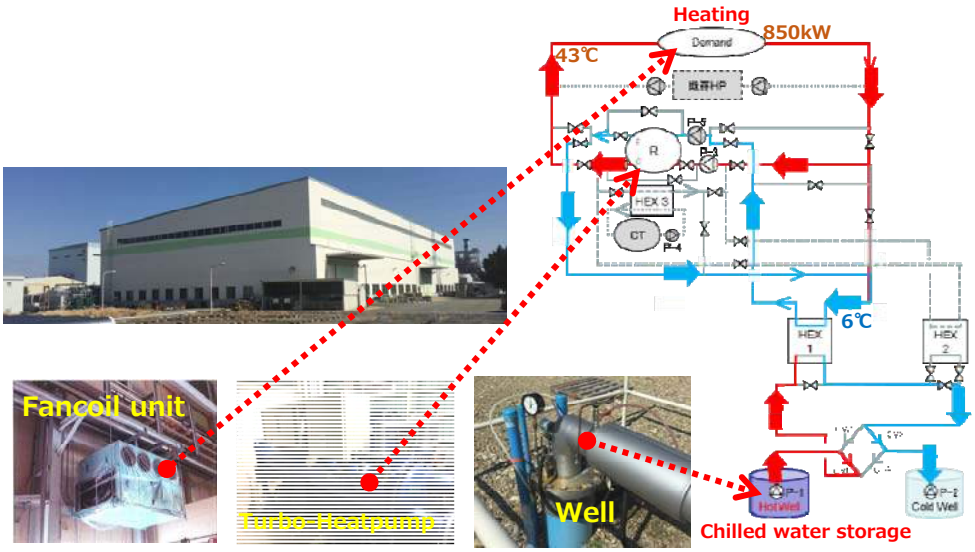

Actual plant of heating and cooling system for the Factory in Takasago City

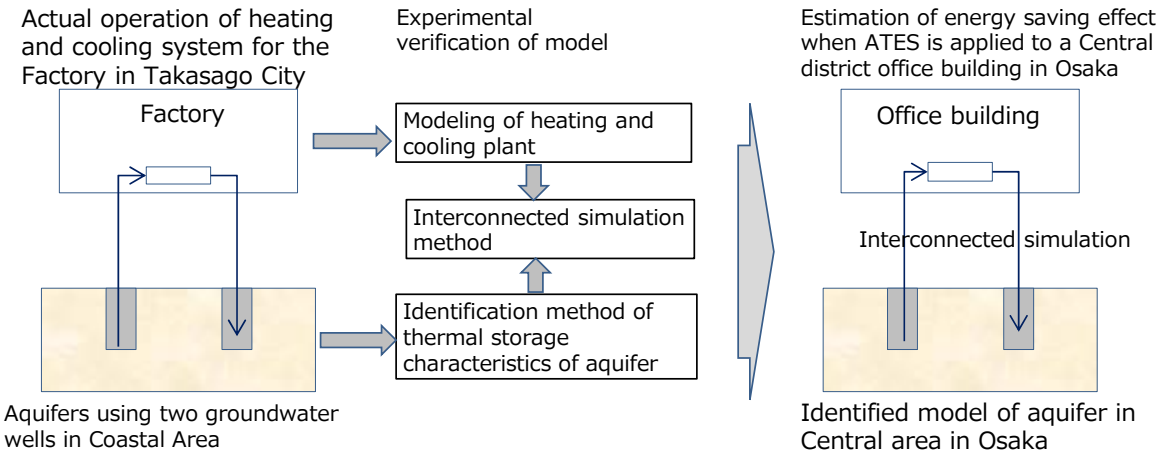

Modeling, experimental verification and estimation of energy saving effect of ATES

O-5

Oral Presentations

March 7th (Wed), 2018

Visualization and structures of membrane proteins by cryo-electron microscopy

Tasuku Hamaguchi, Saori Maki-Yonekura, Koji Yonekura
RIKEN SPring-8 center

Structures of life's molecular machinery are indispensable to understand biological phenomena in details. The current technology, however, still suffer from limitations such as crystallization, stability, heterogeneity and so on. Cryo-electron microscopy (cryo-EM) allows to obtain the 3D structures of biological macro molecules under a natural condition or a condition close to it without crystallization, heavy-atom staining and chemical fixing. Cryo-EM has determined the structures of membrane proteins and protein complexes, e.g. GPCRs, ion channels, transporters, and rotary-ATPases, and the number of high-resolution structures has been increasing explosively, since the direct electron-detection camera was introduced in the field and the structure of TRPV1 was reported at a near-atomic resolution using this new technology [1]. Furthermore, cryo-EM can visualize super-molecular machineries, which are hard or impossible to be crystalized. Those targets include bacterial flagella, injectosome, and cell organelles.

Exosome, an extracellular vesicle excreted from eukaryotic cells, plays an important role in intercellular communications. Reflecting dispositions of the derived cells, the exosome contains many soluble proteins, micro-RNAs and membrane proteins. The exosome-specific membrane proteins include excitatory amino-acid transporters and lysosome-associated membrane glycoproteins. The former regulates an excitation of the postsynaptic action, and this transporter expressed in a central nervous system is responsible for various stresses. We aim at visualization of these targets by cryo-EM. In addition, a membrane protein machinery involved in bacterial motility is also analyzed by cryo-EM and will be presented in this workshop.

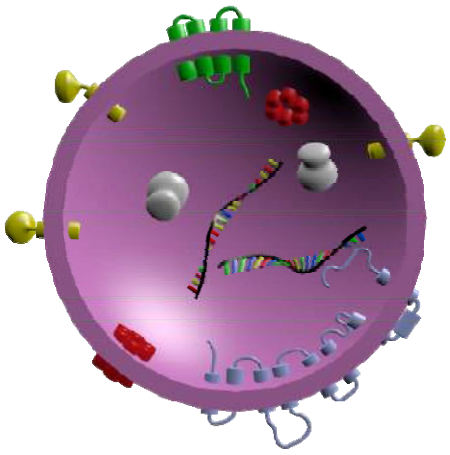

Cartoon of exosome

[1] Liao, M., Cao, E., Julius, D., and Cheng, Y. *Nature* **2013** 504(7478), 107

Cryo-EM structure of the *Blastochloris viridis* RC-LH1 complex at 2.87 Å

Pu Qian

Department of Molecular Biology and Biotechnology, University of Sheffield, Sheffield, UK.

The reaction centre light-harvesting 1 (RC-LH1) complex is the core functional component of bacterial photosynthesis. A 2.87 Å resolution cryo-EM structure of the bacteriochlorophyll *b*-based RC-LH1 from *Blastochloris viridis* reveals the structural basis for absorption of infrared light, and the molecular mechanism of quinone migration across the LH1 complex. The novel triple ring LH1 complex comprises a circular array of 17 β-polypeptides sandwiched between 17 α- and 16 γ-polypeptides. Tight packing of the γ-apoproteins between βs collectively interlocks and stabilizes the LH1 structure which, together with the short Mg-Mg distances of BChl *b* pairs, contributes to the large red-shift of bacteriochlorophyll *b* absorption. The 'missing' 17th γ polypeptide creates a pore in the LH1 ring, and an adjacent binding pocket provides a folding template for a novel quinone, Q_P, which adopts a compact, export-ready conformation prior to passage through the pore and eventual diffusion to the cytochrome bc_1 complex.

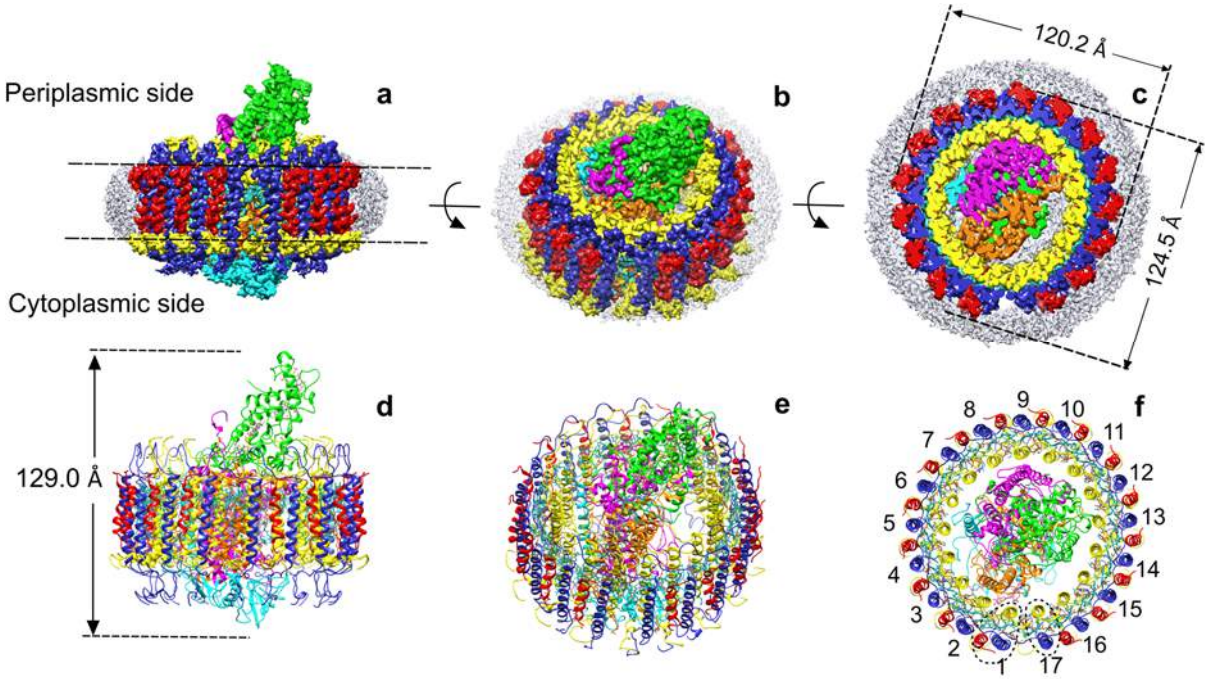

Configuration of Antenna subunits in Photosystem I complex

Shin-Ichiro Ozawa
Research Institute for Interdisciplinary Science, Okayama University, Okayama, Japan

Abstract: In oxygenic photosynthesis, electron transfer is driven by two types of photosystems, Photosystem II (PSII) and Photosystem I (PSI), operating in tandem. In plants and algae, the association of antenna complex, light-harvesting chlorophyll *a*/*b* complex (LHC), significantly increases light-harvesting capacity. LHC consists of LHC subunits of which structures, as well as chlorophyll binding sites, are well conserved. However, the physical property of individual LHC subunit is not identical because chemical species and arrangement of chlorophyll are slightly modified. PSI binds LHCI while PSII binds LHCII, respectively and specifically, to form PSI-LHCI or PSII-LHCII, and it was found that configurations of each LHC subunit are well organized. Structure of PSI-LHCI from pea is resolved at 2.6 Å by X-ray crystal structural analysis and individual LHCI subunit configuration is well described [1]. According to the crystal structure, four LHCI subunits (Lhca1-4) are located in a half-ring arrangement. In contrast to the plant, the arrangement and stoichiometry of LHCI subunits in algal PSI are not sufficiently determined because of the difficulties to isolate intact PSI-LHCI complexes and/or the presence of more LHCI subunits.
It is currently accepted that PSI-LHCI supercomplex of *Chlamydomonas reinhardtii* has nine distinct LHCI subunits (LHCA1-9). Our knowledge of the configuration of individual LHCI subunits is even more limited while the most recent single particle analysis suggested that nine LHCI subunits are arranged in two layers [2]. Recently, our group determined both the stoichiometry and configuration of nine distinct LHCI subunits in PSI-LHCI supercomplex of *C. reinhardtii*[3]. To determine the stoichiometry of the LHCI subunits, we employed uniform labeling of total cellular proteins with ^{14}C, subsequently, the configuration of all LHCI subunits in PSI-LHCI supercomplex was determined by chemical cross-linking in combination with the identification of cross-linked products by immunoblotting and mass spectrometry.
In this talk, I am going to introduce LHCI briefly and discuss functional insights of LHCI subunits in *C. reinhardtii*.

References:
[1] Mazor, Y.; Borovikova, A.; Caspy, I.; Nelson, N., Structure of the plant photosystem I supercomplex at 2.6 Å resolution. *Nat Plants* **2017,** *3*, 17014.
[2] Drop, B.; Webber-Birungi, M.; Fusetti, F.; Kouril, R.; Redding, K. E.; Boekema, E. J.; Croce, R., Photosystem I of *Chlamydomonas reinhardtii* contains nine light-harvesting complexes (Lhca) located on one side of the core. *J Biol Chem* **2011,** *286* (52), 44878-87.
[3] Ozawa, SI.; Bald, T.; Onishi, T.; Xue, H.; Matsumura, T.; Kubo, R.; Takahashi, H.; Hippler, M.; Takahashi, Y., submitted.

XAFS/EELS analyses of nitrogen doped titanium oxide photocatalysts

Tomoko Yoshida[1], Muenaki Yamamoto[2], Akiyo Ozawa[3], Yuma Kato[3], Shinya Yagi[4], Tetsuo Tanabe[1]

[1] *Advanced Research Institute for Natural Science and Technology, Osaka City University*
[2] *Materials, Physics and Energy Engineering, Graduate School of Engineering, Nagoya University*
[3] *Applied Chemistry and Bioengineering, Graduate School of Engineering, Osaka City University*
[4] *Institute for Materials and systems for sustainability, Nagoya University*

Photocatalytic reactions at the surface of titanium dioxide (TiO_2) under UV light irradiation have been attracting much attention in view of their practical applications to environmental cleaning such as self cleaning of tiles, glasses, and windows. Recently, it was found that the doping of nitrogen into TiO_2 contributed to narrowing of the band gap, thus providing a visible-light response [1]. Previous studies demonstrated that nitrogen doping generated new optical absorption bands in the visible-light region and the absorbance evolved with increasing nitrogen. On the other hand, absorbance may not be linearly proportional to the photocatalytic activity [2], and it is thus important to understand the chemical state of doped nitrogen most effective for the visible-light response.

The N K-edge XANES spectrum of the photocatalytic active nitrogen doped TiO_2 showed a characteristic double-peak at 398 and 401 eV, and the XANES spectrum of the inactive photocatalyst a distinct single peak around 401 eV. These features of the XANES spectra were well reproduced by theoretical simulations based on the model where an O atom in TiO_2 were replaced by N ((N)s) for the active photocatalyst, and that of NO_2 ((NO_2)s) for the inactive photocatalyst [3]. The (N)s had proven to be indispensable for band-gap narrowing and photocatalytic activity, and the optimal nitrogen concentration for generating the (N)s was evaluated to be less than 1.8 atom% by EELS analysis.

We also tried to visualize these two different nitrogen species in photocatalytic active and inactive nitrogen doped TiO_2 samples by introducing modern mathematical treatments to energy-filtering TEM. This advanced nanosized mapping clearly showed that the spatial distributions of both (N)s and (NO_2)s species in TiO_2 are the important key to generate visible-light response of a TiO_2 photocatalyst.

[1] Asahi R., Owaki T., Aoki K., Taga Y., *Science.* **2001**, 293, 269-267

[2] Nosaka Y., Matsushita M., Nishino J., Nosaka A. Y., *Sci. Tech. Adv. Mater.*, **2005**, 6, 143-148.

[3] Yoshida T., Niimi S., Yamamoto M., Ogawa S., Nomoto T., Yagi S., *Nucl. Instr. and Meth. B*, **2015**, 365, 79-81

Recommendation for quick freeze replica electron microscopy

Makoto Miyata
1) The OCU Advanced Research Institute for Natural Science and Technology
2) Graduate School of Science, Osaka City University

Quick freeze replica electron microscopy was developed to visualize membrane fusion at a synapse of nerve cell in 1979, and mainly applied to animal cell physiology. In this method, a specimen is frozen and fixed in a moment by slamming it onto a cupper block cooled by liquid helium or nitrogen, and visualized three dimentionally as a pratinum replica. It gives high image contrast, nanometer spacial and submillisecond time resolutions, which cannot be achieved by any other methods. However, recently only a few groups can provide this method over the world, because it needed “advanced craftmanship”. In other words, this exciting special method was going before our project.
Our project is to change this method more friendly to new researchers and subjects. We welcome both intra and inter university collaborations on various subjects including (i) motility machinery, (ii) pathogenic microorganisms, (iii) useful microorganism, and (iv) materials. I will introduce exciting images recently obtained in our project.

References

[1] Heuser, J.E. *J Electron Microscopy* (Tokyo). **2011**, 60 Suppl 1:S3-29.
[2] Trussart, M.; Yus, E.; Martinez, S.; Baù, D. Tahara, Y.O.; Pengo, T.; Widjaja, M.; Kretschmer, S.; Swoger, J.; Djordjevic, S.; Turnbull, L.; Whitchurch, C.; Miyata, M.; Marti-Renom, M.A.; Lluch-Senar, M.; Serrano, L. *Nature Communications*. **2017,** 8, 14665

Molecular physiology of diverse light-senor proteins and their optogenetic applications

Akihisa Terakita and Mitsumasa Koyanagi

Department of Biology and Geoscience, Graduate School of Science, Osaka City University, Osaka, Japan; OCARINA, Osaka City University, Osaka, Japan

Most animal opsins, which bind to a chromophore retinal to form photosensitive pigments (opsin-based pigments), serve as light-sensitive G protein-coupled receptors (GPCRs), which constitute a large protein family of receptors that sense molecules outside the cell and activate inside signal transduction cascades and, ultimately, generate cellular responses.

Many animals capture light information through opsin-based pigments and utilize the information for visual and non-visual functions including regulation of circadian rhythms. Thousands of opsins have been identified from a wide variety of animas thus far. We have characterized diverse opsins, including novel ones, spectroscopically, biochemically, molecular physiologically and evolutionally [1-4], and also investigated their contribution to biological function [5]. Interestingly, we found that some non-visual opsins have unique molecular properties suitable for optogenetics applications, which is the combination of genetics and optics to control well-defined events within specific cells of living tissues and is now a strong application to control cell activities and animal behaviors by light.

A pineal UV-sensitive opsin parapinopsin, which is activated by UV light and deactivated by green light, contributes to the pineal function of lower vertebrate, discrimination of wavelength of lights, UV and green lights [1, 4]. We found that UV and green light illuminations activate and deactivate G protein-mediated signal transduction cascade in the mammalian cultured cells expressing parapinopsin [6]. Therefore we suggest that parapinopsin has optogenetic potentials to regulates cellular responses and animal behaviours in a light wavelength-dependent manner.

References:

[1] Koyanagi et al., *Proc. Natl. Acad. Sci. U.S.A* **2004**, 101, 6687
[2] Tsukamoto et al., *J. Biol. Chem* **2009**, 284, 20676
[3] Koyanagi et al., *Proc. Natl. Acad. Sci. U.S.A* **2013**, 110, 4998
[4] Koyanagi et al., *BMC Biology* **2015**, 17, 73
[5] Nagata et al., *Science* **2012**, 355, 469
[6] Kawano-Yamashita et al., *PLoS One* **2015**, 10, e0141280

Automated single-molecule imaging analysis of cell signaling

Masahiro Ueda

Graduate School of Frontier Biosciences, Osaka University
and Quantitative Biology Center (QBiC), RIKEN

Abstract:

Single-molecule imaging of biomolecules in living cells allows for the investigation of cell signaling and other molecular mechanisms [1]. The techniques have made it possible to directly monitor the behaviors of biomolecules in living cells, in which the locations, movements, turnovers, and complex formations of biomolecules can be detected quantitatively with single molecule sensitivity, providing powerful tools to elucidate molecular mechanisms of intracellular signaling processes. The systematic and comprehensive measurement of a huge number of molecular species at single molecule sensitivity provides detailed information on elementary biological processes and new insights into a system's dynamics, deepening and extending the current biological and medical knowledge. However, technical expertise has been required for both microscope operation and data analysis, which has prevented the analysis from being a standard in medical and biological research. Recently, we have developed an automated single-molecule imaging apparatus for live-cell analysis [2]. All the significant procedures, such as searching for cells suitable for the observation, detecting an in-focus position, image acquisition and single-molecule tracking, are fully automated, allowing us to accomplish a large amount of highly accurate, efficient, and reproducible live-cell imaging experiments. The apparatus could complete single-molecule imaging and analysis of epidermal growth factor receptor (EGFR) for 1,600 cells in a 96-well plate within one day. Changes in the lateral mobility of EGFR on the plasma membrane in response to various ligand and drug concentrations were detected clearly in individual cells, which provided several dynamics and pharmacological parameters including diffusion coefficient, oligomer size, and EC50. Our data show that upon EGF stimulation, EGFR gradually undergoes a transition from the fast-mobile state to slow and immobile states within a 270 nm diameter wide area and simultaneously forms large oligomers that function possibly as a signaling hub for the downstream signaling molecule Grb2. Automated single-molecule imaging is feasible for the systematic analysis of cell signaling and can also be applied to single-molecule screening, thus extensively contributing to biological and pharmacological research.

References:

[1] Ueda, M. et al. *Science* **2001**, 294, 864.

[2] Yasui, M.; Hiroshima, M.; Kozuka, J.; Sako, Y; Ueda, M., under revsion.

Synthesis of π-Conjugated Molecules via Transition-Metal-Catalyzed C–H Functionalization

Tetsuya Satoh

Department of Chemistry, Graduate School of Science, Osaka City University, 3-3-138 Sugimoto, Sumiyoshi-ku, Osaka 558-8585, Japan

Transition-metal-catalyzed regioselective C–H functionalization reactions with the aid of directing groups (–DG) are recognized as important tools for environmentally benign synthesis, since they provide atom- and step-economical routes toward complex molecules from simple substrates. Especially, oxidative coupling of aromatic C–H and unsaturated compounds in the presence of an appropriate oxidant are highly useful for constructing π-conjugated molecules. In earlier examples for such direct transformation, palladium catalysts used to be employed. However, homogeneous palladium catalysts tend to be easily inactivated under oxidative conditions. In addition, substrate scope used to be relatively narrow.

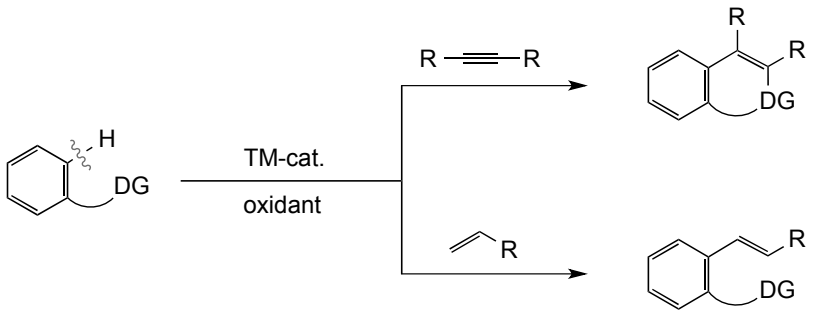

We succeeded in finding that Cp*Rh(III) complexes are stable under oxidative conditions and can effectively promote the oxidative coupling reactions [1]. Particlarly, the annulative coupling of aromatic substrates possessing various heteroatom-containing directing groups with internal alkynes proceeds smoothly under rhodium catalysis to give the corresponding fused heteroaromatic molecules [2].

References:

[1] For review, see: Satoh, T.; Miura, M. *Chem. Eur. J.* **2010**, *16*, 11212.

[2] For representative examples, see: (a) Morioka, R.; Nobushige, K.; Satoh, T.; Hirano, K.; Miura, M. *Org. Lett.* **2015**, *17*, 3130. (b) Iitsuka, T.; Hirano, K.; Satoh, T.; Miura, M. *J. Org. Chem.* **2015**, *80*, 2804.

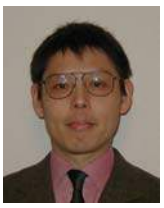

Low-temperature direct bonding of dissimilar materials for advanced electronics

Naoteru Shigekawa

Gradutate School of Engineering, Osaka City University

Seven research projects are currently going on in OCARINA. As members of “Frontier Materials” Project, one of the seven research projects, we have been investigating application of surface-activated bonding (SAB), which is one of low-temperature direct bonding technologies, for fabricating junctions of dissimilar materials. We previously fabricated III-V-on-Si multijunction solar cells [1] and metal-foil-based ultrathick interconnects directly bonded to semiconductor substrates [2] by using SAB. In this presentation, we focus on possibility of SAB-based junctions for realizing novel high-power devices.

The performance of high-power devices is mainly limited by the deterioration in escape of heat during the operation. Diamonds are promising as materials for thermal spreaders because of their excellent insulating properties and large thermal conductivity. It was reported that a diamond film was directly bonded to a Si (100) substrate [3]. The bonding process, however, required a long-period (15 h) loading in a high temperature (> 950 °C), which prevents the method from being applied in semiconductor industries.

We successfully fabricated diamond/Si junctions by using SAB without heating samples during bonding [4]. We found that diamond and Si were firmly bonded to each other by using an SEM. An observation using a TEM and EELS indicated that both sp^2 and sp^3 bondings were distributed in a diamond layer neighboring the bonding interface. We confirmed by XPS characterization that the sp^2 bondings were formed during irradiating fast atom beams of Ar for activating surfaces of samples. It is assumed that the mixture of sp^2 and sp^3 bondings formed on a surface of diamond should play an essential role in successfully bonding diamond and Si at low temperatures.

The authors are grateful to Prof. K. Tsuji in Graduate School of Engineering, Osaka City Univ. for his advice in XPS characterization. This work was supported by the Grant-in-Aid for Challenging Exploratory Research (16K13676) of the Ministry of Education, Culture, Sports, Science, and Technology (MEXT), Japan.

[1] N. Shigekawa, et al. Jpn. J. Appl. Phys. **54**, 08KE03 (2015).
[2] J. Liang, et al. ECS J. Solid State Sci. Technol., **6**, 626 (2017).
[3] G. N. Yushin, et al. Appl. Phys. Lett. **81**, 3275 (2002).
[4] J. Liang, et al. Appl. Phys. Lett. **110**, 111603 (2017).

C–H Activation Catalyzed by Earth Abundant Metals

Laurean Ilies

Department of Chemistry, School of Science The University of Tokyo

7-3-1 Hongo, Bunkyo-ku, Tokyo 113-0033

Transition-metal-catalyzed C–H bond activation is of interest because direct functionalization of simple substrates enables streamlined, rapid creation of molecular complexity. These reactions have been dominated by precious metal catalysis to date, but economical and environmental incentives have boosted the interest into catalysis using Earth abundant metals. This presentation will describe our journey in developing iron catalysis for directed C–H bond activation [1], exploration of catalytic systems based on cobalt [2], manganese [3], and chromium, and exploitation of a dual radical/organometallic reactivity of organoiron species for selective functionalization of C(sp^3) bonds [4].

Scheme 1. **Earth-abundant metal-catalyzed directed C–H activation**

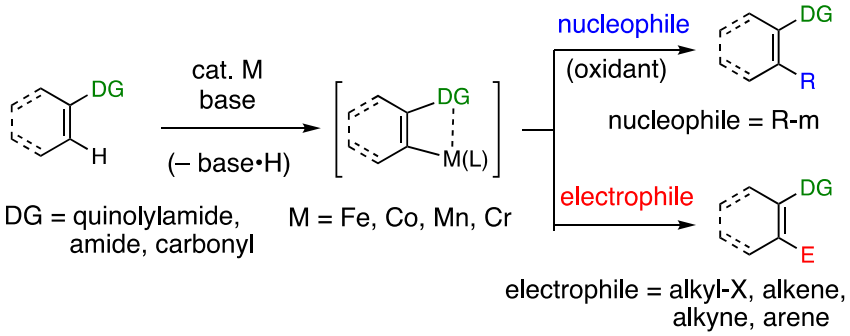

Scheme 2. **Dual reactivity of iron for activation of C(sp^3)–H**

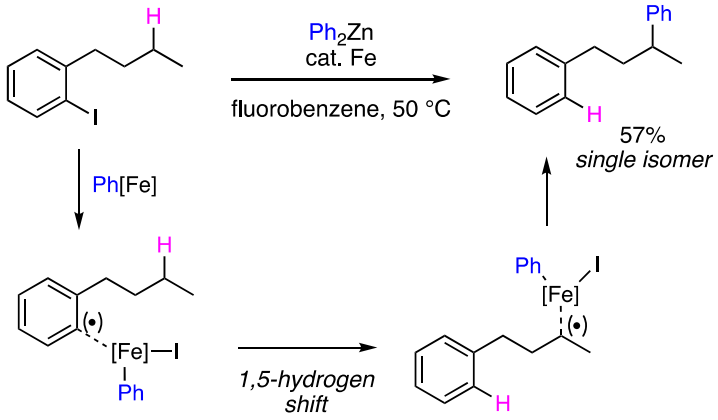

[1] (a) Rui Shang, Ilies, L.; Nakamura, E. *Chem. Rev.* **2017**, *117*, 9086. (b) Ilies, L. *Journal of Organic Synthetic Chemistry*, *Japan* **2017**, *75*, 802.

[2] (a) Chen, Q.; Ilies, L.; Nakamura, E. *J. Am. Chem. Soc.* **2011**, *133*, 428. (b) Ilies, L.; Chen, Q.; Zeng, X.; Nakamura, E. *J. Am. Chem. Soc.* **2011**, *133*, 5221.

[3] Sato, T.; Yoshida, T.; Al Mamari, H. H.; Ilies, L.; Nakamura, E. *Org. Lett.* **2017**, *19*, 5458.

[4] B. Zhou, H. Sato, L. Ilies, E. Nakamura, *ACS Catal.* **2018**, *8*, 8.

Exploiting the Nanoscale Interface at Metal Nanoparticle and Metal-Organic Framework for Catalysis and Sensing Applications

Xing Yi Ling

Division of Chemistry and Biological Chemistry, School of Physical and Mathematical Sciences, Nanyang Technological University, 21 Nanyang Link, Singapore 637371. E-mail: xyling@ntu.edu.sg

Abstract. A major challenge in nanoparticle self-assembly is programming the large-area organization of a single type of anisotropic nanoparticle into distinct superlattices with tunable packing efficiencies. In this talk, I will discuss how nanoscale surface chemistry is used to direct the self-assembly of shape-controlled silver nanoparticles into three distinct two-dimensional plasmonic superlattices at a liquid/liquid interface. Systematically tuning the surface chemistry of the silver nanoparticles leads to a continuous superlattice structural evolution, from close-packed to progressively open structures. Notably, silver octahedra standing on vertices arranged in a square lattice is observed using hydrophobic particles. The structure-to-function characterization reveals that the nanoparticle assembly with the least packing density generates plasmonic 'hotstrips', leading to nearly 10-fold more efficient surface-enhanced Raman scattering compared with the other more densely packed configurations.

In the second part, I will discuss how real-time SERS is developed to directly observe the concentration of CO_2 molecules into a quasi-condensed phase at a nanoscale interface at a metal-organic framework (MOF) and metal nanoparticle surface, even at ambient conditions of 1 bar and 298 K. A systematic spectral evolution is observed throughout our time-dependent SERS studies, which enables us to experimentally visualize the in situ linear-to-bent transformation of CO_2 at the solid-gas interface with increased gas accumulation over time. These direct observations highlight the advantage of surface-sensitive SERS in probing such sophisticated molecular dynamics occurring at the enclosed surface of solid@MOF system, offering valuable insights to further our understanding in solid-gas interactions at ambient operations.

Poster Presentations

Au-nanoparticle-embedded polymer films synthesized on $HAuCl_4$/gelatin aqueous solution irradiated with Ar DBD plasma

[1]Junji Kambayashi, [1]Shiori Azuma, [1]Yusuke Nakamura,
[2]Toshiyuki Isshiki, and [1]Tatsuru Shirafuji
[1]Department of Physical Electronics and Informatics,
Osaka City University, 3-3-138 Sugimoto, Sumiyoshi-ku, Osaka, 558-8585 Japan
[2]Department of Electrical Engineering and Electronics,
Kyoto Institute of Technology, Kyoto 606-8585, Japan

1. Introduction

Solution plasma can be used for various applications including nanoparticle synthesis and liquid treatment [1]. However, there are few reports on thin film formation using solution plasma [2]. In this work, we report that we can synthesize a free-standing film, which is cross-linked gelatin with embedded gold nanoparticles (GNPs), on an aqueous solution irradiated with dielectric barrier discharge (DBD).

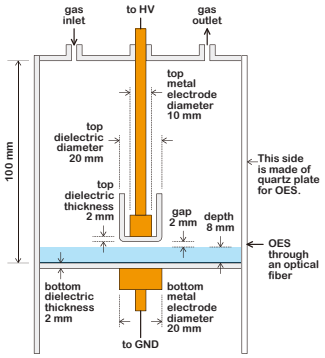

Fig. 1 The DBD reactor used in this study.

2. Experimental procedure

The aqueous solution was $HAuCl_4$ (0.15, 0.30, and 0.60 mM) aqueous solution with gelatin (5, 10, and 20 wt.%). The DBD system used in this study is shown in Fig. 1. Applied voltage was bipolar pulse voltage (amplitude 4 kV, frequency 40 kHz, pulse width 4 μs). Typical discharge time was 10 min. Discharge gas was argon.

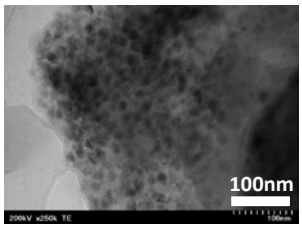

Fig. 2 TEM image of the film.

3. Results and discussion

A film is formed on the aqueous solution by irradiating DBD plasma on the aqueous solution. Infrared absorption spectra of the film and energy dispersive X-ray spectra have indicated that the film is made of cross-linked gelatin and gold. Figure 2 shows a transmission electron microscope (TEM) image of the sample taken from the outer edge of the film, which indicates that the synthesized GNPs are densely incorporated in the film. The size of GNPs seems to be regulated. Such size regulation may be explained in terms of immediate capture of reduced gold by growing film. The film formation process can be controlled by means of the concentration of $HAuCl_4$ and gelatin and discharge duration, which affects the size and concentration of GNPs in the membrane.

References:

[1] T. Shirafuji, et al., *Jpn. J. Appl. Phys.* **2013**, 52, 126202.
[2] H. Furusho, et al., *J. Photopolym. Sci. Technol.* **2007**, 20, 229.

Iridium-Catalyzed Aerobic Dehydrogenative/Decarbonylative Coupling of Salicylaldehydes with Alkynes

Shintaro Yamane,[1] Tomoaki Hinoue,[2] Yoshinosuke Usuki,[1] Masumi Itazaki,[1] Hiroshi Nakazawa,[1] Yoshihiro Hayashi,[3] Susumu Kawauchi,[3] Masahiro Miura,[2] Tetsuya Satoh[1]

[1]*Graduate School of Science, Osaka City University, 3-3-138 Sugimoto, Sumiyoshi-ku, Osaka 558-8585, Japan.*

[2]*Guraduate School of Engineering, Osaka University, Suita, Osaka 565-0871, Japan.*

[3]*Department of Chemical Science and Engineering, Tokyo Institute of Technology, 2-12-1 (E4-6), Ookayama, Meguro-ku, Tokyo 152-8552, Japan.*

Abstract: Transition-metal-catalyzed dehydrogenative coupling reactions have been regarded as useful synthetic tools to prepare useful organic molecules from readily available starting materials. In particular, the coupling of aromatic substrates possessing a heteroatom-containing directing group with internal alkynes has been utilized for constructing fused heteroarenes. We previously demonstrated that salicylaldehydes undergo dehydrogenative coupling with internal alkynes in the presence of a rhodium catalyst and a copper salt oxidant to produce 2,3-disubstituted chromone derivatives.[1] In this study, we succeeded in finding that dehydrogenative, decarbonylative coupling of the same combination of substrates can be carried out efficiently by using an iridium catalyst together with a copper cocatalyst in place of the rhodium system under O_2 (1 atm) to give 2,3-disubstituted benzo[*b*]furan derivatives. Benzo[*b*]furan skeletons can be seen in various synthetic intermediates for pharmaceuticals and biologically active compounds and functional organic materials. The present procedure provides a straightforward, simple method for constructing such important structures.

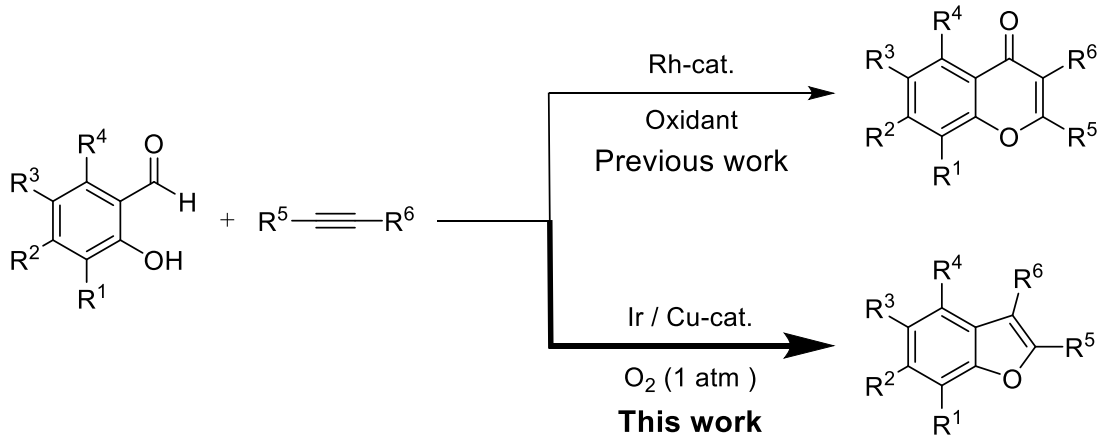

References

[1] Shimizu, M.; Tsurugi, H.; Satoh, T.; Miura, M. *Chem. Asian J.* **2008**, *3*, 881.

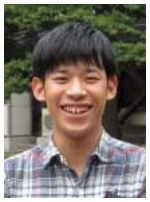

Photoswiching of Birefringence of Diarylethene Single Crystals by Photochromic Reaction

Kohei Morimoto, Hajime Tsujioka, Daichi Kitagawa, Seiya Kobatake
Department of Applied Chemistry, Graduate School of Engineering, Osaka City University, Osaka 558-8585, Japan

Abstract: Photochromic compounds have drawn much attention because the chemical and physical properties are changed by photoirradiation. Diarylethenes are one of the most promising photochromic compounds because of their high fatigue-resistance and high thermal stability of two isomers[1]. In this work, we investigated the photoinduced birefringence change of **1a** and **2a** single crystals. The transmittance spectra of the crystals under crossed Nicols exhibited interference due to birefringence. Fig. 2 shows the interference color change under crossed Nicols and the real color change under open Nicol in **2a** crystal by ultraviolet (UV) light irradiation. The transmittance spectrum due to the interference color was shifted to longer and shorter wavelength in **1a** and **2a**, respectively, as shown in Fig. 3. The results indicate that the birefringence was changed by the photoisomerization reaction. The change in birefringence values of the crystal was obtained by fitting the theoretical formula to the transmittance spectrum. The single crystals of **1a** and **2a** exhibited the birefringence increase and decrease upon irradiation with UV light, respectively. The relationship between the photoinduced birefringence change of diarylethene crystals and their molecular structures was discussed based on the molecular polarizability anisotropy.

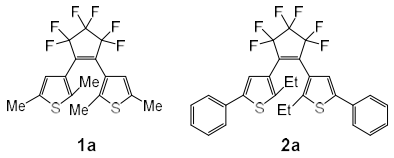

Figure 1. Diarylethenes used in this work.

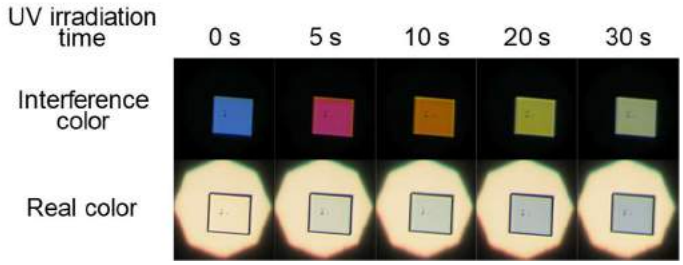

Figure 2. Interference color change under crossed Nicols and real color change under open Nicol of **2a** crystal (thickness: 5.1 μm).

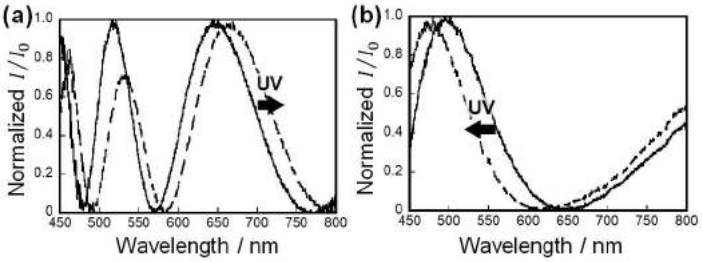

Figure 3. Transmittance spectra of (a) **1a** crystal (thickness: 45.2 μm) and (b) **2a** crystal (thickness: 5.8 μm) under crossed Nicols, before UV irradiation (solid line) and after UV irradiation (dashed line).

References:

[1] M. Irie, T. Fukaminato, K. Matsuda, S. Kobatake, *Chem. Rev.* **2014**, 114, 12174−12277.

Development of Covariance Mapping Method for the Investigation of Coulomb Explosion Processes

Tomomasa Nishimura, Masako Itsukashi, Tomoyuki Yatsuhashi
Graduate School of Science, Osaka City University, 3-3-138 Sugimoto, Sumiyoshi-ku, Osaka 558-8585, Japan

Coulomb explosion is one of the most extreme fragmentation process in chemistry due to the destructive nature of multiply charged molecular cations [1]. We have investigated the relationship between the molecular structure and the ejection of fragment ions by Coulomb explosion for various molecules by using a time-of-flight (TOF) spectroscopy [2]. The qualitative interpretations of ion emissions even for large molecules can be made to some extent; however, the correlations between fragment ions are not known. In this study, we developed the covariance mapping technique, which can be utilized to determine correlations between fragment ions from TOF data. We prepared a data collection and analysis software, which can process 8×10^{11} data within 1 hour. The experimental conditions were optimized for the investigation of Coulomb exploison of diatomic molecules.

Multiple ionization of N_2 was performed with a femtosecond laser pulse (0.8 μm, 40 fs) and the ions formed by Coulomb explosion were detected by a linear-type TOF mass spectrometer. The pressure of N_2 was mainteined in the 10^{-6} Pa range (ca. 4×10^{-13} mol dm^{-3}) to avoid false covariance events. Figure 1 shows a covariance map showing the Coulomb explosion of N_2. The bottom and left traces represent average TOF spectra. The typical feature of an ion generated by Coulomb explosion is the presence of split peaks that are a consequence of the fact that ions with certain kinetic energies are emitted along both the forward (f) and backward (b) direction relative to the ion flight axis. The strong diagonal line in the map corresponds to the auto-correlations. On the other hand, four peaks indicated by dashed circles show the correlation of N_f^{3+} and N_b^{3+}, N_f^{2+} and N_b^{3+}, N_f^{3+} and N_b^{2+}, and N_f^{2+} and N_b^{2+}, respectively. We conclude that the origin of the respective fragment ion pairs is definitively identified as being N_2^{6+}, N_2^{5+}, N_2^{5+}, and N_2^{4+}.

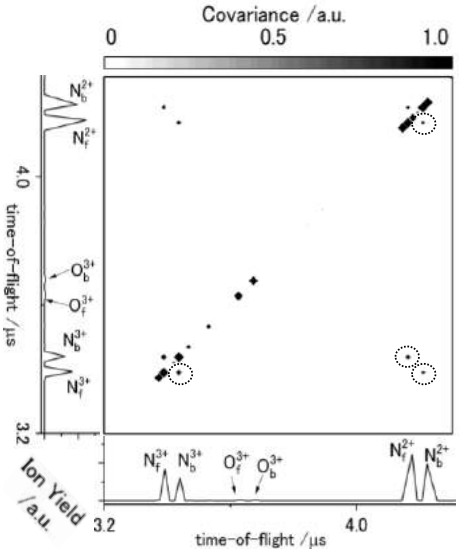

Figure 1 A covariance map showing the ion correlations in the Coulomb explosion of N_2.

References

[1] Yatsuhashi, T.; Nakashima, N. *J. Photochem. Photobiol. C* **2018** in press.
[2] Tanaka H.; Nakashima, N.; Yatsuhashi, T. *J. Phys. Chem. A* **2016**, *120*, 6917.

Synthesis of Single-Nano-Sized Iron Nanoparticles from Liquid/Liquid Dispersion System by Femtosecond Laser Irradiation

Yuki Horikawa, Takuya Okamoto, Tomoyuki Yatsuhashi

Graduate School of Science, Osaka City University, 3-3-138 Sugimoto, Sumiyoshi-ku, Osaka 558-8585, Japan

Iron nanoparticles (FeNPs) have come to occupy an important position in magnetic and biomedical materials. The production of FeNPs have been reported by using nanosecond ultraviolet lasers, whereas femtosecond laser was rarely used [1]. In this study, we report the synthesis of FeNPs by using water and *n*-hexane mixed solvent to control the size of FeNPs as well as to remove the unwanted carbon aggregates.

We chose ferrocene as a reactant, and *n*-hexane or water and *n*-hexane mixture as solvent. The reactant solution was exposed to focused femtosecond laser pulses (0.8 μm, 40 fs, 0.4 mJ, 1 kHz) for 10 min. Transmission electron microscopy (TEM) was used to investigate the morphology and size of FeNPs. When *n*-hexane was used as a solvent, FeNPs as well as carbon aggregates were formed in abundance. The mean and maximum diameters of FeNPs were 10 nm and 50 nm, respectively (Fig.1a). On the other hand, we obtained dispersed FeNPs with negligible amout of carbon aggregates when water and *n*-hexane mixture was used as solvent (Fig.1b). It is emphasized that single-nano-sized FeNPs are dominantly formed. The mean and maximum diameters of FeNPs were 4.6 nm and 10 nm, respectively. We conclude that heterogeneous reaction environment (*n*-hexane droplets in water) regulates the growth of FeNPs. In addition, hydrophobic carbon aggregates originating form cyclopentadienyl ligands were separated into a hydrocarbon phase [2].

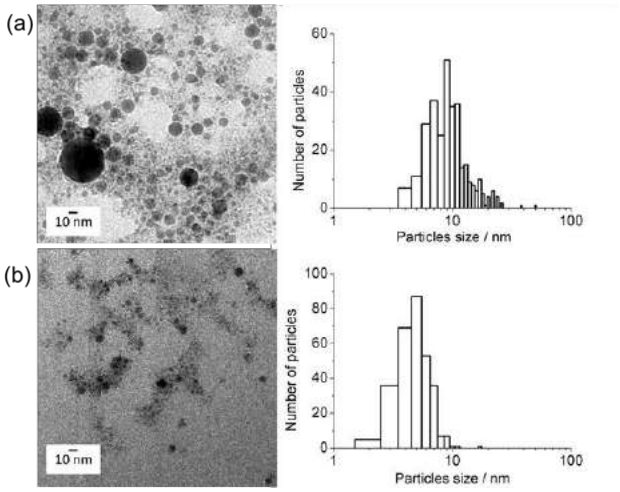

Fig.1 TEM images and paticles size distribution of FeNPs collected from (a) *n*-hexane solution and (b) water layer of water and *n*-hexane mixture.

References

[1] Wesolowski, M. J.; Kuzmin, S.; Wales, B.; Sanderson, J. H.; Duley, W. W. *J. Mater. Sci*. **2013**, *48*, 6212.

[2] Okamoto, T.; Mitamura, K.; Hamaguchi, T.; Matsukawa, K.; Yatsuhashi, T. *ChemPhysChem* **2017**, *18*, 1007.

Stereoselective Synthesis of the Tripeptide of SF-2132

Akira Sawai, Ai Sekihara, Yoko Yasuno, Tetsuro Shinada
Graduate School of Science, Osaka City University
3-3-138 Sugimoto, Sumiyoshi, Osaka 558-8585, Japan

SF-2132 (**1**), isolated from the culture broth of *Nocardiopsis* sp. SF-2132, exhibits antimicrobial activities against mycobacteria, Gram-positive bacteria, and Gram-negative bacteria.[1] This hexapeptide contains four unusual amino acids. Among them, the structures of the β-arginine and the dehydroamino acid moieties have not been established yet. In this presentation, we would like to report the stereoselective synthesis of the tripeptide unit *E*-**2** and *Z*-**3**. *E*-tripeptide **2** was synthesized via the Negishi cross coupling reaction of iodo dehydroamino acid **4** under the mild condition.[2] Stereoselective synthesis of *Z*-isomer **3** was furnished by the selective dehydration reaction of **5** via a cyclic sulfamidite.[3] Comparison of NMR data of *E*-**2**, *Z*-**3** and **1** suggested that the olefin geometry of **1** was putatively assigned to be *Z*-configuration.

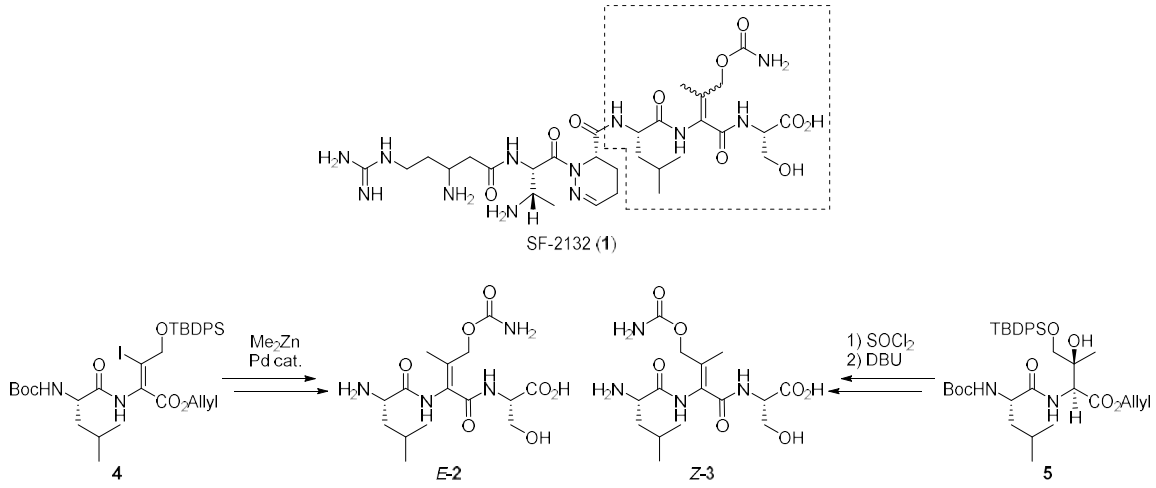

[1] Kondo, Y.; Tohyama, H.; Shomura, T.; Sezaki, M.; Niwa, T.; Kojima, M. Meiji Seika Kenkyu Nenpo, **1985**, *24*, 27.
[2] Yasuno, Y.; Nishimura, A.; Yasukawa, Y.; Karita, Y.; Ohfune, Y.; Shinada, T. *Chem. Commun*. **2016**, *52*, 1478.
[3] Stohlmeyer, M. M.; Tanaka, H.; Wandless, T. J. *J. Am. Chem. Soc.* **1999**, *121*, 6100.

Annealing temperature dependency of directly-bonded SiC/Si junction characteristics

K. Shimozato, J. Liang, and N. Shigekawa
Graduate School of Engineering
Osaka City University
Sugimoto 3-3-138, Sumiyoshi, Osaka 558-8585, Japan
E-mail : m17tb029@ka.osaka-cu.ac.jp

M. Arai
New Japan Radio Co. Ltd.

Abstract:

We measured electrical characteristics and die shear strength of directly-bonded n—SiC(1×10^{17}cm^3)/p$^+$-Si junction with the emphasis on their dependence on the annealing condition during bonding. As reported for GaAs/GaAs junction[1], the electrical characteristics of directly-bonded junction are varied by annealing conditions. In this work, we separated annealing process into two steps. We performed lower-temperature annealing at the first step and higher-temperature one at the second step. Figure 1 shows capacitance-voltage (C-V) characteristics of junction prepared with different first step annealing temperatures. The impurity concentration obtained from each C-V curve is also shown in this figure. Figure 2 shows the dependence of bonding strength on the annealing temperature in the first step. A concentration close to that for n$^-$-SiC layers obtained by characterizing Schottky junctions is observed for higher annealing temperatures in the first step. With increasing annealing temperature at the first step, the impurity concentrations tend to approach the concentration of SiC and the bonding strength shows a high numerical value. These results show directly-bonded SiC/Si junction characteristics depend on the annealing temperature at the first (lower-temperature) step in the bonding process.

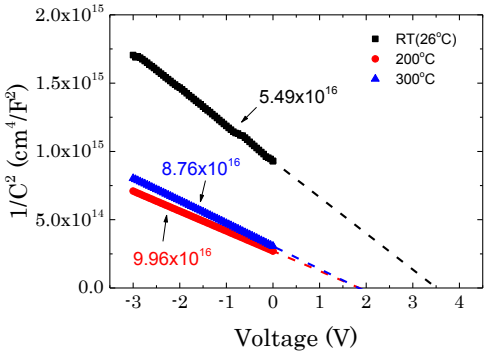

Fig. 1 C-V characteristics of n-4H-SiC/p$^+$-Si junctions.

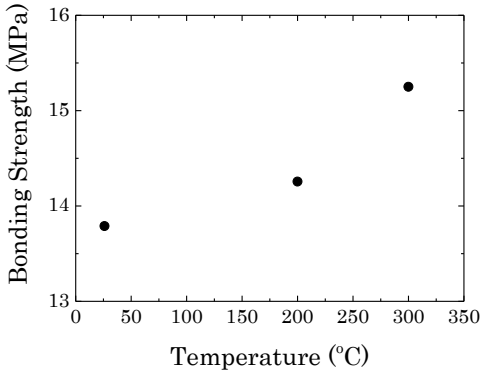

Fig. 2 Bonding strength of SiC/Si junctions.

References:

[1]M. J. Jackson, et al. J. Appl. Phys. 110, 104903 (2011).

Light-induced hydrogen production by photosystem I-Pt nanoparticle immobilized in porous glass plate nanopores

Makoto Hirano,[1] Tomoyasu Noji,[2] Keisuke Kawakami,[2] Teturo Jin,[3] Masaharu Kondo,[4] Hirozo Oh-oka,[5] Nobuo Kamiya,[2,1]

[1] Graduate School of Science, Osaka City University, [2] The OCU Advanced Research Institute for Natural Science & Technology (OCARINA), Osaka City University, [3]Inorganic Functional Materials Research Institute, National Institute of Advanced Industrial, Science and Technology (AIST),[4]Department of Life Science and Applied Chemistry, Graduate School of Engineering, Nagoya Institute of Technology, [5]Department of Biological Sciences, Graduate School of Science, Osaka University,

Abstract: Artificial photosynthesis that converts solar energy into chemical energy, has attracted a lot of attention as one of answers to solve the energy problem. Natural photosynthesis is efficiently achieved by pigment-protein complexes, named photosystem I (PSI) and photosystem II. PSI produces the high reducing power to convert carbon dioxide to sugar using solar energy. Utilization of natural photosynthetic proteins for the construction of artificial devices is an attractive approach, because the high quantum efficiencies of light-induced charge separation are near 100%. For example, a light-induced hydrogen production system has been reported using a conjugate of PSI and Pt nanoparticle (PSI-PtNP) [1]. More recently, the hydrogen production system working even under aerobic condition has been constructed by immobilizing the PSI-PtNP and cytochrome c_6 (cyt c_6) in a nanoporous glass plate (PSI-PtNP/PGP) with a pore diameter of 50 nm [2]. The hydrogen evolution activity of the PSI-PtNP/PGP was low because the reduction rate of PSI by cyt c_6 was limited by the cyt c_6 diffusions in the PGP. In this study, we optimized the method immobilizing the PSI-PtNP and cyt c_6 into PGP. As a result, the maximum rate of the hydrogen production was faster 6.5-times than that of the previous report. Furthermore, we investigated photochemical activity of PSI inside PGP by measuring fluorescence spectra and flash-induced transient absorption changes. We will discuss the relation between the electron transfer rates in PGP and the hydrogen evolving efficiencies.

References:

[1] L. M. Utschig, N. M. Dimitrijevic, O. G. Poluektov, S. D. Chemerisov, K. L. Mulfort and D. M. Tiede, *J. Phys. Chem. Lett.*, **2011**, 2, 236-241.

[2] T. Noji, T. Suzuki, M. Kondo, T. Jin, K. Kawakami, T. Mizuno, H. Oh-oka, M. Ikeuchi, M. Nango, Y. Amao, N. kamiya, T. Dewa, *Res. chem. Intermed*. **2016**, 42, 7731-7742

Dehydrogenative Coupling of Aromatic Carboxylic Acids and Unsaturated Compounds under Rhodium Catalysis

○Asumi Sakai,[1] Takeshi Okada,[2] Tetsuya Satoh,[1] Yoshihiro Hayashi,[3] Susumu Kawauchi,[3] Masahiro Miura[2]

[1]*Department of Chemistry, Graduate School of Science, Osaka City University, 3-3-138 Sugimoto, Sumiyoshi-ku, Osaka 558-8585, Japan*

[2]*Graduate School of Engineering, Osaka University, 2-1 Yamagaoka, Suita 565-0871, Japan*

[3]*Department of Chemical Science and Engineering, Tokyo Institute of Technology, 1-12-1 Ookayama, Meguro-ku, Tokyo 152-8552, Japan*

The transition-metal catalyzed dehydrogenative coupling reactions of aromatic substrates possessing a hetero atom-containing directing group with unsaturated compounds via regioselective C-H bond cleavage are powerful synthetic tools for constructing π-conjugated molecules. Among directing groups, a carboxylic group coordinates to a metal center weekly to allow smooth dissociation and coordination. Previously, our group has reported that the dehydrogenative coupling of benzoic acids with unsaturated compounds such as alkenes and alkynes can be conducted effectivity in the presence of a rhodium catalyst and a suitable oxidant through *ortho* C-H bond cleavage [1].

In this work, we have found that the dehydrogenative coupling of indole-3-carboxylic acids with alkenes proceeds involving C-H activation at their 4-position . Futhermore, the carboxylic function of the 4-alkenylated products can be removed upon treatment with a CuO catalyst [2] to produce 2,3-unsubstituted 4-alkenylindole derivatives.

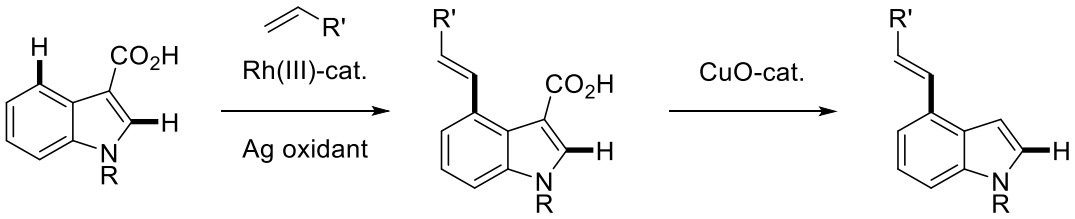

[1] K. Ueura, T. Satoh, M. Miura, *Org. Lett*. **2007**, *9*, 1407-1409.

[2] L. J. Goossen, G. Deng, L. M. Levy, *Science*. **2006**, *313*, 662-664.

Synthesis, Properties, and Reactivities of (Nitronyl Nitroxide-2-ide)Copper Complex Bearing Phenanthroline ligand

Kiyomi YAMADA[1], Shuichi SUZUKI[2], Masatoshi KOZAKI[1,3], Keiji OKADA[1,3]

[1] Graduate School of Science, Osaka City University, [2] Graduate School of Engineering Science, Osaka University, [3] Osaka City University Advanced Research Institute for Natural Science and Technology (OCARINA), Sugimoto, Osaka 558-8585.

Radical metalloids have a metal-carbon bond at the C2-position in **NN** (nitronyl nitroxide), and only a few studies have been reported mainly from our laboratory. Recently, we reported that a Pt complex exhibited a large shift in the oxidation potential of the **NN** moiety to the negative direction by ~0.6 V compared to that of the parent NN (**NN-H**) [1]. Furthermore, an Au complex was successfully used as a stable reagent in the Pd(0)-mediated cross-coupling reaction with aryl iodides (ArI) to afford aryl-substituted NNs (**Ar-NN**s) in excellent yields [2]. In order to develop further variation of these properties, we have developed various radical metalloid reagents. In this study, we designed and synthesized the Cu(I)-**NN** complex bearing 1,10-phenanthroline (**1**).

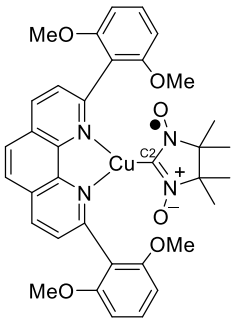

1

The copper complex **1** could be readily prepared in high yield and turned out to be stable in solid under aerated condition. The structure of **1** was confirmed by MS, ESR, and X-ray crystal structure analysis. The copper complex **1** has a extremely low oxidation potential of the **NN** moiety (–0.56 V vs Fc/Fc^+), which is ~ –1 V negative compared to that of **NN-H**. The cross-coupling reaction of **1** with aryl halides proceeded in good yields in the presence of $Pd_2(dba)_3$•$CHCl_3$ and DPPF (1,1'-bis(diphenylphosphino)ferrocene) (Scheme 1). Aryl iodides were more reactive than aryl bromides for both of electron-rich and -poor aryl halides. Moreover, the reactions proceeded with heteroaromatic systems in good yields.

Scheme 1.

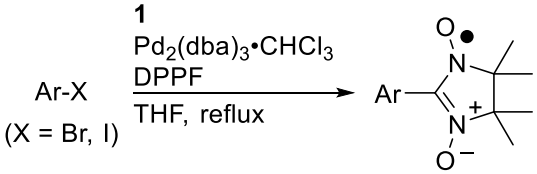

References:

[1] Zhang, X.; Suzuki, S.; Kozaki, M.; Okada, K. *J. Am. Chem. Soc.* **2012**, *134*, 17866–17868.

[2] Tanimoto, R.; Suzuki, S.; Kozaki, M.; Okada, K. *Chem. Lett*. **2014**, *43*, 678–680.

Stereoselective Syntheses of β-Hydroxy Amino Acids by Isonitrile Aldol Reaction

Kazuma Fuku, Yoko Yasuno, Tetsuro Shinada
Graduate School of Science, Osaka City University
3-3-138 Sugimoto, Sumiyoshi, Osaka 558-8585, Japan

β-Hydroxy amino acids, such as β-hydroxyvaline and β-hydroxyisoleucine, are often found as components of bioactive natural products. In this presentation, we would like to report stereoselective syntheses of β-hydroxy-α-amino acids by the aldol reaction of isonitrile **1** possessing a camphorsulfonamide chiral auxiliary.

Isonitrile aldol reaction of **1** with ketone **2** in the presence of 5 mol% of copper catalyst **3** and Et_3N in dichloroethane (DCE) at 0 °C provided **4** which were hydrolyzed to give *N*-formyl-β-hydroxy amino acid esters **5** [58–72% yield (2 steps), dr = 2:1–>10:1].[1] The scope and limitation will be discussed.

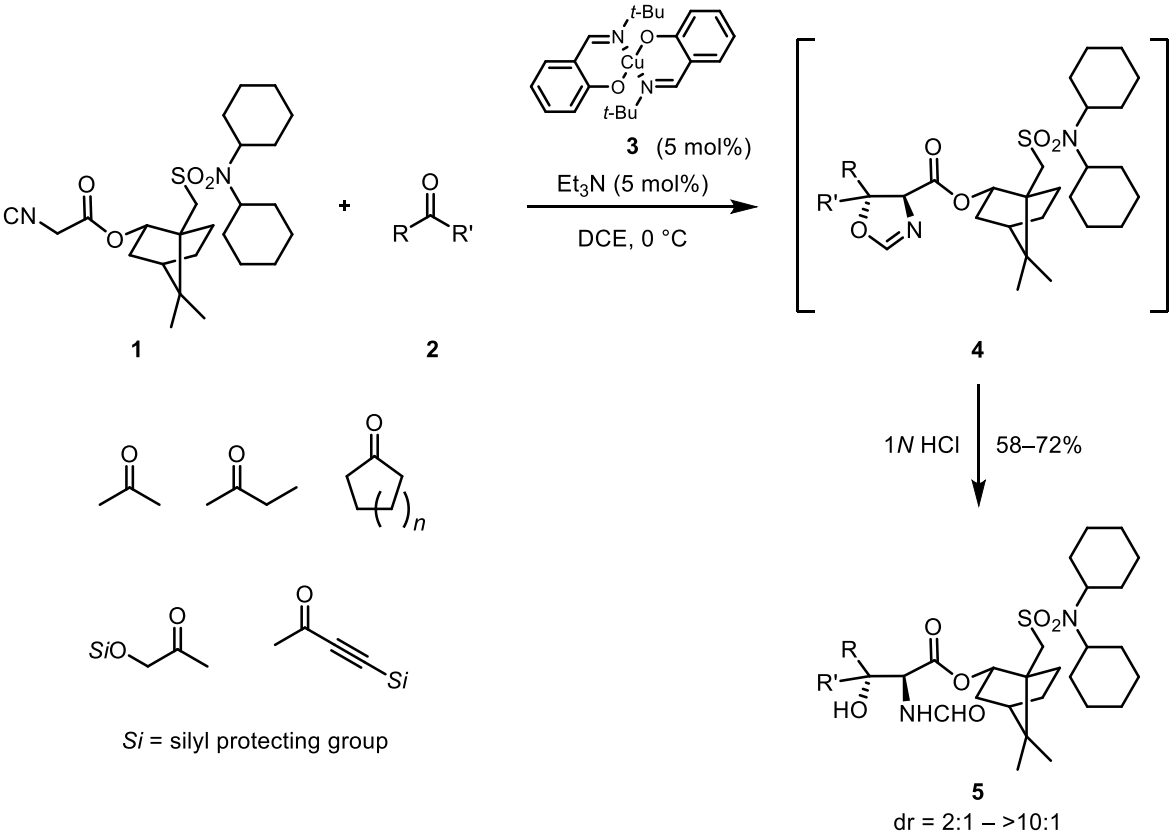

[1] Shinada, T.; Oe, K.; Ohfune, Y. *Tetrahedron Lett.* **2012**, *53*, 3250.

One-pot Synthesis of Anthraquinones by $Sc(OTf)_3$-catalyzed Tandem Reaction

Yohei Toriyama, Yoko Yasuno, Tetsuro Shinada
Graduate School of Science, Osaka City University
3-3-138 Sugimoto, Sumiyoshi, Osaka 558-8585, Japan

A tandem reaction using a single catalyst has attracted much attention as an efficient synthetic method.[1–3] In the last annual meeting, we reported one-pot conversion of **1** to cyclic compounds **4** in the presence of catalytic amount of $Sc(OTf)_3$.[4] In this reaction process, two different reactions, (i) dehydration and (ii) Diels–Alder (DA) reaction were promoted by $Sc(OTf)_3$ in an efficient manner. During the course of our continuous studies, we found that the DA product **4** underwent (iii) aromatization reaction in the presence of $Sc(OTf)_3$. These results led us to investigate a new $Sc(OTf)_3$-catalyzed tandem reaction including three different reactions (i)–(iii) in one-pot. Indeed, various anthraquinones listed below were prepared from **1** and **2**. The scope of the new tandem reaction will be discussed.

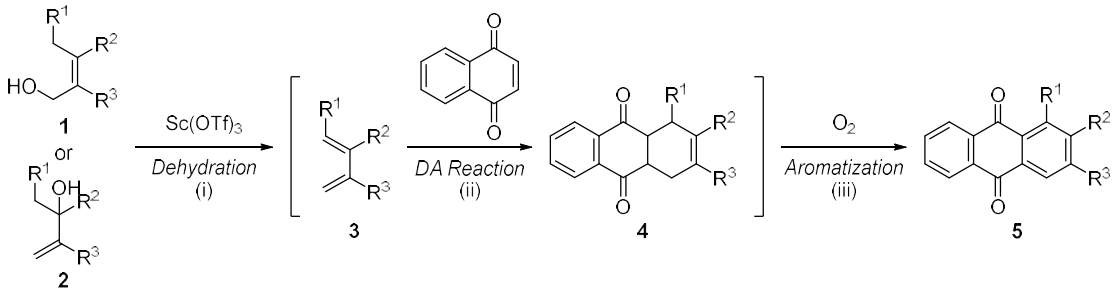

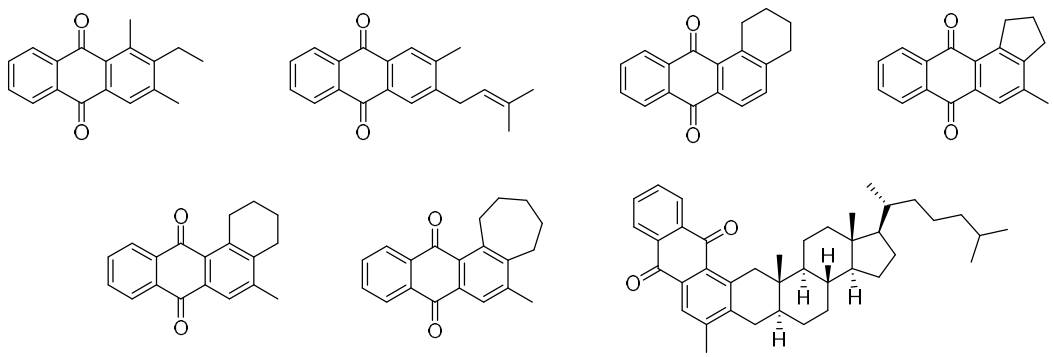

[1] Wasilke, J. C.; Obrey, S. J.; Baker, R. T.; Bazan, G. C. *Chem. Rev.* **2005**, *105*, 1001.
[2] Shindoh, N.; Takemoto, Y.; Takasu, K. *Chem. Eur. J.* **2009**, *15*, 12168.
[3] Camp, J. E. *Eur. J. Org. Chem.* **2017**, 425.
[4] The Chemical Society of Japan 97 th Spring Annual Meeting, **2017**, 3C6-35.

Total Synthesis of SF-2132

Ai Sekihara, Akira Sawai, Yoko Yasuno, Tetsuro Shinada
Graduate School of Science, Osaka City University
3-3-138 Sugimoto, Sumiyoshi, Osaka 558-8585, Japan

SF-2132 (**1**), isolated from the culture broth of *Nocardiopsis* sp. SF-2132, is a unique class of unusual amino acid-rich peptides.[1] In the precedented paper, we reported the stereoselective synthesis of the tripeptide chain **5** including the dehydroamino acid moiety of **1**.[2] These synthetic and spectroscopic analysis suggested that the dehydroamino acid moiety of the natural product has *Z*-configuration. In this presentation, we would like to report the first total synthesis of **1** or **2** by coupling of fragments (*R*)/(*S*)-**3**, **4** and **5**. Stereochemistry of the β-arginine moiety of **1** and **2** will be discussed.

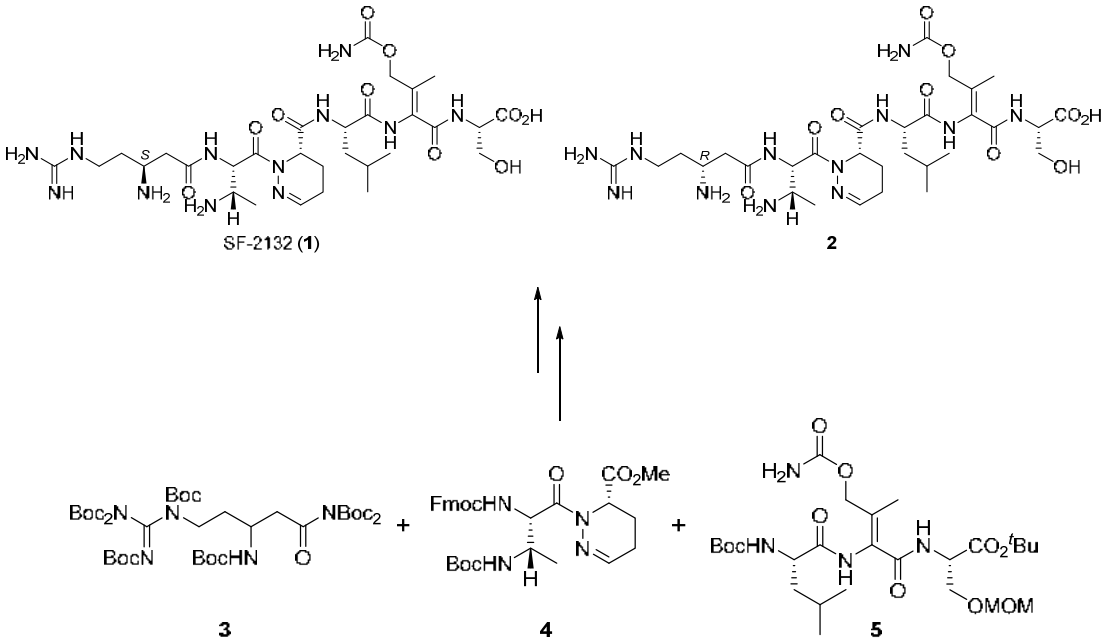

[1] Kondo, Y.; Tohyama, H.; Shomura, T.; Sezaki, M.; Niwa, T.; Kojima, M. Meiji Seika Kenkyu Nenpo **1985**, *24*, 27.
[2] The Chemical Society of Japan 98 th Spring Annual Meeting, **2018**, 1D2-17.

Long-lived Molecular Tetracations of Fluorine-containing Aromatic Compounds

Akihiro Kitashoji, Tomoyuki Yatsuhashi

Department of Chemistry, Graduate School of Science, Osaka City University

Abstract: Multiply charged molecular cations (MMCs) have the potential to be a novel chemical species due to their high electron affinity and charge-dependent reactions. However, little is known about MMCs because they are quite unstable due to Coulombic repulsion. In this study, we showed that intact tetracations of hexafluorobenzene (C_6F_6) and octafluoronaphthalene ($C_{10}F_8$) were produced by femtosecond laser pulses. $C_6F_6^{4+}$ is the smallest tetracation ever observed for aromatic compounds. We investigated the reactivity of $C_6F_6^{z+}$ and $C_{10}F_8^{z+}$ (z = 1–4) by using the time-of-flight mass spectrometer equipped with an ion gate and a curved-field reflectron.

Figure 1 shows the time-of-flight mass spectra of a) C_6F_6 and b) $C_{10}F_8$ ionized by a femtosecond laser pulse (0.8 μm, 35 fs, $>10^{14}$ W cm^{-2}). Intact tetracations of C_6F_6 and $C_{10}F_8$ were clearly identified (see insets) in abundance. Each charge states of $C_6F_6^{z+}$ were successfully selected by a homebuilt Bradbury-Nielsen ion gate (gate width: 36.5±0.5 ns, rise and fall time: >3 ns) [1] as shown in Figure 2. Supposing that the fragmentation of MMCs occurs in the first field-free drift region, the product ions are recorded at times that are different from their precursor ions. However, such product ions were not observed for $C_6F_6^{z+}$ (z = 1–4) and $C_{10}F_8^{z+}$ (z = 2–4). Therefore, the lifetimes were estimated to be more than 9 μs for $C_6F_6^{4+}$ and 11 μs for $C_{10}F_8^{4+}$. We conclude that tetracations are potential candidates as novel reactive species based on the relatively long lifetime and the expected high potential energy (>50 eV).

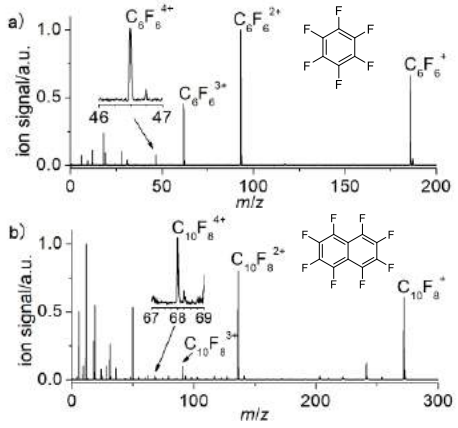

Figure 1. Time-of-flight mass spectra of a) C_6F_6 and b) $C_{10}F_8$.

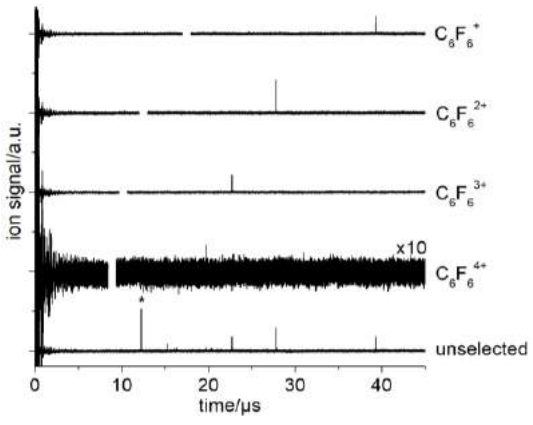

Figure 2. Time-of-flight spectra of a single charge state of $C_6F_6^{z+}$ (z = 1–4) selected by Bradbury-Nielsen ion gate. * indicates H_2O^+.

References:

[1] Kitashoji, A.; Yoshikawa, T.; Fujihara, A.; Kamamori, T.; Nashima, S.; Yatsuhashi, T. *ChemPhysChem* **2017**, *18*, 2007.

Synthetic Study of Phomopsin A

Yuma Karita, Yoko Yasuno, and Tetsuro Shinada
Graduate School of Science, Osaka City University
3-3-138 Sugimoto, Sumiyoshi, Osaka 558-8585, Japan

Phomopsin A (**1**) isolated from *Diaporthe toxica* is known to be a mycotoxin.[1] According to the complex structural feature as well as its potent microtubule depolymerization activity, **1** has attracted much attention as a synthetic target. Structure of **1** is characterized by the constrained 13-membered cyclophane ring consisted of β-OH-DOPA, β-OH-Ile, and β,γ-ΔVal. In this presentation, we would like to report our efforts toward the first total synthesis of **1** via the cyclophane intermediate **2**.

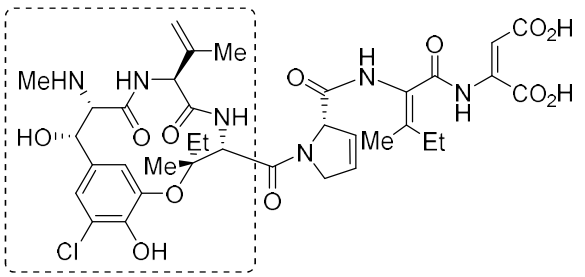

Phomopsin A (**1**)

Three fragments **3**[2], **4**[3] and **5**[4] were sequentially condensed to give cyclization precursor **6** which was subjected to macrocyclization reaction under the high dilution conditions. After the optimization, cyclophane **2** was obtained in 83% from **6**. Recent progress on the conversion of **2** to the target natural product will be reported.

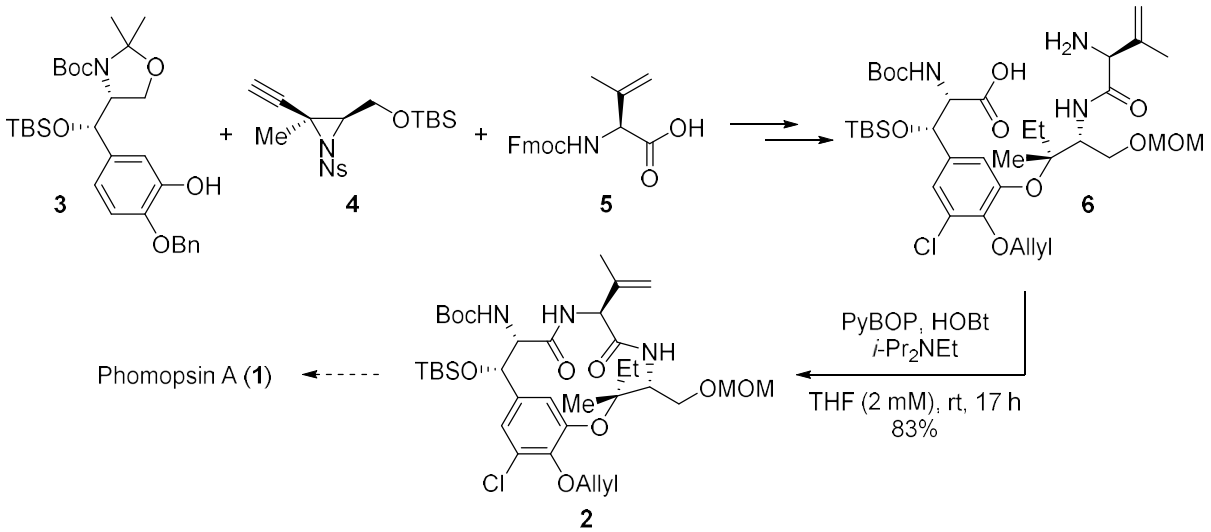

[1] Culvenor, C. C. J.; Beck, A. B.; Clarke, M.; Cockrum, P. A.; Edgar, J. A.; Frahn, J. L.; Jago, M. V.; Lanigan, G. W.; Payne, A. L.; Peterson, J. E.; Petterson, D. S.; Smith, L. W.; White, R. R. *Aust. J. Biol. Sci.* **1977**, *30*, 269.
[2] The Chemical Society of Japan 97 th Spring Annual Meeting, **2017**, 2C7-47.
[3] Forbec, E. M.; Evans, C. D.; Gilleran, J. A.; Li, P.; Joullié M. M. *J. Am. Chem. Soc.* **2007**, *129*, 14463.
[4] The Chemical Society of Japan 97 th Spring Annual Meeting, **2017**, 2C7-36.

Template for the abstract

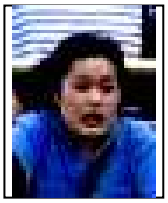

Hydrolysis of Organophosphates Catalyzed by Plussian Blue Analogs

Chihiro Terashima, Hiroyasu Tabe, Yusuke Yamada
Graduate School of Engineering, Osaka City University
3-3-138 Sugimoto Sumiyoshi-ku, Osaka-shi, 558-8585, JAPAN

Abstract: Prussian blue analogs ($M^N[M^C(CN)_6]$, M^N = $Fe^{II/III}$, Mn^{II}, Co^{II}, Ga^{III}, M^C = Fe^{II}, Co^{III}, Ru^{II}, Ir^{III}, Pt^{IV}) were examined as heterogeneous catalysts for hydrolysis of organophosphates. The catalytic activity of the Prussian blue analogs depends on not only M^N ions regarded as potential active sites but also M^C ions with coordinatively saturated structure.

【Introduction】

Removal of organophosphates used as agricultural chemicals has been strongly demanded, because organophosphates are listed as the 2nd cause of poisoning accidents in Japan. Organophosphates are currently removed by adsorbents such as activated carbon, however, complete removal of organophosphates at high concentration can be hardly achieved. Thus, catalytic decomposition of organophosphates is another promising method for removal of organophosphate. We report herein that Prussian blue analogs (PBAs, Fig. 1) exhibits catalytic activity for the hydrolysis of organophosphorus compounds.

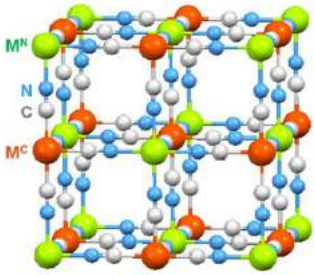

Fig. 1 Partial structure of

【Experiments】

Heterogeneous catalysis of each PBA was evaluated in a buffer solution containing 4-nitrophenylphosphate disodium salt and stirred at 60 ° C.

【Results】

Catalytic activity of various PBAs ($M^N[M^C(CN)_6]$, M^N = $Fe^{II/III}$, M^C = Fe^{II}, Pt^{IV}, Ir^{III}, Co^{III}, Ru^{II}) for hydrolysis of 4-nitrophenylphosphate (NPP) was compared based on the formation rates of 4-nitrophenol (NP) (Fig. 2). The initial reaction rates of 86, 6.9 , 5.6, 2.6 and 1.7 × 10^7 M s^{-1} for PBAs with M^C = Fe^{II}, Pt^{IV}, Ir^{III}, Co^{III} and Ru^{II}, respectively, depend on the M^C ions. The highest activity of Prussian blue (M^C = Fe^{III}) resulted from the higher oxidation sate of Fe ions at M^N sites in the mixed valence state.

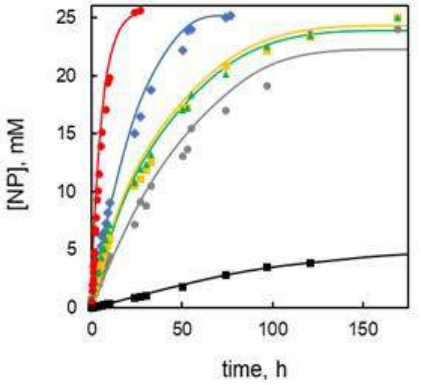

Fig. 2 Time profiles of NP production by hydrolysis of NPP (25 mM) catalyzed by $K_{0.1}[Fe^{III}(H_2O)_{1.4}]_{1.3}$-$[Fe^{II}(CN)_6]$ (●), $Fe^{II}_x[M^C(CN)_6]$ (M^C = Co^{III} (●), Ru^{II} (■), Ir^{III} (◆), Pt^{IV} (▲)) ([NPP]/[$Fe^{II/III}$] = 100) or no catalyst (■) in 2-[4-(2-hydroxyethyl)-1-piperazinyl]ethane-sulfonate buffer (0.75 mL, 100 mM, pH 8.2) at 60 °C.

Synthetic Study of Deoxyustiloxin D

Kenta Sakai, Yoko Yasuno, and Tetsuro Shinada
Graduate School of Science, Osaka City University
3-3-138 Sugimoto, Sumiyoshi, Osaka 558-8585, Japan

Ustiloxin D (**1**) is a unique class of unusual peptides which is characterized by the presence of a 13-membered cyclic core with an ether linkage.[1] This natural product reveals potent inhibitory activities against tubulin polymerization. Based on the X-ray analysis of ustiloxin D and tubulin complex,[2] we proposed that potent biological activity would be maintained in the designed analog **2**. In this presentation, we would like to report our synthetic efforts.

Fragments of **3**, **4**, and **5** were sequentially combined. The resulting acyclic molecule was subjected to macrocyclization reaction to provide **6**. Conversion of **6** via coupling reaction with **7** to provide the target analog **2** will be reported.

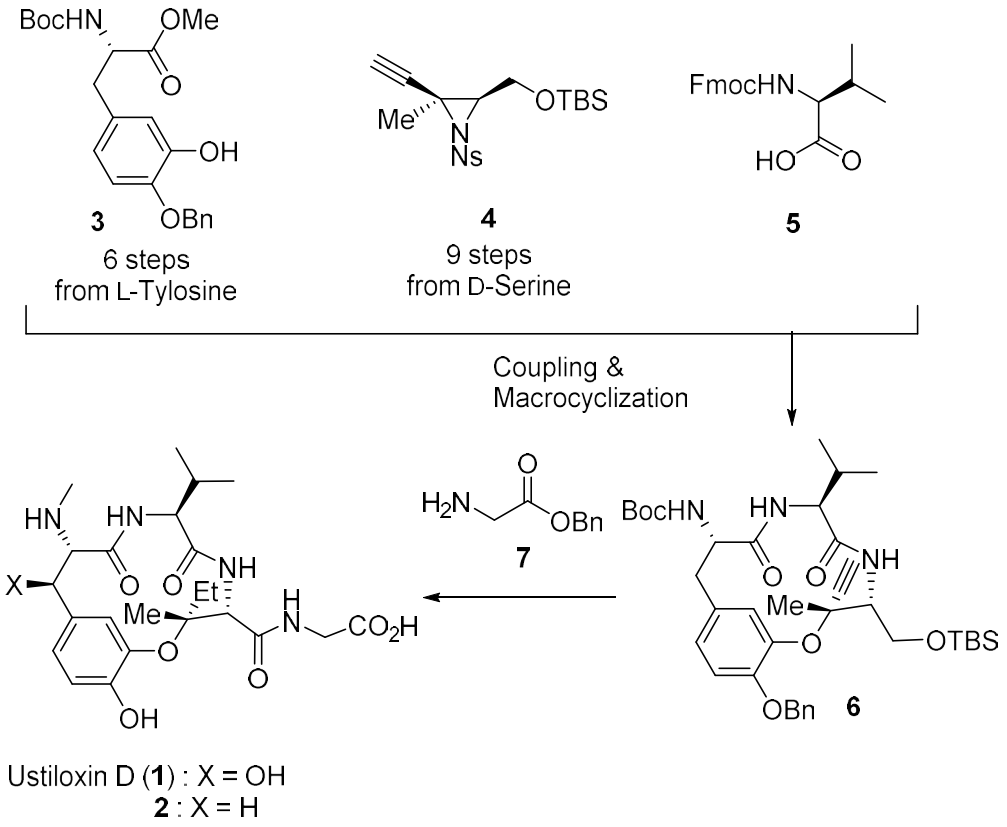

[1] Koiso, Y.; Natori, M.; Iwasaki, S.; Sato, S.; Sonoda, R.; Fujita, Y.; Yaegashi, H.; Sato, Z. *Tetrahedron Lett*. **1992**, *33*, 4157.
[2] Ranaivoson, F. M.; Gigant, B.; Berritt, S.; Joullié, M.; Knossow, M. *Acta Crystallogr. D* **2012**, *68*, 927.

Improvement of water permeability of a bone-regeneration scaffold by irradiating atmospheric pressure plasma jet

[1]Yuki Hamamoto, [1]Masato Oshiro, [2]Kumi Orita,
[2]Yoshihiro Hirakawa, [2]Hiromitsu Toyoda, and [1]Tatsuru Shirafuji
[1]Department of Physical Electronics and Informatics, Graduate School of Engineering, Osaka City University, Osaka, 558-8585 Japan
[2]Department of Orthopedic Surgery, Graduate School of Medicine, Osaka City University, Osaka, 545-8585 Japan

1. Introduction

An atmospheric pressure plasma jet (APPJ) employing dielectric barrier discharge of helium gas is known to be a source of "plasma bullets", which propagate in high-purity helium gas channels [1]. A plasma bullet propagates to the direction independent of gas-flow direction, and nicely separated when they encounter branches of gas channels. These unique features of "plasma bullets" may be used for the treatment of internal surfaces of an interconnected porous scaffold used in bone regeneration.

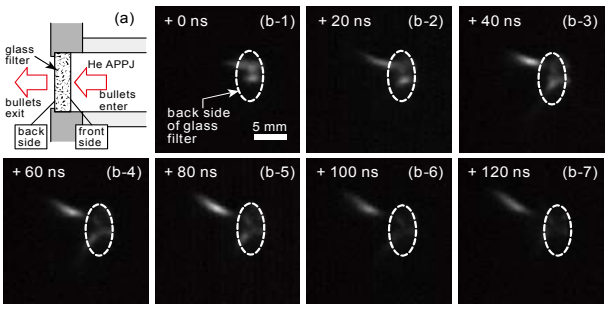

Fig. 1 Propagation of plasma bullets out of a glass filter.

2. Experimental procedure

We have irradiated a helium APPJ to a glass filter. The glass filter is used as a substitute of a scaffold made of expensive HA or β-TPC. The thickness and pore channel diameter of the glass filter are 3.15 mm and 160-250 μm. The scaffold was hydrophobic treated using fluorinated compounds before APPJ irradiation. Plasma bullets were injected from one side of the scaffold. We have expected that the bullets penetrate the scaffold and ejected from the other side of it.

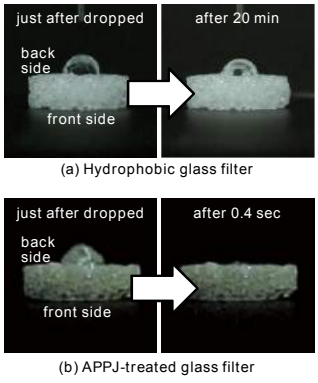

Fig. 2 Water permeability of the glass filter before and after the plasma-bullet treatment.

3. Results and discussion

Figures 1(b-1) to 1(b-7) show time-evolution of plasma bullets on the back side of the APPJ-irradiated glass filter, which indicates that the bullets penetrate the glass filter and exit from its back side. Figures 2(a) and 2(b) show that water permeability of the back side of the glass filter before and after the APPJ treatment. These results indicate that the internal surfaces of channels in the glass filter have become hydrophilic by propagation of plasma bullets through the scaffold.

References:

[1] M. Teschke, J. Kedzierski, E. G. Finantu-Dinu, D. Korzec, and J. Engemann, *IEEE Trans. Plasma Sci.* **2005**, 33, 310.

Characterization of damages in n-Si due to irradiation of Ar fast atom beams

Y. Matsumoto, K. Hisamoto, J. Liang and N. Shigekawa
Graduate School of Engineering
Osaka city University,Japan
Sugimoto 3-3-138,Sumiyoshi,Osaka 558-8585, Japan
a14tmX0E36@st.osaka-cu.ac.jp

Abstract:

Surface-activated bonding (SAB) technologies have widely been applied for bonding semiconductors[1]. The SAB process includes irradiation of Ar fast atom beams (FAB), which plays a role of activating surface of semiconductor. It is noted that damages are formed at the bonding interfaces by the FAB irradiation. The damages can be healed by annealing interfaces at low temperatures[2]. However, the temperature and duration of annealing are not yet optimized since they are likely to depend on the depth and density of damages[3].

We investigated the depth of damages due to irradiation of Ar FAB. Irradiated n-Si was etched by TMAH and Au/n-Si Schottky diodes were fabricated on unveiled Si surfaces. The acceleration voltage and irradiation time were 1.4 kV and 600 s, respectively. We measured current-voltage (I-V) and capacitance-voltage (C-V) characteristics of Schottky diodes. Figure 1 shows the dependence of Schottky barrier height (SBH) that were derivated from the I-V characteristics on the etching depth. We found that SBH was decreased from 0.75 to 0.63 eV by the FAB irradiation. SBH was recovered by etching the irradiated n-Si surfaces to a depth of ≈ 60 nm. We observed a similar relation in SBH obtained from the C-V measurement. Their results suggested that damages were formed in a ≈ 60–nm thick region of the n-Si surface and they lowered SBH of Au/n-Si junctions.

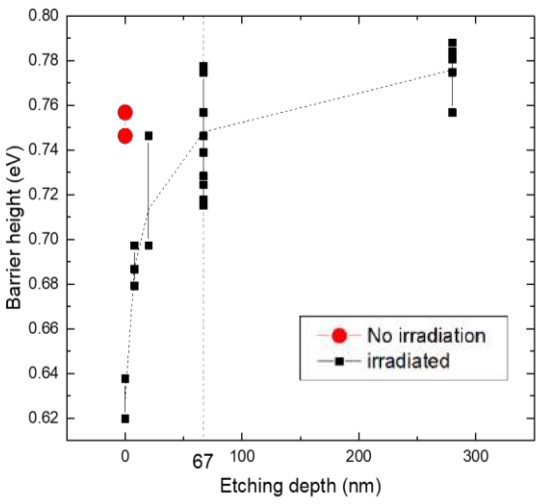

Fig.1 Relationship between Schottky barrier height obtained from I-V characteristics and etching depth.

References:

[1] J. Liang, et al. Jpn. J. Appl. Phys. **54**, 030211 (2015).

[2] S. Hisamoto, et al. IMFEDK, pp. 40-41 (2016).

[3] T. Seki, et al. Nucl. Instrum. Methods Phys. Res. B **164-165**, 650 (2000).

Synthesis and Properties of Soluble Bis(trioxytriphenylamine) Derivatives

Kento Shimode,[1] Shuichi Suzuki,[2] Masatoshi Kozaki,[1,3] Keiji Okada[1,3]

[1]*Graduate School of Science, Osaka City University*, [2]*Graduate School of Engineering Science, Osaka University,* [3]*Osaka City University Advanced Research Institute for Natural Science and Technology (OCARINA), Sugimoto, Osaka 558-8585.*

Abstract:

Generally, radical cation species of triphenylamine derivatives without *p*-substitutents are unstable and undergo dimerization because of the large spin density at the para-positions. We have designed and synthesized oxygen-bridged triphenylamine (trioxytriphenylamine: **TOT**). We sucessfully prepared its radical cation and radical-substituted **TOT** radical cations and clarified their unique magnetic properties. [1] More recently, we synthesized a **TOT**-dimer (**bisTOT**), and investigated magnetic properties of their dicationic species [2]. However, the radical cation species of **bisTOT** was difficult to obtain because of 1) the proximate first and second oxidation potentials (E_{OX}^1 = +0.10 V, E_{OX}^2 = +0.20 V, vs Fc/Fc^+, ΔE_{OX} = 0.10 V) and 2) low solubility of the neutral and dicationic species. In order to obtain insight into **TOT**-dimer radical cation species, we designed and synthesized **TOT**-dimers **1** and **2**. Compound **1** and **2** were prepared via long steps (6 and 7 steps with an overall yield of 12% and 9 %, respectively) from known 1-bromo-3-methoxy-5-pentylbenzene as a starting compound. Compound **1** and **2** exhibited good solubility in usual organic solvents such as CH_2Cl_2 and toluene. Compound **1** showed a larger separation of oxidation potentials (E_{OX}^1 = –0.03 V, E_{OX}^2 = +0.13 V vs Fc/Fc^+, ΔE_{OX} = 0.16 V) in benzonitrile compared with **bisTOT**. From the absorption spectra and ESR spectra in CH_2Cl_2, radical cation species of **1** and **2** were suggested to be in a mixed-valence state of Class II and Class II/III border, respectively. We could succesfully isolate radical cation $\mathbf{1}^{\bullet+}$ in a pure form.

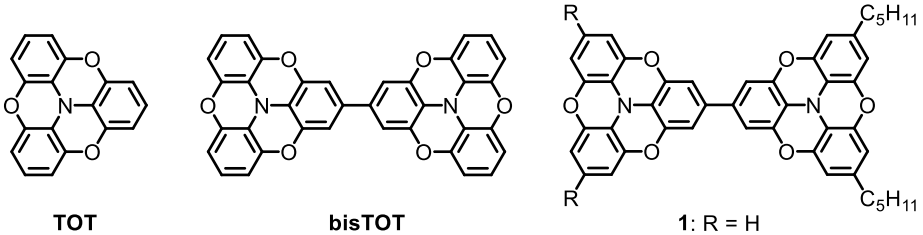

[1] Okada, K. et al. *Angew. Chem., Int. Ed.* **2005**, *44*, 4056–4058. Wang, X. et al. *J. Am. Chem. Soc*. **2013**, *135*, 14912–14915. Okada, K. et al. *Chem. –Asian. J.* **2012**, *7*, 1604–1609. Okada, K. et al. *Angew. Chem., Int. Ed.* **2012**, *51*, 3193–3197.

[2] Okada, K. et al. *Eur. –J. Chem.* **2017**, *23*, 16014–16025.

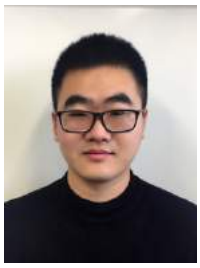

Identification of *S. pombe* genes involved in spore maturation

Bowen ZHANG[1], Yuhei TAHARA[1,2], Makoto MIYATA[1,2]
and Taro NAKAMURA[1,2]

1) Graduate School of Science, Osaka City University, Japan

2) The OCU Advanced Research Institute for Natural Science and Technology (OCARINA), Osaka City University, Japan

The fission yeast *Schizosaccharomyces pombe* form spores in response to nitrogen starvation. The spores are dormant cells with high resistance to various stresses, such as heat, digestive enzymes and organic solvents. Spore maturation is a result of significant cellular structure morphological changes, mainly including spore wall formation and simultaneous outer forespore membrane (FSM) autolysis. The spore wall is critical for resistance of spores to the external stresses and it is formed in the lumen of the FSM, a double layer compartment surrounding a spore. During spore maturation, the inner layer of the FSM becomes the future plasma membrane and the outer one disappears ultimately. By random mutagenesis, the *spoE22* strain was originally isolated as a mutant showing defect in the outer layer FSM autolysis. Under an electron microscope, the surface of the *spoE22* spores was also found to be abnormally smooth, without spike structure seen in wild type spores. This study demonstrated that this defect of outer FSM autolysis was caused by the absence of Meu5, an RNA binding protein whose expression is upregulated during meiosis [1, 2]. Meu5 binds to poly(A) domain, stabilizing the mRNAs of more than 80 target genes. To screen the genes that are directly involved in the outer FSM lysis, we observed the FSM of the strains in which the Meu5 target gene is disrupted. According to the observation result, several genes were supposed to be related to outer FSM autolysis.

1. Amorim M.J.; Cotobal C; Duncan C; Mata J. Global coordination of transcriptional control and mRNA decay during cellular differentiation. *Molecular Systems Biology* **2010,** 6:380

2. Watanabe T.; Miyashita K.; Saito T.T.; Yoneki T.; Kakihara Y.; Nabeshima K.; Kishi Y.A.; Shimoda C.; Nojima H. Comprehensive isolation of meiosis-specific genes identifies novel proteins and unusual non-coding transcripts in *Schizosaccharomyces pombe*. *Nucleic Acids Research* **2001**, 29(11): 2327-2337.

The Short Step Synthesis and Properties of Triazapyrene Derivatives

Yuta Omura,[1] Yoshimitsu Tachi,[1] Keiji Okada,[1,2] Masatoshi, Kozaki[1,2]

[1]Graduate School of Science, Osaka City University, [2]Osaka City University, Advanced Research Institute for Natural Science and Technology (OCARINA)

Abstract: Introducing multi-nitrogen atoms into polycyclic aromatic hydrocarbons is effective methods for developing novel n type organic semiconductors. However, there are limited number of reports of nitrogen-rich polycyclic aromatic compounds due to the lack of an effective synthetic method. In our research, using pyrene as a framework, we developed a short step synthetic method for triazapyrene derivatives that involves Pd-catalyzed cross-coupling reactions via C–H activation and Cu-catalyzed annulation reactions.[1]

Scheme 1. Synthesis of triazapyrene **1**

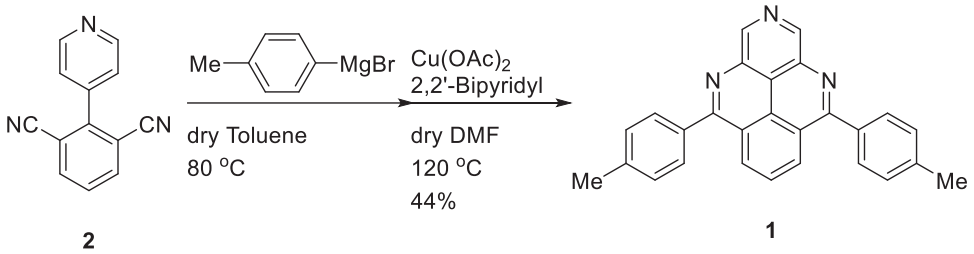

2 **1**

The direct palladium-catalyzed C–H substitution was carried out using 1,3-dicyanobenzene and 4-bromopyridine hydrochloric acid salt to afford 4-(2,6-dicyanophenyl)pyridine (**2**). The reaction of **2** with Grignard reagents and the Cu-catalyzed C-N bond formation produced **1** in 44% yield (Scheme 1). Both absorption and emission bands of triazapyrene **1** with three pyridine rings observed in longer wavelength region compared to the corresponding bands of pyrene. While reduction wave of pyrene was not observed, triazapyrene **1** shows reversible reduction waves at –1.94 V vs Fc/Fc^+. Crystal structural analysis establishes that the large dihedral angles between the pyrene core and the *p*-tolyl group (51° and 59°) and the planar pyrene cores have π-stack packing. The detailed synthesis and properties of triazapyrene derivatives will be reported.

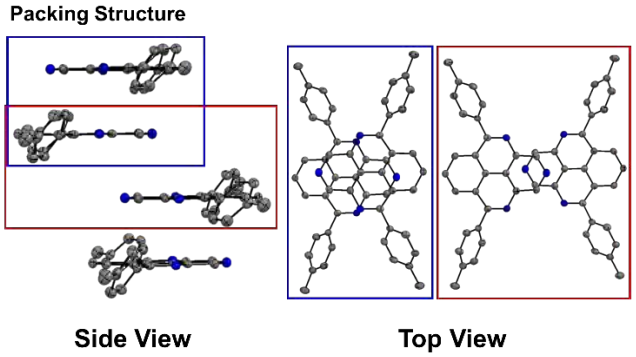

Figure 1. Packing structure of triazapyrene **1**

[1] Ihanainen, N. E.; Kumpulainen, E. T. T.; Koskinen, A. M. P. *Eur. J. Org. Chem*. **2015**, 3226–3229. Zhang, L.; Ang. G. Y.; Chiba, S. *Org. Lett*. **2010**, *12*, 3682–3685.

Visible light-driven carbon-carbon bond formation from CO_2 as a feedstock with the system containing malic enzyme and dye

Takayuki Katagiri[1], Shusaku Ikeyama[2], Yutaka Amao[1,2,3]
[1]*Graduate School of Science, Osaka City University,*
[2]*The Advanced Research Institute for Natural Science and Technology, Osaka City University*
[3]*Research Center for Artificial Photosynthesis (ReCAP), Osaka City University*

Recently, solar energy based CO_2 utilization technologies including artificial photosynthesis have been received much attention. As one of these technologies, CO_2 conversion system consisting of photosensitizer and catalyst were constructed. To use CO_2 as a feedstock, effective catalyst for carbon-carbon bond formation from CO_2 is required. For example, malic enzyme (ME) catalyzes a reaction of introducing CO_2 as a carboxy group to pyruvate (C3 compound) to form malate (C4 compound) *via* oxaloacetate in the presence of natural co-enzyme NADPH. More recently, we reported that multi-electron reduced form of diphenylviologen (PV) act as an artificial co-enzyme for ME [1,2].

In this study, novel water soluble viologen, 1,1'-bis(*p*-sulfonatophenyl)-4,4'-bipyridiniu dichloride (PSV) based on PV, was synthesized as an artificial co-enzyme for ME. The electrochemical and photoreduction properties of PSV were investigated. Quenching of photoexcited state of water soluble zinc porphyrin (ZnP) was also studied using fluorescence spectroscopy. In addition, PSV was applied for visible light-driven oxaloacetate and malate production system.

The first and second reduction potential of PSV were -0.38 and -0.72 (*vs* Ag/AgCl), respectively. The photoreduction properties of PSV in the visible light-irradiation with photosensitization of ZnP. As a result of photo-irradiation, the absorption maximum at 650 and 710 based on two-electron reduced form of PSV (PSV^0) was increased with irradiation time. When a sample solution containing triethanolamine (TEOA), water soluble porphyrin (P), PSV, pyruvate, Mg^{2+} and ME in CO_2 saturated pH 7.4 bis-tris buffer was irradiated with visible-light, oxaloacetate and malate were produced. Thus, visible light-driven carbon-carbon bond formation system was constructed with ME and PSV.

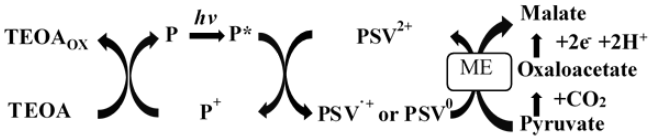

Fig.1 Visible light-driven malate production from pyruvate and CO_2 *via* oxaloacetate with ME.

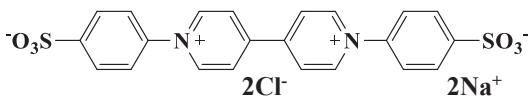

Fig.2 Chemical structure of 1,1'-bis(*p*-sulfonatophenyl)-4,4'-bipyridinium salt

[1] Y. Amao, S. Ikeyama, T. Katagiri, K. Fujita, *Faraday Discuss.*, **2017**, 198, 73
[2] T. Katagiri, S. Ikeyama, Y. Amao, *J. Photochem. Photobiol. A*, **2018** *in press*

Allosteric effect of a zinc porphyrin receptor with sterically bulky shielding units

Tomoaki, Nishimura;[1] Yoshito, Sasaki; [1] Yoshimitsu, Tachi; [1] Keiji, Okada; [1,2] Masatoshi, Kozaki[1,2]

[1]Graduate School of Science, Osaka City University, [2]Osaka City University, Advanced Research Institute for Natural Science and Technology (OCARINA)

Abstract: Artificial allosteric systems are attractive as intelligent receptors and biomimetic catalysts. Only a few studies have been reported allosteric systems using organic molecules as external sitmuli[1]. We prepared zinc porphyrin receptor **1** with sterically bulky shielding units (**HPhB**) to allosterically regulate ligand-binding ability using chemical stimuli. Receptor **1** recognizes a specific guest molecule through multiple supramolecular binding sites. The formation of **1•2** would reduce the binding constant between diethynylporphyrin (**DEP**) and 4-phenylpyridine (**PhPy**) because of the shielding of **DEP** by **HPhB**.

UV-vis spectral titration in toluene suggested that **1** and **2** formed stable 1:1 complex **1•2** through hydrogen bonds between a diamidopyridine (**DAP**) and uracil (**U**) unit and coordination bonds between tetraphenylporphyrin (**TPP**) and pyridine units (**Py**). The binding constant between **DEP** in **1•2** and **PhPy** was 0.089 times smaller than that between **1** and **PhPy**. These results suggest that ligand-binding ability of **DEP** in **1** was allosterically inhibited by the formation of **1•2**. We will present molecular design and the allosteric effect in detail.

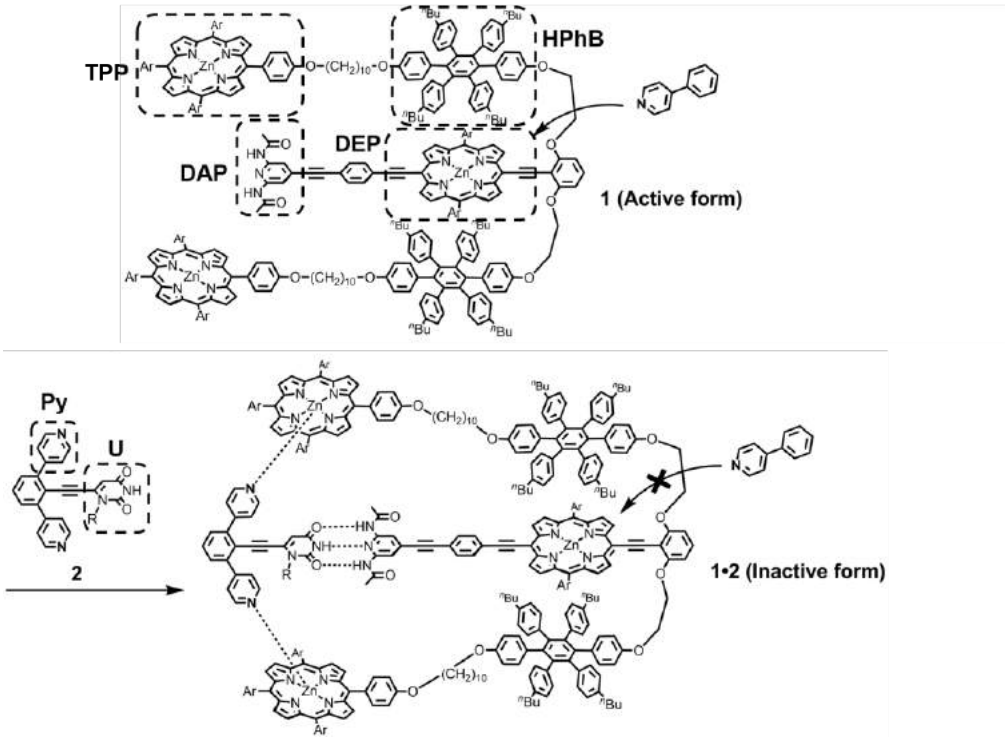

References

[1] Sasaki, Y.; Suzuki, S.; Okada, K.; Kozaki, M. *Tetrahedron Lett*. **2016**, *57*, 4082–4085.

Fabrication of semiconductor/patterned metal layer junctions

T. Hishida, S. Kohno, J. Liang, and N. Shigekawa
Graduate School of Engineering
Osaka City University
Sugimoto 3-3-138, Sumiyoshi, Osaka 558-8585, Japan
E-mail: a14tme0g29@ex.media.osaka-cu.ac.jp

Abstract:

III-V-on-Si multijunction solar cells are promising as high-efficiency and low-cost photovoltaics. We previously fabricated InGaP/GaAs//Si triple-junction cells by using surface-activated bonding (SAB) and achieve a high efficiency (~26%) [1]. However, it was found that damages were introduced to the bonding interface by Ar beam irradiation in the surface-activating process. This led to the increase in the interface resistance [2]. A practical solution is likely to be provided by using patterned ohmic metal with passivation layer on the Si bottom cells.

In this work, we successfully fabricated a p^+-Si // patterned Al with SiO_2 / p^+-Si junction by SAB of a p^+-Si substrate and a patterned Al layer and a subsequent annealing (500℃ 1hour). The resistivity of p^+-Si substrate was 0.002-0.005 Ω·cm. A schematic cross section and a scanning electron microscope (SEM) image of the junction are shown in Fig. 1 and 2, respectively. Figure 3 shows the current-voltage (*I-V*) characteristics of the junction. Excellent ohmic properties were confirmed.

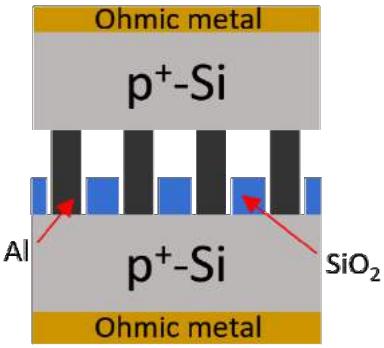

Fig.1. A schematic cross section of a p^+-Si/patterned Al with SiO_2/p^+-Si junction.

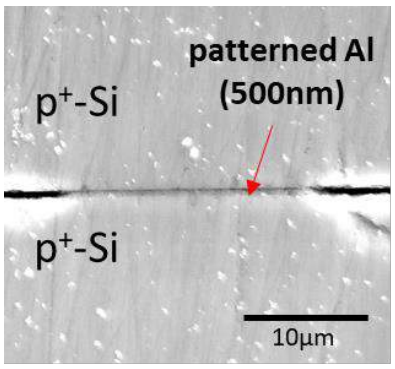

Fig. 2. An SEM image of a p^+-Si/patterned Al with SiO_2/p^+-Si junction.

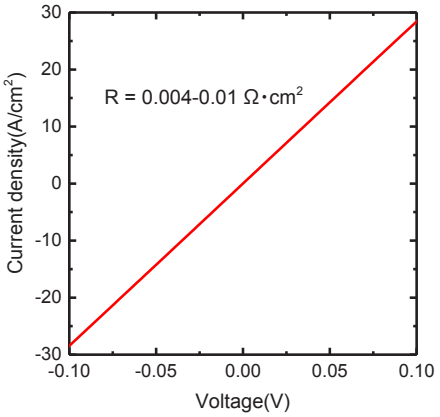

Fig. 3 *I-V* characteristics of a p^+-Si/patterned Al with SiO_2/p^+-Si junction.

References:

[1] N. Shigekawa, et al. Jpn. J. Appl. Phys. **54**, 08KE03 (2015).

[2] J. Liang, et al. Jpn. J. Appl. Phys. **54**, 030211 (2015).

Analysis of neural connection between pineal organ and some brain regions in zebrafish

Makomo Kakiya[1], Seiji Wada[1], Emi Kawano-Yamashita[1], Mitsumasa Koyanagi[1, 2], Akihisa Terakita[1, 2]

[1]Department of Biology and Geosciences, Graduate School of Science, Osaka City University, Osaka, Japan; [2]OCARINA, Osaka City University, Osaka, Japan

Many lower vertebrates capture light not only with eyes but also with pineal organs, which are known as a melatonin-secretion organ in mammalian brains. Interestingly, pineal organs of teleosts can detect wavelength of lights in addition to light intensity. Several lines of evidence suggested that pineal photoreceptive pigments, exorhodopsin and parapinopsin are localized in different cells and are involved in the intensity detection and the wavelength discrimination, respectively [1, 2]. Because previous studies suggest that neural responses of the photoreceptor cells transmit to the brain, analyses of neural projection of the photoreceptor cells via ganglion cells is important to speculate physiological functions of the pineal photoreception.

Previous histological studies by anterograde-tracing suggested that light information captured by the pineal photoreceptor cells might transmit into the several regions of brain including mesencephalon via ganglion cells in zebrafish. However, it has not been uncovered whether light information about the wavelength discrimination transmits to the regions. In this study, we tried histological analysis to identify regions which the pineal photoreceptor cells expressing parapinopsin project to, with some kinds of transgenic zebrafish.

[1] Kawano-Yamashita E.; Koyanagi M.; Terakita A. *Springer* **2014**, 1-21

[2] Koyanagi M.; Kawano E.; Kinugawa Y.; Oishi T.; Shichida Y.; Tamotsu S.; Terakita A. *Proc. Natl. Acad. Sci. USA* **2004** 6687-91.

Photocatalytic activity of gallium oxynitride for H_2 evolution under visible light irradiation

Yuma Kato[1], Muenaki Yamamoto[2], Akiyo Ozawa[1]and Tomoko Yoshida[3]

[1] *Graduate School of Engineering, Osaka City University*
[2] *Graduate School of Engineering, Nagoya University*
[3] *Advanced Research Institute for Natural Science and Technology, Osaka City University*

Recently, we found that gallium oxide (Ga_2O_3) showed photocatalytic activity for water splitting reaction under ultra violet light irradiation [1]. In order to generate visible light response in Ga_2O_3 photocatalysts, we tried nitriding Ga_2O_3 in our previous study, however, H_2 evolution reaction did not proceed over the nitrided Ga_2O_3. In this study, gallium oxynitride (GaON) samples were prepared by nitriding gallium oxide hydroxide (GaOOH) and we examined whether GaON samples promote H_2 evolution from an aqueous methanol solution under visible light irradiation.

GaOOH powder was obtained by autoclaving gallium nitrate aqueous solution at 120 ℃ for 6 h followed by filtration and drying. Nitriding of GaOOH was performed by calcination under NH_3 flow. Detailed nitriding conditions are summarized in Table 1.

Diffuse reflectance spectra (DRS) indicated that absorption bands appeared in the visible light region after nitriding (Fig.1). N K-edge XANES and N 1s XPS spectra of the prepared samples showed the peaks attributed to nitrogen species and the peaks became sharper with higher nitriding temperatures. These results suggested that prepared samples actually contained nitrogen. In XRD measurement of the prepared samples, as nitriding temperature exceeded 973 K, gallium nitride (GaN) phase started to appear, and the samples had higher crystallinity with higher nitriding temperature. Similar results were obtained from the Ga K-edge EXAFS measurement. H_2 evolution reactions using prepared samples were performed under visible light irradiation (λ>420 nm).This reaction did not proceed over GaN reference sample while the sample (e) promoted H_2 evolution.

Table 1. Nitriding condition of GaOOH

Entry	temp (K)	time (h)	NH_3 flow rate (mL/min)
(a)[1]	-	-	-
(b)	773	15	60
(c)	873	15	60
(d)	973	15	60
(e)	1073	15	60
(f)	1173	15	60
(g)[2]	-	-	-

[1]GaOOH, [2]GaN (reference samples)

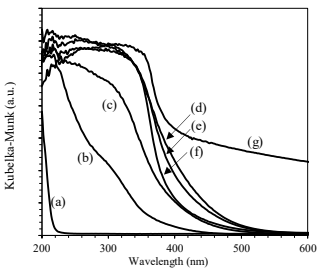

Figure 1. DRS spectra of prepared samples (a-g) the samples described in Table 1.

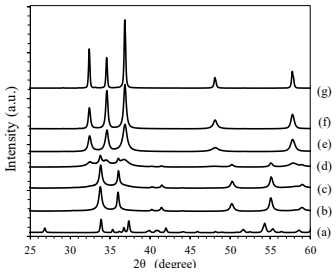

Figure 2. XRD patterns of prepared samples (a-g) the samples described in Table 1.

[1] M. Akatsuka, T. Yoshida, N. Yamamoto, M. Yamamoto, S. Ogawa, S. Yagi, *J. Phys. Conf. Ser.* **2016,** 712, 012056.

Estimating spectral sensitivities of various opsins based on biochemical responses of cultured cells expressing opsins

Tomohiro Sugihara[1], Takashi Nagata[1], Benjamin Mason[2], Mitsumasa Koyanagi[1,3], Akihisa Terakita[1,3]

[1]Department of Biology and Geosciences, Graduate School of Science, Osaka City University, Osaka, Japan; [2]Department of Genetics, Stanford School of Medicine, Stanford University, Stanford, CA, United States; [3]OCARINA, Osaka City University, Osaka, Japan

Many animals capture light information by light sensitive proteins, opsins for various photoreceptive functions. Thousands of opsins have been identified from ocular and extraocular tissues of a wide variety of vertebrates and invertebrates. Spectral sensitivity of the opsin provides basic and important information to speculate its relevant physiology but spectral characteristics of not a few opsins still unknown. Basically, we express opsins in cultured cells and obtain functional recombinant opsin-based pigments. However, lower expression level of opsins often limits to analyze their spectral sensitivities by spectroscopic method.

We recently focused on a light-induced second messenger change in cultured cells and have succeeded in quantitatively analyzing wavelength-dependent cAMP changes in cultured cells expressing opsins even in their low expression level. In this study, we showed that the method based on cAMP changes is useful to obtain spectral sensitivities of opsins of which absorption spectra have been unknown [1].

[1] Sugihara, T.; Nagata, T.; Mason, B.; Koyanagi, M.; Terakita, A. *PLoS One* **2016**, 11(8)

Contribution of parapinopsin “bistability” to light-responses in the zebrafish pineal organs

Baoguo Shen[1], Seiji Wada[1], Emi Kawano-Yamashita [1], Mitsumasa Koyanagi[1, 2], Akihisa Terakita[1, 2]

[1]Department of Biology and Geosciences, Graduate School of Science, Osaka City University, Osaka, Japan; [2]OCARINA, Osaka City University, Osaka, Japan

Pineal-related organs in lower vertebrates can discriminate UV and visible lights. We previously found that a pineal-specific opsin, parapinopsin, which serves as a UV -sensitive pigment in the wavelength discrimination [1-3]. Parapinopsin has a unique molecular property called “bistable nature” different from that of visual opsin: upon UV-light absorption, parapinopsin converts to a stable photoproduct, which reverts to the dark state upon subsequent visible light absorption. This bistable nature is never found in vertebrate visual opsins of which photoproduct is unstable [1] and therefore has been considered to contribute to the photoregeneration of opsins in photoreceptor cells. In order to obtain a clue to understanding a contribution of the bistable nature to photoreceptor cell responses in the wavelength discrimination, we established a mutant zebrafish, which expresses UV-sensitive visual opsin instead of parapinopsin in the pineal photoreceptor cells. We performed calcium imaging for the pineal organ of the mutant and wild-type zebrafish with a multiphoton microscope. The result suggested that the bistability of parapinopsin contributes to the pineal color opponency. In addition, we discussed effect of parapinopsin bistability on photoreceptor sensitivity under strong light conditions.

[1] Koyanagi, M.; Kawano, E.; Kinugawa, Y.; Oishi, T.; Shichida, Y.; Tamotsu, S.; Terakita, A. *PNAS* **2004**, 101, 6687-6691.
[2] Wada, S.; Kawano-Yamashita, E.; Koyanagi, M.; Terakita, A. *PLoS One* **2012**, e39003.
[3] Koyanagi, M.; Wada, S.; Kawano-Yamashita, E.; Hara, Y.; Kuraku, S.; Kosaka, S.; Terakita, A. *BMC biology* **2015**, 13, 73.

Effects of micro-bubble assistance on the performance of 3D integrated micro solution plasma

Reiya Nakagawa, Hiroto Masunaga, Yodai Ishida,
and Tatsuru Shirafuji
Department of Physical Electronics and Informatics,
Osaka City University, 3-3-138 Sugimoto, Sumiyoshi-ku, Osaka, 558-8585 Japan

1. Introduction

Plasma in liquid has attracted much attention because of their possible applications for solving water-related environmental issues. We have previously proposed a novel three-dimensionally integrated micro solution plasma (3D IMSP) reactor, which can generate a large number of microplasmas in a porous dielectric material filled with a gas/liquid mixed medium [1]. However, 3D IMSP is not effective for the treatment of an aqueous solution with a high electrical conductivity [2], which was one of disadvantages of 3D IMSP. In this work, we have introduced micro bubbles into the 3D IMSP reactor in order to treat water with higher electrical conductivity.

2. Experimental procedure

We employed micro-bubble generator (Hack UFB, FB11) as a substitute of the liquid circulation pump used in our previous 3D IMSP reactor [1], in which the circulation speed is faster than in conventional 3D IMSP. The aqueous solutions used for this experiment had electrical conductivities of 1, 10, 100, 200, 500, and 1000 μS/cm, which were prepared by mixing KCl with deionized water and methylene blue.

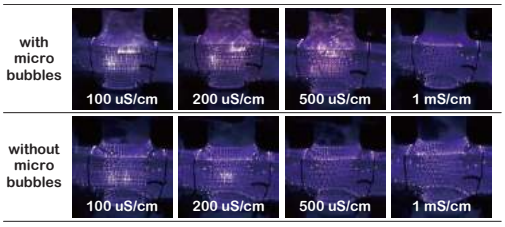

Fig. 1 Effects of micro-bubble assistance on the operation of 3D IMSP.

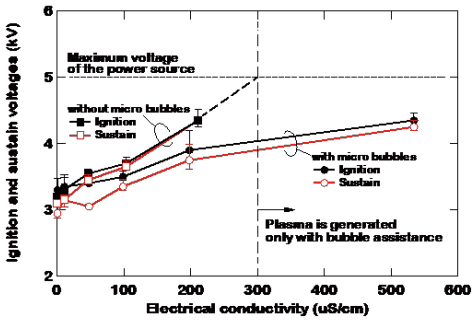

Fig. 2 Effects of micro-bubble assistance on the ignition and sustain voltages of 3D IMSP.

3. Results and discussion

As shown in Fig. 1, we can confirm that the micro-bubble assisted 3D IMSP reactor can generate plasma in the aqueous solution with electrical conductivity up to 500 μS/cm, while conventional 3D IMSP cannot. Furthermore, micro-bubble assistance has an effect of reducing the ignition and sustain voltages of 3D IMSP as shown in Fig. 2. Although the results are not shown here, we have confirmed that micro-bubble assisted 3D IMSP can decompose methylene blue without reducing decomposition efficiency.

References:

[1] T. Shirafuji and Y. Himeno, *Jpn. J. Appl. Phys.* **2013**, 52, 11NE03.
[2] T. Shirafuji, J. Ueda, A. Nakamura, S.-P. Cho, N. Saito, and O. Takai, *Jpn. J. App. Phys.* **2013**, 52, 126202.

Template for the abstract

Effect of nitrogen codoping on strontium doped $NaTaO_3$

Akiyo Ozawa[1,2], Keita Kobayashi[2], Muneaki Yamamoto[3], Tomoko Yoshida[4]

1 Applied Chemistry and Bioengineering, Graduate School of Engineering, Osaka City University, 3-313-8, Sugimoto, Sumiyoshi-ku, Osaka, Japan

2 Corporate Research Laboratories, Research & Development Division, Sakai Chemical Industry, Co., Ltd., 5-1, Ebisujima-cho, Sakai-ku, Sakai, Japan

3 Materials, Physics and Energy Engineering, Graduate School of Engineering, Nagoya University, Furo-cho, Chikusa-ku, Nagoya, Japan

4 Osaka City University Advanced Research Institute for Natural Science and Technology, 3-313-8, Sugimoto, Sumiyoshi-ku, Osaka, Japan

For potential applications in environmental protection and solar energy conversion, heterogeneous photocatalytic reactions over semiconductor surfaces have been researched. Among them, $NaTaO_3$ having perovskite crystal structure was reported to provide high photocatalytic activity under UV light irradiation. For example, Sr doped $NaTaO_3$ modified by Ag nanoparticles can reduce CO_2 to CO with high efficiency [1]. However, the band gap of $NaTaO_3$ is too large to proceed photocatalytic reactions under visible-light irradiation. Most solar energy is concentrated in the visible light region, therefore, from the perspective of effective utilization of sun light, many oxides/ complex oxides have been improved to use visible light. Nitrogen doping of oxides or complex oxides has been reported to be an effective method for allowing the use of visible light. However, high concentration nitrogen doping into $NaTaO_3$ by thermal treatment in ammonia atmosphere was rarely achieved [2]. Zhao et al reported that $NaTaO_3$ doped with La can proceed to dope nitrogen, La-N co-doping into $NaTaO_3$ exhibited high activity for reduction of water in the presence of methanol solution as a scavenger [3]. However, the role of cation doping in nitrogen doping was not well understoodSr content in the sample. In this study, we synthesized nitrogen strontium codoped $NaTaO_3$ by solid state process and investigated effects of synthesis condition on the chemical state of doped nitrogen. In calcination at 1073 K in NH_3, the Sr- N codoped sample in which the Na site was substituted by 50 mol% of Sr contained 2 crystalline phase, $NaTaO_3$ and $Sr_2Ta_2O_7$. On the other hand, in calcination at 1223 K in NH_3, the sample maintained the crystal structure of $NaTaO_3$ even if containing 50 mol% Sr ion . As the amount of Sr doping increased, Sr-N codoping into $NaTaO_3$ inhibited generation of Ta_3N_5 in calcination under NH_3 and enhanced nitrogen doping into $NaTaO_3$.

References:

[1] H. Nakanishi, K. Iizuka, T. Takayama, A. Iwase, A. Kudo, ChemSusChem **2017**, 10, 112.

[2] X. Wang, G. Liu, Z. Chen, F. Li, G. Q. Lu, H. Cheng, Chem. Lett. **2009**, 38 (3), 214.

[3] Z. Zhao, R. Li, Z. Li, Z. Zou, J. Phys. D: Appl. Phys. **2011**, 44, 165401.

Template for the abstract

Effects of Ga_2O_3 structure on the CO_2 reduction with water over Ga_2O_3 photocatalyst

Yu Kawaguchi[1], Muneaki Yamamoto[2], AkiyoOzawa[1], Yuma Kato[1], Kokoro Yoshioka[1], Tetsuo Tanabe[3] and Tomoko Yoshida[3]

[1]*Graduate School of Engineering, Osaka City University, Osaka, Japan*

[2]*Graduate School of Engineering, Nagoya University, Nagoya, Japan*

[3]*Advanced Research Institute for Natural Science, Osaka City University, Osaka, Japan*

Abstract: Gallium oxide photocatalyst (Ga_2O_3) has been the focus of attention, because it can convert CO_2 and water into CO, H_2 and O_2 under UV light irradiation. Recently, we revealed that a Ga_2O_3 photocatalyst prepared by calcining a gallium nitrate powder at around 800 K showed much higher activity for CO production than an Ag loaded β-phase Ga_2O_3, and the Ga_2O_3 had the crystalline structure of mixed phases of γ- and β- Ga_2O_3 [1]. However, the reason for high activity of this Ga_2O_3 has not been revealed yet. In this study, we investigated that the reason for high activity for the Ga_2O_3 with mixed phases of γ- and β-phase.

Ga_2O_3 prepared by calcination of gallium nitrate powder for 4 h in air at 773 K. Fig.1 shows time course of CO production rate in the photocatalytic reduction of CO_2 with water over the Ga_2O_3, and Fig. 2 shows XRD patterns for this Ga_2O_3 before and after 1 h, 3 h and 5 h reaction test. As shown these figures, the photocatalytic activity of this Ga_2O_3 increased with time, and GaOOH phase formed and grew in this Ga_2O_3. The Ga_2O_3 introduced GaOOH in advance (Ga_2O_3-3wL) showed higher CO production activity than that of only Ga_2O_3 (Fig. 3), indicating that the presence of GaOOH enhanced CO production. On the other hands, the activity of single phase of GaOOH was low (shown in Fig. 3), suggesting the mixed phases of γ, β-phase Ga_2O_3 and GaOOH is important to have high activity. FT-IR measurement revealed that CO production would be enhanced with the increased CO_2 adsorption on GaOOH phase.

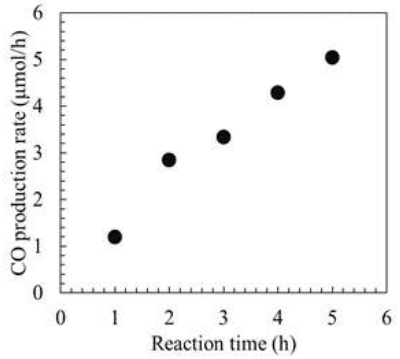

Fig. 1 Time course of CO production rate for Ga_2O_3.

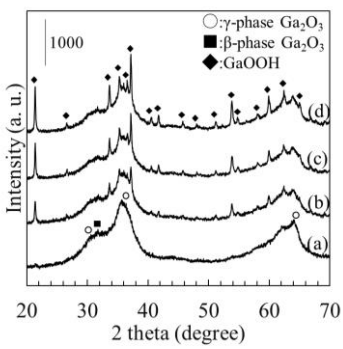

Fig. 2 XRD patterns of Ga_2O_3 (a) before and after (b) 1 h, (c) 3 h and (d) 5 h reaction.

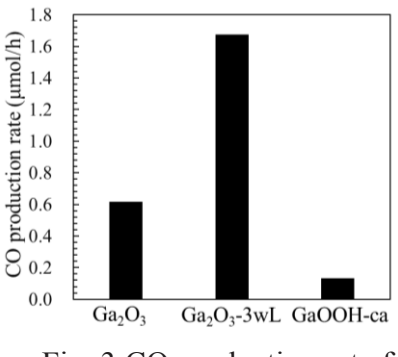

Fig. 3 CO production rate for Ga_2O_3, Ga_2O_3-3wL and commercial available GaOOH (GaOOH-ca) after 5 h reaction.

References: [1] Kawaguchi. Y.; Akatsuka. M.; Yamamoto. M.; Yoshioka. K.; Ozawa. A.; Kato. Y.; Yoshida. T. *J Photochem. Photobiol. A Chem.* **2017**.

The Allosteric Receptor Containing a Zn-porphyrin and a Recognition Site for a Photo-responsive Stimulus Molecule

Chisato Okamoto,[1] Yoshimitsu Tachi,[1] Shuichi Suzuki,[2] Keiji Okada,[1,3] Masatoshi, Kozaki[1,3]

[1]Graduate School of Science, Osaka City University, [2]Graduate School of Engineering Science, Osaka University [3]Osaka City University, Advanced Research Institute for Natural Science and Technology (OCARINA)

Abstract: Artificial allosteric systems with molecular recognition sites are attracting much attention because of the possible applicability to intelligent catalysts and sensors.[1] Here, we designed **1** and **2** as an allosteric receptor and a photo-responsive stimulus molecule, respectively. Receptor **1** has a zinc diethynyldiphenylporphyrin unit (**DEDPP**) as an active site and a diamidopyridine (**DAP**) and zinc tetraphenylporphyrin terminals (**TPP**) as molecular recognition sites. Stimulus molecule **2** has both a pyridinyl (**Py**) and uracil terminals (**U**). Receptor **1** is able to form a 1:1 complex with *trans*-**2** by **DAP**-**U** multiple hydrogen bonds or a **TPP**-**Py** coordination bond. A ligand is still accessible to **DEDPP** in this 1:1 complex (**Active form**). On the other hand, *cis*-**2** can form a 1:1 tight complex with receptor **1** by the concomitant formation of the coordination and the multiple hydrogen bonds. Consequently, a bulky hexaphenylbenzene unit is fixed close to **DEDPP** and the ligand-binding ability of the zinc porphyrin center is allosterically suppressed (**Inactive form**).

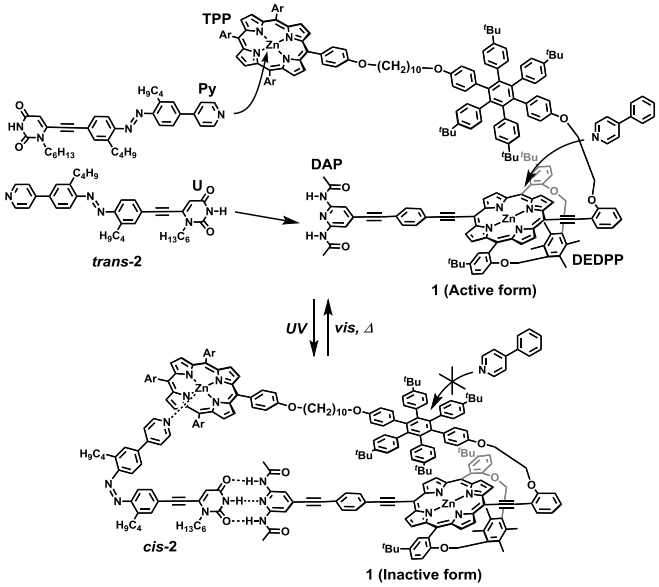

Allosteric receptor **1** was prepared in 32% yield by linking an alkyl chain **3** to a linear conjugated chain **4** under the conditions of the Williamson ether synthesis. UV-vis spectra in toluene suggested that **2** reversibly isomerized using UV light (365 nm) and visible light (470 nm). Both the formation of **1**•*cis*-**2** and the inhibition of ligand-binding ability of **DEDPP** were monitored by UV-vis absorption measurement. The detailed synthesis and properties of these compounds will be presented.

Scheme 1. Synthesis of allosteric receptor **1**.

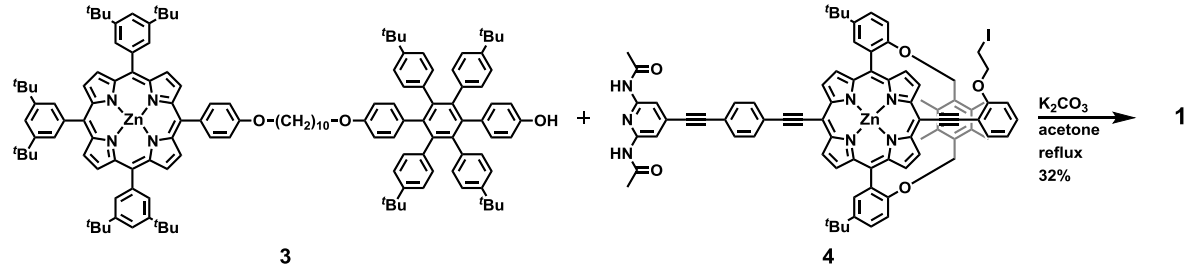

[1] Sasaki, Y.; Suzuki, S.; Okada, K.; Kozaki, M. *Tetrahedron Lett.* **2016**, *57*, 4082–4085.

Template for the abstract

YgiT, antitoxin of *mqsR-ygiT* TA system, enhances motility and biofilm formation in *Escherichia coli*

Ryoma Yokoi[1] and Yoshihiro Yamaguchi[1,2]

[1]*Department of Biology, Graduate school of Science, Osaka City University*

[2]*The OCU Advanced Research Institute for Natural Science and Technology (OCARINA)*

Abstract:

All free-living bacteria contain toxin or suicide genes, which regulate cell growth and cell death, reminiscent of the programmed cell death or apoptosis in mammalian cells. These toxin genes are co-transcribed with their cognate antitoxin genes and thus the systems are referred to as the toxin-antitoxin (TA) systems. Although prolonged induction of a toxin causes eventual cell death, it causes pseudo-dormancy to the cells, in which all cellular metabolic function are maintained intact. Dormancy of the cells caused by TA toxins is considered to play important roles in biofilm formation. Bacterial biofilms have a definitive role in medical device-associated diseases and also mediate resistance to antibiotics and phagocytosis. MqsR is potent toxin encoded by the *mqsR-ygiT* TA system in *Escherichia coli*. Although it has been reported that MqsR causes an eight-fold induction of biofilm formation and that it also causes the activation of a two-component system, the *qseB-qseC* operon, which is known to play an important role in biofilm formation, MqsR has been shown to function as an mRNA interferase specific for GCU sequences.

Here, we show that overproduction of YgiT antitoxin in the cell increases cell motility and biofilm formation, indicating that YgiT antitoxin by itself is able to directly act as a regulator for motility and biofilm formation (Fig. 1). We analyzed the amount of flagellin and curli fimbriae involved in cell motility. It was suggested that the over production of YgiT significantly repressed the expression of curli fimbriae but not flagellin. Since YgiT itself can bind to the palindromic sequences in its own promoter region similar to the MqsR-YgiT complex, it is possible that YgiT itself functions as a regulator binding to the promoter regions to repress or activate some genes leads to enhance cell motility and biofilm formation. We are screening the gene(s) enhancing cell motility after induction of YgiT.

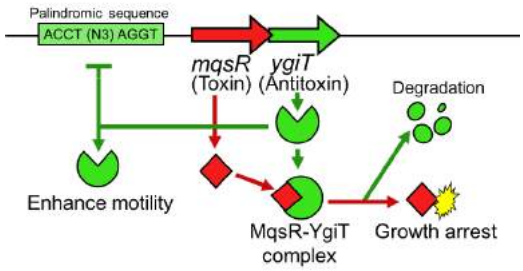

Fig. 1 : MqsR-YgiT toxin-antitoxin system

Selective formate reduction catalyzed with aldehyde dehydrogenase using artificial co-enzyme based on reduced form of methylviologen

Tomoya Ishibashi[1], Shusaku Ikeyama[2], Yutaka Amao[1,2]

[1]*Graduate School of Science, Osaka City University,*

[2]*The Advanced Research Institute for Natural Science and Technology, Osaka City University*

CO_2 is reduced to methanol via formic acid and formaldehyde with the system of reduced methylviologen ($MV^{\cdot+}$) as an artificial co-enzyme, formate (FDH), aldehyde (AldDH) and alcohol dehydrogenases (ADH) [1]. The enzymatic kinetic parameters for FDH catalyzing CO_2 conversion to formic acid with $MV^{\cdot+}$ or ADH catalyzing formaldehyde conversion to methanol with reduced $MV^{\cdot+}$ have been clarified. However, the kinetic parameters for AldDH catalyzing formic acid conversion to formaldehyde with $MV^{\cdot+}$ have not been clarified. In this study, the parameters for formic acid reduction with $MV^{\cdot+}$ and AldDH were determined by enzymatic kinetic analysis.

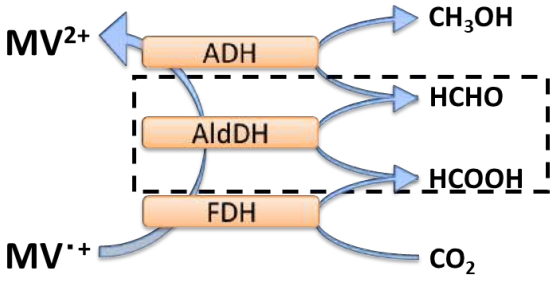

Figure 1. CO_2 -methanol conversion with three dehydrogenases (ADH, AldDH, FDH) and reduced methylviologen

$MV^{\cdot+}$ (25~500 μM), sodium formate (2.0 mM) and AldDH (1.3 μM) in 1.0 mM sodium pyrophosphate buffer (pH = 7.4) was reacted for 1 min at 30.5 ℃ in argon atmosphere. Sodium dithionite was used as a reducing agent for MV. The decrease amount of formic acid as a formaldehyde production after 1 min was measured by ion chromatography. The decrease amount of formic acid was plotted against the concentration of $MV^{\cdot+}$ as initial production rate of formaldehyde. Table 1 shows the kinetic parameters for FDH, AldDH and ADH with $MV^{\cdot+}$. Comparing the kinetic parameters with FDH and ADH, it was found that the affinity between $MV^{\cdot+}$ and AldDH is stronger than FDH and ADH.

Table 1. The enzymatic kinetic parameters for dehydrogenases with reduced MV [2],[3]

	V_{max}(μM· min^{-1})	K_m(μM)	k_{cat}(min^{-1})	k_{cat}/K_m(M^{-1}· min^{-1})
FDH	17.8	212	1.90	9,000
AldDH	34.1	87.5	25.7	293,000
ADH	7.13	311	3.57	11,400

V_{max} : Maximum velocity, K_m : Michaelis constant, k_{cat} : Turnover number, k_{cat}/K_m : Catalytic efficiency

References

[1] Y. Amao, T. Watanabe, *Chem. Lett.*, **2004**, 33, 1544.

[2] S. Ikeyama, Osaka City University, **2017** *Doctor's thesis.*

[3] R. Kataoka, Oita University, **2014** *Master's thesis.*

Light-Driven Water Oxidation Reaction Catalyzed by Cyano-Bridged Metal Complexes with Core-Shell Structure

Akira Kitase, Hiroyasu Tabe, Yusuke Yamada
Graduate School of Engineering, Osaka City University
3-3-138 Sugimoto Sumiyoshi-ku, Osaka-shi, 558-8585, JAPAN

Abstract: Artificial photosynthesis is a promising method to convert chemical energy from solar energy. Artificial photosynthesis for water splitting includes several steps, 1) light harvesting and chargeseparation, 2) water reduction and 3) water oxidation. In these steps, water oxidation is the bottle neck to realize artificial photosynthesis, thus, a highly active water oxidation catalyst (WOC) is strongly demanded. Recently, cyano-bridged metal complexes, known as Prussian blue analogues, have been reported as efficient WOCs [1, 2]. We report herein the preparation of core-shell structured cyano-bridged metal complexes having a catalytically active shell, $Co^{II}_{1.5}[Co^{III}(CN)_6]$, with various thickness and an inert core, $M^N_x[M^C(CN)_6]$ (M^N = Cu^{II}, Co^{II}; M^C = Fe^{III}, Co^{III}) to reduce the using amount of Co ion [3]. Light-driven water oxidation was examined under visible-light irradiation in a phosphate buffer solution (pH 8.0) containing cyano-bridged metal complexes with core-shell structure as a catalyst, $[Ru(bpy)_3]^{2+}$ as a photosensitizer and $Na_2S_2O_8$ as a sacrificial oxidant. $Cu^{II}_{1.5}[Fe^{III}(CN)_6]$@$Co^{II}_{1.5}[Co^{III}(CN)_6]$ (190 nm core and 8 nm shell) exhibited catalytic activity as high as $Co^{II}_{1.5}[Co^{III}(CN)_6]$ even though it contains small amount of Co ion.

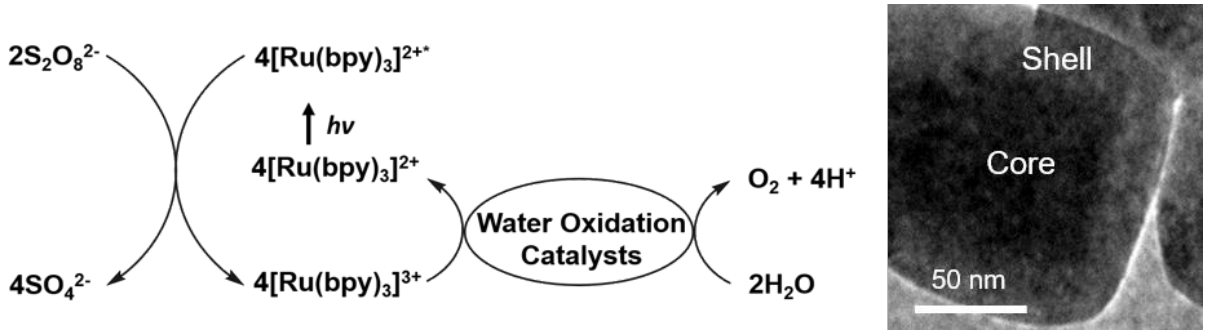

Figure 1: Overall catalytic cycle of light-driven water oxidation (left) and TEM image of $Cu^{II}_{1.5}[Fe^{III}(CN)_6]$@$Co^{II}_{1.5}[Co^{III}(CN)_6]$ (right).

References:

[1] Yamada, Y.; Oyama, K.; Gates, R.; Fukuzumi, S. *Angew. Chem. Int. Ed*. **2015**, 54, 5613.
[2] Yamada, Y.; Oyama, K.; Suenobu, T.; Fukuzumi, S. *Chem. Commun.* **2017**, 53, 3418.
[3] Li, C. H.; Peprah, M. K.; Asakura, D.; Meisel, M. W.; Okubo, M.; Talham, D. R. *Chem. Mater*. **2015**, 27, 1524.

Template for the abstract

Title: Persister formation mechanism mediated with DNA binding protein, YjjJ

Name of author(s): Yuki Maeda(1), Yoshihiro Yamaguchi(1,2)

Affilication and address of author(s):

1:Department of Biology, Graduate School of Science, Osaka City University;

2:The OCU Advanced Research Institute for Natural Science and Technology (OCARINA), Osaka City University

Abstract:

Reminiscent of eukaryotic apoptotic programmed cell death, bacteria also contain a large number of suicide genes, which are in general co-expressed with their cognate antitoxic genes. These systems called the toxin-antitoxin (TA) systems are associated with cellular dormancy, and play major roles in persistent multi-drug tolerance of many human pathogens. Especially the overexpression of HipA, the toxin in HipA-HipB TA system, induces persister state in which the cells show high stress tolerance containing antibiotics treatment. We showed that despite being a homologue of HipA, YjjJ has different cellular target(s) than that of HipA. Helix-turn-helix DNA binding motif present in the N-terminal of YjjJ is consistent with the data that YjjJ has DNA binding activity. It was also showed that HipB, the cognate antitoxin of HipA, also acts as an antitoxin for YjjJ.

Here, we report functional characterization of YjjJ. We tested if yjjJ is involved in persister formation. Although the deletion of hipA, hipBA or yjjJ gene has little effect on persister formation, the deletion of yjjJ and hipA genes significantly increased persister cell formation indicating that both hipA and yjjJ are important for multi-drug tolerance in E. coli. We constructed various YjjJ mutants and found that YjjJ S200E and N-terminal truncated mutant (N10) have no effect on cell growth. Since DNA binding motif presents in the truncated region, we examined the DNA binding activity of these YjjJ mutants. Neither S200E nor N10 truncated mutant binds to genomic DNA suggesting that YjjJ binds to DNA and repress specific gene(s) expression resulting in cell growth arrest. As a step towards identification of the target genes of YjjJ, we investigated the DNA binding specificities by an in vitro selection approach. We show that YjjJ is able to bind preferentially to specific DNA sequences. The consensus sequences are CCCTATAGTGAGTCGTATTA (Seq1) and GGATCCCCGCTGAGCA- ATAACTAGA (Seq2). Interestingly, Seq2 contains the CRISPR repeat sequence which is involved in the bacterial defense system against phage. Then we analyzed the effect of hipB-hipA and hipB-yjjJ TA systems on phage resistance in E. coli. The deletion of yjjJ gene increased the phage sensitivity indicating that yjjJ may play an important role in phage defense mediated with CRISPR system.

Photocatalytic Hydrogen Generation Systems Inside Cross-Linked Crystals of Hen Egg White Lysozyme

Hikaru Takahashi,[a] Hiroyasu Tabe,[a] Satoshi Abe,[b] Takafumi Ueno,[b] Yusuke Yamada[a]

a) Graduate school of Engineering, Osaka city University
3-3-138 Sugimoto Sumiyoshi-ku, Osaka-shi, 558-8585, JAPAN
b) School of Life Science and Technology, Tokyo Institute of Technology, 4259-B55, Nagatsuta-cho, Midori-ku, Yokohama 226-8501, JAPAN

Abstract: Photocatalytic hydrogen evolution systems can be constructed by combining a photosensitizer and a hydrogen evolution catalyst in the presence of an appropriate electron donor. Cooperative immobilization of a photosensitizer and metal nanoparticles acting as hydrogen evolution catalysts on a mesoporous metal oxide can provide a heterogeneous system, which is more robust than homogeneous systems. However, amorphous nature of conventional mesoporous materials disturbs precise and periodical immobilization of catalytic components [1]. In this study, cross-linked crystals of hen egg white lysozyme (CL-HEWL) were employed as mesoporous supports to construct an efficient photocatalytic H_2 generation system. Rose Bengal (RB) and platinum nanoparticles (PtNPs), which act as a photosensitizer and H_2 generation catalysts, respectively, were immobilized inside CL-HEWL. Single-crystal X-ray structure analyses of the CL-HEWL suggested that a coordination site of a Pt ion locates in immediate proximity to potential adsorption sites for RB (Figure 1). Effective H_2 generation was achieved under visble light irradiation in the presence of *β*-dihydronicotinamide adenine dinucleotide (NADH) acting as a sacrificial electron donor (Figure 2) [2].

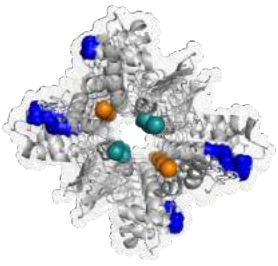

Figure 1. Crystal structure of CL-HEWL immobilizing RB and precursors of PtNPs. The Pt atoms are represented by spheres. Blue residues indicate potential adsorption sites for RB.

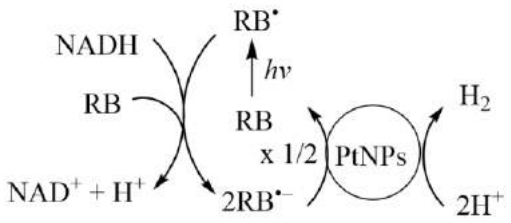

Figure 2. The overall photocatalytic cycle of H_2 generation.

References: [1] Yamada, Y.; Tadokoro, H.; Fukuzumi, S., *RSC Adv*. **2013,** 3, 25677.
[2] Tabe, H.; Takahashi, H.; Shimoi, T.; Abe, S.; Ueno, T.; Yamada, Y., *Appl. Catal. B.*, in press (DOI: 10.1016/j.apcatb.2018.01.046).

In-vitro reconstitution of light-harvesting complexes of a siphonous green alga, *Codium fragile*

Yuki Isaji[1], Rei Tohda[4], Nami Yamano[2], Tetsuko Nakaniwa[4], Genji Kurisu[4,5], Ritsuko Fujii[2,3]

[1]Faculty of Science, [2]Graduate School of Science, [3]OCARINA, Osaka City University, Osaka 558-8585, Japan; [4]Institute for Protein Research, Osaka University, Osaka 565-0871, Japan; [5]CREST, JST, Saitama 332-0012, Japan

Abstract: Photosynthetic light-harvesting complexes plays the crucial role of absorbing sunlight and transferring the excitation energy to photoreaction center [1]. A siphonous green alga, *Codium fragile* has a unique light-harvesting complexes, siphonaxanthin-chlorophyll *a*/*b*-binding protein (SCP) [2]. Siphonaxanthin bound to the SCP absorbs green region of light which is abundant under the sea whereas it dissolved in organic solvent absorbs blue [2]. The reason of the large bathochromic shift has been considered to the specific interaction between siphonaxanthin and aminoacid residue, but it is not clarified yet. In-vitro reconstitution is one of the powerful method to investigate the specific interaction for photosynthetic light-harvesting complex which requires pigments for their folding process [3]. Therefore we aim to perform in-vitro reconstitution of SCP in order to figure out the specific interaction.

In this study, we prepared the pigments from cultivated siphonous green alga, and performed in-vitro reconstitution by using the inclusion body containing artificially expressed SCP-protein [4] and the natural pigments following the protocol established for plant light-harvesting complex [5] (See Fig.1). We will present our recent progress on the poster.

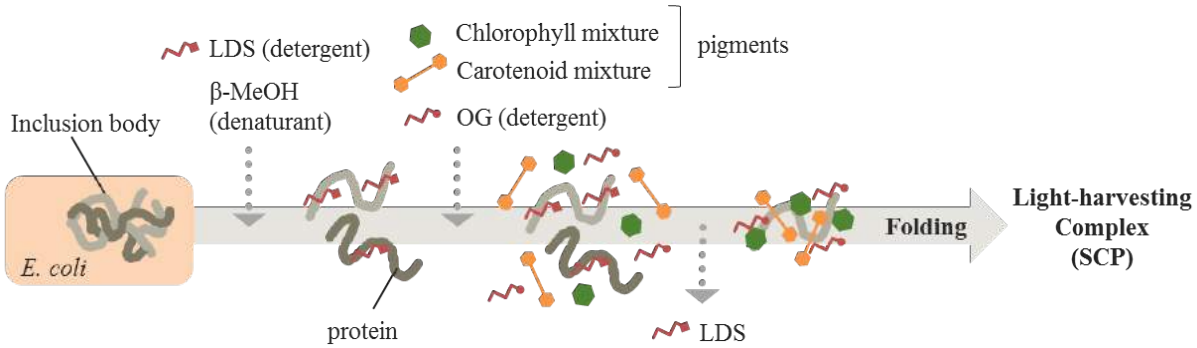

Figure 1. Concept of the Reconstitution of light-harvesting complex [5]

References:

[1] R. Croce and H. van Amerongen, Nature Chem. Biol. 10 **2014**, 492-501.

[2] Z.-X. Chu and J. M. Anderson, Biochem. Biophys. Acta 806 **1985**, 154-160.

[3] R. Croce, S. Weiss, R. Bassi, *J. Biol. Chem.* 274 **1999**, 29613–29623.

[4] T. Nakaniwa et al., unpublished result

[5] A. Natali, et al., *J. Vis. Exp.* 92 **2014**, e51852.

Investigation of amino acid residues involved in spectral tuning of butterfly long-wavelength-sensitive opsins

Tomoka Saito[1], Mitsumasa Koyanagi[1,2], Tomohiro Sugihara[1], Kentaro Arikawa[3], Akihisa Terakita[1,2]

[1]Department of Biology and Geosciences, Graduate School of Science, Osaka City University, Osaka, Japan; [2]OCARINA, Osaka City University, Osaka, Japan; [3] Departmrnt of Evolutionary Studies of Biosystems, The Graduate University for Advanced Studies (SOKENDAI), Kanagawa, Japan;

Absorption spectra of opsin-based pigments are tuned from UV to red region based on interactions between the chromophore and surrounding amino acid residues. Both vertebrates and invertebrates possess long-wavelength-sensitive (LWS) opsins, which underlie color vision. It has been also known that LWS opsins have independently evolved in each lineage, which implies the diverse mechanisms of spectral tuning. In vertebrate LWS opsins, the spectral tuning mechanisms have been well understood by spectroscopic analyses with recombinant pigments and their mutants. However, the spectral tuning mechanisms of invertebrate LWS opsins, such as insects, are largely unknown due to difficulty in obtaining recombinant pigments. Here we successfully estimated the spectral sensitivity curves of two kinds of butterfly LWS opsins by using our new method based on light-dependent change of second messenger in opsin-expressing cultured cells [1], showing the wavelengths of their maximum sensitivities are at ~570nm and ~545nm, respectively. Then we analyzed a series of chimeric and site-directed mutants to identify amino acid residues responsible for the spectral tuning that accounts for the different absorption maxima. Based on the results, we discuss the spectral tuning mechanisms of the butterfly LWS opsins, compared with those of vertebrate ones.

[1] Sugihara, T.; Nagata, T.; Mason, B.; Koyanagi, M.; Terakita, A. *PLoS One* **2016**, 11(8)

Catalytic Activity of Thiocyanato-Bridged Polynuclear Metal Complexes for Hydrolysis of Organophosphates

Masaaki Matsushima, Chihiro Terashima, Hiroyasu Tabe, Yusuke Yamada
Graduate School of Engineering, Osaka City University
3-3-138 Sugimoto, Sumiyoshi-ku, Osaka-shi, 558-8585 JAPAN

Abstract: Organophosphates used for agricultural pesticides are ranked as the 2nd cause of poisoning accidents in Japan. Thus, the removal of organophosphates has been strongly demanded. Recently, cyano-bridged polynuclear metal complexes have been reported to exhibit catalytic activity for organophosphate hydrolysis, in which complexes having the low crystallinity exhibit higher catalytic activity. We report herein catalysis of thiocyanato-bridged polynuclear metal complexes ($Fe^{III}_n[M^S(SCN)_6]$; M^S = Ir^{III}, Rh^{III}, Pt^{IV}), which have nonlinear M^S–S–C bonds beneficial to decrease the crystallinity, for organophosphate hydrolysis. (Figure 1).

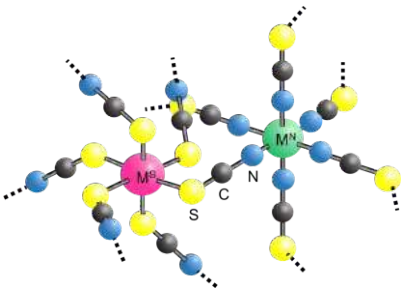

Figure 1. Partial structure of thiocyanato-bridged polynuclear metal complexes.

The precursor compounds, $\{(n\text{-}C_4H_9)_4N\}_3[M^S(SCN)_6]$ (M^S = Ir^{III} and Rh^{III}) and $K_2[Pt^{IV}(SCN)_6]$, were synthesized according to the previous reports [1,2]. Then, $Fe^{III}_n[M^S(SCN)_6]$ (M^S = Ir^{III}, Rh^{III}, Pt^{IV}) complexes were obtained as precipitates by mixing a solution of the corresponding complex and that of $Fe^{III}(NO_3)_3$ under ambient conditions. X-ray diffraction patterns of $Fe^{III}_n[M^S(SCN)_6]$ showed that $Fe^{III}_{2/3}[Pt^{IV}(SCN)_6]$ has the high crystallinity while $Fe^{III}[Ir^{III}(SCN)_6]$ and $Fe^{III}[Rh^{III}(SCN)_6]$ have the low crystallinity. Heterogeneous catalysis of each complex was evaluated by the hydrolysis of 4-nitrophenylphosphate disodium salt (NPP) in a buffer solution (pH 8.3) (Figure 2). Turnover frequencies (TOFs) of $Fe^{III}[Ir^{III}(SCN)_6]$ and $Fe^{III}[Rh^{III}(SCN)_6]$ for NPP hydrolysis were 0.44 and 0.41 h^{-1}, respectively, higher than that of $Fe^{III}_{2/3}[Pt^{IV}(SCN)_6]$ (TOF = 0.24 h^{-1}).

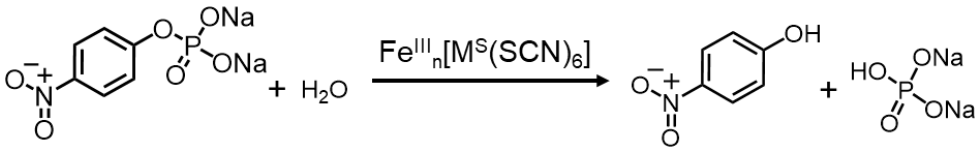

Figure 2. Catalytic hydrolysis of 4-nitrophenylphosphate disodium salt.

References:
[1] Fricke, H. H.; Preetz, W. *Z. Anorg. Allg. Chem.* **1983**, 507, 23.
[2] Siebel, E.; Fischer, R. D. *Chem.–Eur. J.* **1997**, 3, 12.

Synthesis and Characterization of $Li_2Co_{1.8}Ni_{0.2}O_4$ as Zero-Strain Lithium Insertion Material

Kensuke Kajikawa, Yusuke Yamada, Kingo Ariyoshi
Graduate School of Engineering, Osaka City University
3-3-138 Sugimoto, Sumiyoshi, Osaka, 558-8585, Japan

Lithium-ion batteries are the key components for portable electronic devices, electric vehicles, and renewable energy storage systems. The performance of lithium-ion batteries depends on lithium insertion materials used as positive and negative electrodes. Zero-strain lithium insertion materials are beneficial to obtain long-life batteries, because no change in the lattice dimension during charge and discharge results in low mechanical stress. In this study, we report the synthesis and characterization of $Li_2Co_{1.8}Ni_{0.2}O_4$ having spinel framework as a novel zero-strain lithium insertion material. Lithium cells with $Li_2Co_{1.8}Ni_{0.2}O_4$, which was prepared by solid-state reaction at 450°C, showed reversible capacities of about 110 mA h/g at constant operating voltage of 3.5 V, indicating that the lithium-insertion reaction of $Li_2Co_{1.8}Ni_{0.2}O_4$ proceeds in a two-phase manner as shown in Fig. 1. To examine change in the

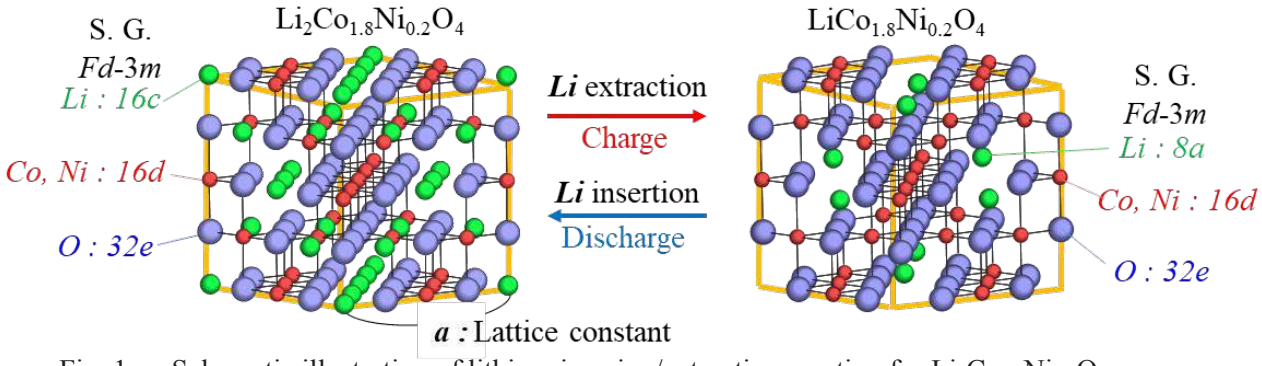

Fig. 1 Schematic illustration of lithium inserion/extraction reaction for $Li_2Co_{1.8}Ni_{0.2}O_4$.

crystal structure of $Li_2Co_{1.8}Ni_{0.2}O_4$ during lithium insertion/extraction reactions, X-ray diffraction measurements of the electrode charged to 4.2 V were carried out. As shown in Fig. 2, no significant change in the diffraction peaks before and after charge evidenced that $Li_2Co_{1.8}Ni_{0.2}O_4$ is the zero-strain material.

In the poster session, we discuss the mechanism of "zero-strain" reaction of $Li_2Co_{1.8}Ni_{0.2}O_4$.

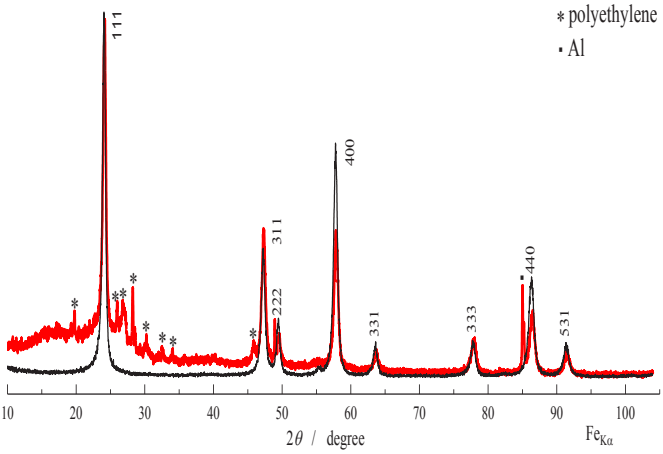

Fig. 2 Powder X-ray diffraction patterns of $Li_2Co_{1.8}Ni_{0.2}O_4$ before (black) and after charge (red). Cubic lattice constant did not change during lithium insertion/extraction reaction.

Color opponency with a single kinds of bistable opsin in the zebrafish pineal organ.

Seiji Wada[1], Baoguo Shen[1], Emi Kawano-Yamashita[1], Takashi Nagata[1], Masahiko Hibi[2], Satoshi Tamotsu[3], Mitsumasa Koyanagi[1,4], Akihisa Terakita[1,4]

[1]Department of Biology and Geosciences, Graduate school of Science, Osaka City University, Japan; [2]Division of Biological Science, Graduate School of Science, Nagoya University, Japan;[3]Department of Biological Sciences, Faculty of Science, Nara Women's University, Japan;[4]OCARINA, Osaka City University, Japan;

Color perception is achieved through antagonistic responses to wavelengths of light, i.e., "color opponency". Ocular and extraocular color opponency has been considered to require multiple color-opsins. Human trichromacy involves red-, green- and blue-sensitive cone opsins, which are exclusively present in different photoreceptor cells. Intriguingly, it was reported that pineal organs of lower vertebrates discriminate UV and visible light; pineal ganglion cells receiving the light information from several pineal photoreceptor cells exhibit suppression and promotion of neural firings to UV and visible light, respectively. We have found that parapinopsin is a UV-sensitive pigment and is possibly the common molecular basis for UV-sensitivity in the color opponency of pineal related organs [1-3]. Interestingly, parapinopsin has a molecular property called bistable nature; upon UV light-absorption, the UV-sensitive parapinopsin converts to a stable photoproduct that is sensitive to visible light, and this photoproduct reverts to the original dark state upon visible light absorption, showing interconvertibility between the dark state and its photoproduct. Therefore, parapinopsin has two stable "color states", unlike other vertebrate color opsins of which photoproduct is unstable. However, a contribution of the bistable nature providing the visible light-sensitive photoproduct in the pineal color opponency has not been understood. In this study, we carried out calcium imaging using parapinopsin-deficient zebrafish to obtain a clue to how the bistable nature of parapinopsin contributes to pineal color opponency. As a result, we found the pineal color opponency is achieved through the photo-interconversion of parapinopsin. Based on obtained results, we discuss the mechanism of pineal color opponency with a single kind of opsin, parapinopsin.

[1] Koyanagi M.; Kawano E,; Kinugawa Y.; Oishi T.; Shichida Y.; Tamotsu S.; Terakita A. *PNAS* **2004**, 101, 6687-6691

[2] Wada S.; Kawano-Yamashita E.; Koyanagi M.;Terakita A. *PLoS One* **2012**, e39003

[3] Koyanagi M.; Wada S.; Kawano-Yamashita E.; Hara Y.; Kuraku S.; Kosaka S.; Kawakami K.; Tamotsu S.; Tsukamoto H.; Shichida Y.; Terakita A. *BMC Biology* **2015**, 13, 73.

Study on the structure and CO_2 reduction activity of Al_2O_3 supported Ga_2O_3 photocatalyst

Ryota Ito[1], Muneaki Yamamoto[2], Akiyo Ozawa[1], Yuma Kato[1], Yu Kawaguchi[1],Masato Akatsuka[2], Tetsuo Tanabe[3] and Tomoko Yoshida[3]

[1]Graduate School of Engineering, Osaka City University, Osaka, Japan

Graduate School of Enjineering, Nagoya University, Nagoya, Japan

Advanced Reserch Institute for Natural Science, Osaka City Univercity, Osaka, Japan

Nowadays photocatalysts are expected to provide a solution for energy crisis and global warming. In particular, photocatalytic CO_2 reduction to give industrial usable products such as CO gas has attracted much attention. It has been reported that Ga_2O_3 works as a photocatalytst for CO_2 reduction with water [1]. In order to improve the photocatalytic activity of Ga_2O_3, in this study, Ga_2O_3 was loaded on Al_2O_3 support having high surface area. Preparing Al_2O_3 supported Ga_2O_3 (Ga_2O_3/Al_2O_3) samples with various amounts of loaded Ga_2O_3, their activities on photocatalytic CO_2 reduction with water were examined, and the correlation of the photocatalytic activity and the amount of loaded Ga_2O_3 and their structure was investigated in detail.

Ga_2O_3/Al_2O_3 samples were prepared by impregnation of γ-phase Al_2O_3 with aqueous solution of gallium nitrate followed by dry and calcination in air at 823 K for 4 h. The loading amouts of Ga_2O_3 were 5, 10, 20, 40 and 60 wt%. Pure Al_2O_3 and Ga_2O_3 samples (refreed as 0 and 100 wt%, repectively) were also prepared in the similar procedure.

Fig.1 compares prodution rates of CO, which is the product of the photocatalytic CO_2 reduction, for all prepared Ga_2O_3/Al_2O_3 samples. Among them, 40 wt% Ga_2O_3/Al_2O_3 showed the highest CO production rate with CO selectivity similar to that of 100wt% Ga_2O_3. This indicates that the activity of the photocatalytic CO_2 reduction of Ga_2O_3 was enhanced with its loading on Al_2O_3 support.

Fig.2 shows the difference XRD patterns for all prepared samples which were obtained by subtracting the XRD pattern of Al_2O_3 support from that of each sample. Samples with loading amounts of less than 20 wt% consisted of single α-phase Ga_2O_3, while 40 and 60 wt% Ga_2O_3/Al_2O_3 consisted of α and γ phases. This suggests that existance of either α or γ phase or coexistence of the both phase enhanced the photocatalytic activty. Understaning the role of each phase on the phtocatalytic activity remains for future work.

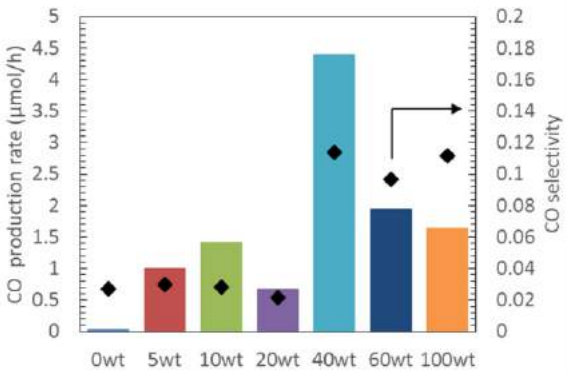

Fig.1 CO production rates for prepared samples after 5 h reaction.

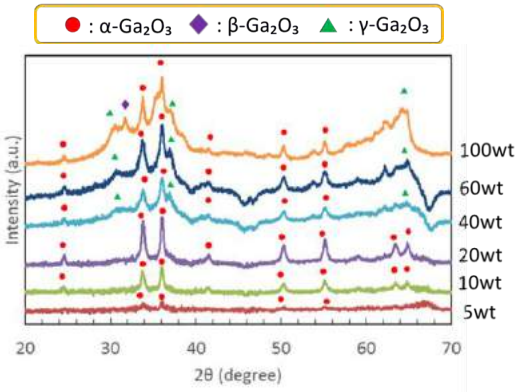

Fig.2 Difference XRD patterns of Ga_2O_3/Al_2O_3 and Ga_2O_3 samples.

References:[1] L.Zhang *et al.*,108th Symposium of Catal. Soc. A,1D15 (2011).

Effect of photon energy on photocatalitic CO_2 reduction with water by Ag loaded Ga_2O_3

Kokoro Yoshioka[1], Yu Kawaguchi[2], Muneaki Yamamoto[3],
Akiyo Ozawa[2] Tetsuo Tanabe[4] and Tomoko Yoshida[4]

[1] Faculty of Engineering, Osaka City University, [2] Graduate School of Engineering, Osaka City University, 3Graduate School of Engineering, Nagoya University, 4 Advanced Research Institute for Natural Science, Osaka City University

Gallium oxide (Ga_2O_3) photocatalysts can promote CO_2 reduction with water to produce CO, H_2 and O_2 under UV photon irradaition. Recentry, it has been reported that Ag loading on Ga_2O_3 as co-catalyst significantly improved the photocatalytic activity for CO_2 reduction to CO[1]. In this study, we investigated the influence of photon energy on CO production as the result of photocatalytic redcution of CO_2 with water over Ag loaded Ga_2O_3 (Ag/Ga_2O_3).

0.5 wt% Ag/Ga_2O_3 samples were prepared by impregnation (IMP) and photodeposition (PD) methods. In the photocatalytic reduction tests, the prepared samples were photo-irradiated using a 300 W Xe lamp controling photon energy with band path or cut filters.

Fig. 1 shows energy spectra of photons after energy selection by filters (254bp, 33U and 37L) together with energy spectrum of a Xe lamp (no filter). Fig. 2 shows diffuse reflectance (DR) spectra of Ag/Ga_2O_3 samples after 5 h reaction by using photons filtered by 37L. The DR spectra showed a large absorption band at wavelength shorter than 290 nm, a small shoulder around 300 nm and a broad band around 450 nm. They were respectively assigned to the band gap transition of the Ga_2O_3, the absorption of Ag small clusters and a localized surface plasmon resonance (LSPR) of Ag nanoparticles. The LSPR band was broadened to the longer wavelength for Ag/Ga_2O_3(PD) compared to that of Ag/Ga_2O_3(IMP). This suggests that sizes of precipitated Ag nanoparticles were larger on the former than that on the later [1].

In the reduction test by using photons filterd by 37L, both Ag/Ga_2O_3(IMP) and Ag/Ga_2O_3(PD) were inactive. On the ther hand, by using photons filtered by 254bp, 33U and no filters, the photocatalytic CO_2 reduction proceeded over both samples, and Ag/Ga_2O_3(IMP) showed higher CO selectivity. These results suggested that the band gap excitation of Ga_2O_3 is necessary for the CO_2 reduction, while the CO selectivity depends on the size of Ag particles. Fig.3 compares the CO selectivity for Ag/Ga_2O_3(IMP) for photons flitered by 33U and 254bp and non-filtered. Note that CO selectivity depended on the photon energy giving the highest CO selectivity for the photons filtered by 33 U.

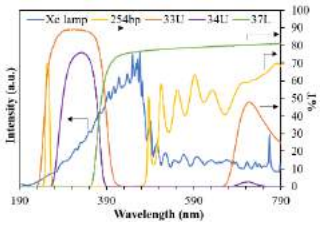

Fig. 1 Energy spectra of photons after energy selection by filters together with energy spectrum of a Xe lamp (no filter).

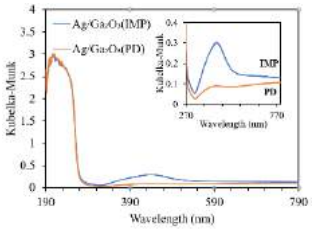

Fig. 2 DR spectra of Ag/Ga_2O_3 samples after 5 h reaction by using photons filtered by 37L.

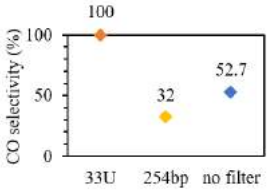

Fig. 3 The change of CO selectivity for Ag/Ga_2O_3(IMP) by the kind of the filter .

[1] N. Yamamoto, T. Yoshida, S. Yagi, Z. Like, T. Mizutani, S. Ogawa, H. Nameki and H. Yoshida, e-J. Surf Sci. Nanotech., 2014, 12, 263

DNA-binding activity of the multifunctional enzyme, nucleoside diphosphate kinase

Chinami Sako[1], Masaaki Miyamoto[2], Satoshi Akanuma[3], and Ryoji Masui[1]

[1]Grad. Sch. Sci., Osaka City Univ., [2]RFC, Kobe Univ., [3]Facl. Hum. Sci., Waseda Univ.

Nucleoside diphosphate kinase (NDPK) is a phosphotransferase that catalyzes of the γ-phosphate from nucleoside triphosphate (NTP) to nucleoside diphosphate (NDP) and critical for maintaining the cellular NTP pools. Some eukaryotic NDPKs have DNA-binding activity and are involved in various cellular functions such as metastasis suppression and transcriptional regulation. The DNA-binding activity of those NDPKs has been characterized biochemically, but their DNA-binding site and binding mode are still unclear. In this study, we first examined the universality of the DNA-binding activity using seven different NDPKs. As a result, three NDPKs including human NM23-H2 and reconstructed ancestral NDPKs bound to DNA, whereas the other four including NDPK from *Schizosaccharomyces pombe* and *Thermus thermophilus* did not. These results suggest that DNA-binding activity is not universally shared among NDPKs. Human NM23-H2 had an ability to bind to double-stranded DNA as well as single-stranded DNA including G-quadruplex DNA. However, NM23-H2 did not bind to 15-mer/bp or less oligo DNAs even if those contained G-rich motifs. In some cases DNA binding was inhibited in the presence of ATP. Replacement of the autophosphorylation site His with Ala abolished inhibition of DNA binding by ATP. These results raise the possibility that DNA binds near the nucleotide-binding site of NDPK. Further, replacement of two basic residues common to NDPKs with DNA-binding activity (Arg42 and Lys135 of NM23-H2) with Ala decreased the DNA-binding activity increased the inhibitory effect of ATP. These results suggest that positively charged Arg42 and Lys135 are involved in DNA-binding activity. In the tertiary structure of NM23-H2, these two residues are located at outer surface of the hexameric ring and near the subunit interface, suggesting that DNA binds to this region. NDPK with DNA-binding activity bound to single-stranded DNA stronger than double-stranded DNA and also to circular plasmid DNA. We also investigated the length the dependence and sequence specificity of DNA binding. Based on these results, we discuss the DNA-binding sites in NDPK.

Characterization of arrestin binding to parapinopsin, a photopigment involved in pineal wavelength discrimination

Takashi Nagata[1], Mitsumasa Koyanagi[1,2], Emi Kawano-Yamashita[1], Seiji Wada[1], Akihisa Terakita[1,2]

[1]*Department of Biology and Geosciences, Graduate School of Science, Osaka City University, Osaka, Japan;* [2]*OCARINA, Osaka City University, Osaka, Japan*

Many lower vertebrates including fish have extraocular photosensitive organs, pineal and related organs, which are suggested to transmit spectral (color) information on ambient light, especially the ratio of ultraviolet (UV) and visible light, to the brain. We have previously reported that parapinopsin, a photosensitive protein opsin, is responsible for the UV reception in the pineal organ of lampreys and also revealed some properties of parapinopsin such as its photoreaction and the interaction with other proteins involved in intracellular signaling cascades [1-3]. Upon light absorption, parapinopsin converts to a thermally stable active state that drives a cellular signaling cascade. This is in contrast to the property of visual opsins (i.e. visual pigments), of which active states are not stable and lose activation ability of the signaling cascade during the process of bleaching. Additionally, we previously found that arrestins, which bind to active state of opsin to shut off the signaling, are different for parapinopsin and visual pigments; that is, parapinopsin and visual pigments bind to β-arrestin (non-visual arrestin) and visual arrestin, respectively [4]. In the current study, we characterized light-dependent binding of β-arrestin by parapinopsin in comparison with a visual pigment by live-cell assays using luciferase-based luminescent reporters. Our results suggest that the molecular mechanism of parapinopsin for arrestin binding could be different from that of visual pigments.

[1] Koyanagi, M.; Kawano, E.; Kinugawa, Y.; Oishi, T.; Shichida, Y.; Tamotsu, S.; Terakita, A. *Proc Natl Acad Sci U S A* **2004,** *101* (17), 6687-91

[2] Tsukamoto, H.; Farrens, D. L.; Koyanagi, M.; Terakita, A. *J Biol Chem* **2009,** *284* (31), 20676-83

[3] Kawano-Yamashita, E.; Koyanagi, M.; Wada, S.; Tsukamoto, H.; Nagata, T.; Terakita, A. *PLoS One* **2015,** *10* (10), e0141280

[4] Kawano-Yamashita, E.; Koyanagi, M.; Shichida, Y.; Oishi, T.; Tamotsu, S.; Terakita, A. *PLoS One* **2011,** *6* (1), e16402.

Construction of Composite Photocatalysts for Water Oxidation Using Silica Nanoparticles Assembly as a Mesoporous Support

Gentato Sakamoto, Hiroyasu Tabe, Yusuke Yamada
Graduate School of Engineering, Osaka City University
3-3-138 Sugimoto Sumiyosi-ku, Osaka-shi, 558-8585, JAPAN

Abstract: H_2 is regarded as a clean fuel to realize a sustainable society, because only water is emitted after burning. Photocatalytic water splitting is an ideal strategy to convert solar energy to chemical energy, H_2. A photocalytic water splitting system can be constructed by combination of a photosensitizer, a water reduciton catalyst for H_2 evolution, and a water oxidation catalyst for O_2 evolution. However, concomitant use of an H_2-evolution catalysts and water oxidation catalysts in a reaction solution fails to produce H_2, because of the back electron transfer between the catalysts. Such undesired back electron transfer can be avoided by co-immobilization of the catalysts on a support. As we reported previously, a novel photocatalytic H_2-evolution system was constructed utilizing the interparticle spaces of silica-alumina nanoparticles assembly by immobilization of Pt nanoparticles and a photosensitizer.[1] We report herein that concomitant immobilization of a water oxidation catalyst, iridium hydroxide, and a photosensitizer, $[Ru(2,2'\text{-bipyridine})_3]^{2+}$, in the interparticle spaces of silica-nanoparticles assembly, which successfully evolve O_2 from water under visible-light irradiation in the presence of a sacrificial oxidizing agent, $S_2O_8^{2-}$ (Fig.1). Then, co-immobilization of iridium hydroxide and PtNPs in the interparticle spaces of silica-nanoparticles assembly was examined for photocatalytic water-splitting (Fig.2).

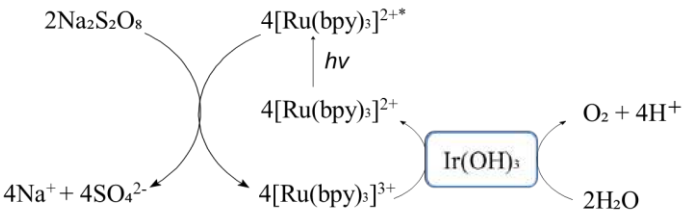

Figure 1. Catalytic cycle of the photocatalytic water oxidation reaction.

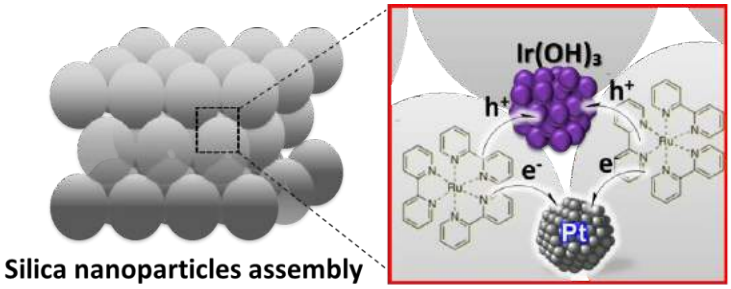

Figure 2. Simultaneous immobilization of iridium hydroxide and PtNPs in the pore of silica nanoparticles assembly.

Reference: [1] Yamada, Y.; Tadokoro, H.; Naqshbandi, M.; Canning, J.; Crossley, M.; Suenobu, T.; Fukuzumi, S. *ChemPlusChem* **2016**, 81, 521.

Subcellular localization of internal structure in gliding machinery of *Mycoplasma mobile*

Isil Tulum[1,2] , Kenta Kimura[1] and Makoto Miyata[1,2]
1) Graduate School of Science, Osaka City University, Osaka, Japan
2) OCARINA , Osaka City University, Osaka, Japan

Mycoplasmas are parasitic and occasionally commensal bacteria which lack peptidoglycan layer. They represent the smallest self-replicating organisms and are fastidious nutritional requirements. *Mycoplasma mobile*, a fish pathogen, exhibits a unique gliding motility with an average speed of 2.0 to 4.5 μm/s based on ATP hydrolysis. This motility has been shown not to be related to other mechanisms of bacterial motility, nor does it involve motor proteins known to be involved in eukaryotic cell motility. The gliding machinery is a complex composed of surface and internal components. The internal structure consists of at least ten proteins and seven of them are tandemly coded with very short gaps on the genome. Two proteins, coded by the ORFs, MMOBs 1660 and 1670 are paralogs of F_1-ATPase/synthase α and β subunits, respectively [1]. F_1F_o ATPases have been identified in most bacteria, including *Mycoplasmas*. Interestingly, besides the conventional F_1F_o ATPase (Type 1), phylogenetic studies identified two types of F_1-like ATPase clusters, Type 2 and Type 3 which had emerged during mycoplasma evolution [2].
In this study, subcellular localization of α-subunits of Type 1, Type 2, and Type 3 F_1-like ATPases and individual subunits of Type 2 F_1-like ATPase subunit paralogs were visualized by the previously developed EYFP tagging using total internal reflection fluorescence microscopy (TIRFM) [3]. Five out of six proteins of internal structure colocalized with surface gliding structure, suggesting that internal structure is associated with the gliding machinery. Two of the Type 2 F_1-like ATPase transformants exhibited enhanced binding activity and one of the transformants exhibited significantly decreased binding activity, suggesting these proteins may involve in the gliding mechanism. The phylogenetic tree construction and sequence analyses showed that gliding related Type 2 F_1-like ATPase and surface gliding proteins also exist in newly identified gliding *Mycoplasmas*, *Mycoplasma agassizi* and *Mycoplasma testudineum* (pathogens of desert tortoise). Although the proteins of internal structure were highly conserved, the surface gliding proteins and 16S rDNA sequences were distinct, suggesting that the surface structure differs according to the host surface while the internal gliding structure remains conserved to generate the force.

References

[1] Miyata M and Hamaguchi T. *Current Opinion in Microbiology.*2016, 29,15-21.
[2] Béven L, Charenton C, Dautant A, Bouyssou G, Labroussaa F, Sköllermo A, Persson A, Blanchard A, and Sirand-Pugnet P. *PLoS ONE*. 2012, 7(6): e38793.
[3] Tulum I, Yabe M, Uenoyama A and Miyata M. *Journal of Bacteriology.* 2014, 196(10), 815.

Motor Evolved from F-ATPase for *Mycoplasma mobile* Gliding

Takuma Toyonaga[1], Takayuki Kato[2], Akihiro Kawamoto[2],
Noriyuki Kodera[3], Toshio Ando[3], Keiichi Namba[2,4]
and Makoto Miyata[1,5]

1. Graduate School of Science, Osaka City University, Japan
2. Graduate School of Frontier Biosciences, Osaka University, Japan
3. Bio-AFM Frontier Research Center, Kanazawa University, Japan
4. OCARINA, Osaka City University, Japan
5. Quantitative Biology Center, Riken (QBiC), Japan

Mycoplasma mobile, a fish pathogenic bacterium, glides on solid surfaces with a unique mechanism. The gliding machinery is divided into two parts: surface and internal structures. The internal structure of the gliding machinery has 28 filaments, and each filament is a polymer of 17 particles made of paralogs of ATP synthase catalytic subunits [1, 2]. Thus these particles are suggested to be the motors for gliding. Previously, we visualized the 3D structure of the motor by electron cryomicroscopy and single particle image analysis. Two hexamers similar to ATP synthase were paired by a frame and attached with eight arm-like extensions. In the present study, we analyzed the image of internal filaments obtained by negative-staining electron microscopy. The filaments were aligned at regular intervals with bridging structures, suggesting that the filaments form a sheet by the arms of the motor. The sheet formation may contribute to the directionality and cooperativity of leg movements. To clarify the movement of the motor, we have observed the motor by high-speed atomic force microscopy.

[1] Miyata, M.; Hamaguchi, T. *Curr. Opin. In Microbiol.* **2016**, 29, 15-21.
[2] Nakane, D.; Miyata, M. *Proc. Natl. Acad. Sci. USA* **2007**, 104, 19518-19523.

Template for the abstract

Gliding Behavior Analyses of *Mycoplasma gallisepticum*

Masaki MIZUTANI[1], Makoto MIYATA[1,2]
1) Graduate School of Science, Osaka City University, Osaka, Japan
2) OCARINA, Osaka City University, Osaka, Japan

Mycoplasma gallisepticum, an avian pathogen, is closely related to human-pathogenic mycoplasmas, *Mycoplasma pneumoniae* and *Mycoplasma genitalium*. It attaches to animal tissue surfaces and glides to spread infected area. The gliding system is totally different from that of *Mycoplasma mobile*, well-studied mycoplasma gliding[1,2]. The gliding machinery in *Mycoplasma gallisepticum* is composed of an internal core and surface adhesion proteins. The surface adhesion proteins catch sialylated oligosaccharides (SOs) on host surface and propel the cell forward using force generated by the internal core. In the present study, we analyzed the gliding behavior in detail by using phase-contrast or dark-field optical microscopy.

Mycoplasma gallisepticum glided at a speed of 0.27 ± 0.09 μm/s on the KOH washed glass coated with SOs and bovine serum albumin (BSA). To examine the gliding direction, we measured the changes of cell axis for 5-s invertals. The averaged gliding direction relative to the cell axis was 0.6 ± 44.6 degrees, showing that the gliding direction is not biased to the left or right from the cell axis. In general, some gliding bacteria show the rolling of cell body in gliding[3,4]. To check whether *Mycoplasma gallisepticum* rotate or not in gliding, we attached a 40-nm colloidal gold to a gliding cell and observed by dark-field microscopy. The cell and the colloidal gold parallelly moved keeping constant intervals, indicating that the cell body is not rolling in gliding movement. To investigate the relationship between cytoadhesion and gliding, we added 0 to 0.5 mM of free sialyllactose (SL), an SO, to gliding cells to decrease the number of binding adhesin. The gliding speed linearly decreased to 0.10 μm/s, but the gliding cell ratio sigmoidally reduced to 1.8%, indicating drag caused by adhesins or the cell body. To determine the direct energy source of gliding, we treated gliding cells with detergent to permeabilize the cell membrane, resulting in the removal of cytoplasm[5]. The cells treated with only detergent stopped gliding simaltaniously with permeabilization, but some permeabilized cells treated with detergent containing ATP continued gliding at 0.02–0.03 μm/s for at least 1 min, indicating that the direct energy source of their gliding is possibly ATP.

[1] Nakane, D.; Miyata, M. *Journal of Bacteriology* **2009**, 191, 3256－3264
[2] Indikova, I.; Vroka, M.; Szostak, M. P. *Veterinary Research* **2014**, 45, 99
[3] Morio, H.; Kasai, T.; Miyata, M. *Journal of Bacteriology* **2016**, 198, 283－290
[4] Nakane, D.; Sato, K.; Wada, H.; McBride, M. J.; Nakayama, K. **2013** *PNAS* 110, 11145－11150
[5] Uenoyama, A.; Miyata, M. **2005** *PNAS* 102, 12754－12758

Structural changes of Gli123 protein, essential for *Mycoplasma mobile* gliding

Daiki MATSUIKE[1], Yuhei O. TAHARA[1, 2], Tasuku HAMAGUCHI[1, 2], Munehito ARAI[3], Makoto MIYATA[1, 2]

1) Department of Biology, Graduate School of Science, Osaka City University, Japan

2) The OCU Advanced Research Institute for Natural Science and Technology (OCARINA), Osaka City University, Japan

3) Graduate School of Arts and Science, The University of Tokyo, Japan

Abstract:

M. mobile, a fish pathogenic bacterium glides on solid surfaces based on ATP energy by a unique energy-conversion mechanism. Three huge proteins clustering on the surface of the gliding machinery are essential for this mechanism. Gli349 shaped like an eighth music note (♪), acts as a leg protein by binding to sialylated oligosaccharides on solid surfaces. Gli521 shaped an interrogation mark (?), transmits the force to Gli349 as a crank protein [1]. Gli123 is a 123 kDa protein responsible for the assembly of surface gliding proteins in the "neck" part on cell surface [2].

Previously, we reported that three-dimensional reconstitution of Gli123 shaped like a "mushroom" with dimensions, 20.0, 14.5, and 16.0 nm, based on negative-staining electron microscopy (EM), which was common with recombinant Gli123 (rGli123) isolated from *Escherichia coli* cells.

In the present study, we focus on the conformational change of the rGli123 according to the ionic strength, which was detected by light scattering. Rotary-shadowing EM showed that rGli123 forms globular and filamentous structures with the lengths of 19.7 ±3.0 nm and 47.9 ± 9.4 nm under 300 mM and 200 mM ammonium acetate, respectively. Limited proteolysis showed flexibility of N-terminal 450 amino acid residues in the whole 1132 residues, suggesting that the flexible part can be assigned to the N terminus including a tansmembrane segment. Now, we are analyzing the conformation of molecule on a cell using the limited proteolysis and immunoblotting.

References:

[1] Miyata, M.; Hamaguchi, T. *Current Opinion in Microbiology*. **2016**, 29, 15-21.

[2] Uenoyama, A.; Miyata M. *Journal of Bacteriology*. **2005**, 187, 5578-5584.

Structural Basis for Regulation of Contractile Function by Phosphorylation of Cardiac Troponin I and T: Distance Measurements Using Dipolar ESR Spectroscopy

Toshiaki Arata[1,2,3]

K. Sakai[3], H. Yamashita[3], C. Zhao[3], T. Somiya[3], S. Takai[3], S. Ueki[4], and M. Miki[5]

[1]Dept. Biol., Grad. Sch. Sci., and [2]OCARINA, Osaka City Univ.; [3]Dept. Biol. Sci., Grad. Sch. Sci., Osaka Univ., Osaka; [4]Tokushima Bunri Univ., Kagawa; [5]Univ. Fukui, Fukui. Japan

Continuous wave (CW) [1] electron spin/paramagnetic resonance (ESR/EPR), and pulsed EPR methods PELDOR/DEER [2] and DQC [3], can determine a distribution of the distance 0.8-8.0 nm between two spin labels (nitroxide radical) attached chemically to protein by site-directed genetic mutagenesis (SDSL-EPR). We applied these methods to huge protein complexes like motor proteins myosin in muscle fibers [4] and kinesin-microtubule [5] and clock protein KaiABC complex [6] and detect their functional structural changes at atomic level. Muscle contraction is triggered by Ca^{2+}. Using EPR measurements we detected large Ca^{2+}-induced structural changes between troponin (Tn) subunits [7] but unexpectedly small structural change of tropomyosin (Tm) on the actin filament for switching-on and allowing myosin to produce force [8]. Heart muscle beating is fine-tuned by phosphorylation of cardiac troponin (cTn) I and T. Here we focussed on the N-extension of cTnI (NxTnI) and N-domain of cTnT (N-cTnT) whose structures are unkown. The CWEPR spectra from two spin labels attached on i and i+4 residues of NxTnI of full length cTnI were well fitted by narrow 0.9 nm (alpha-helix) and broad 1-2 nm distance distributions (unstable conformation). Upon cTnC-cTnI formation, the 43/47 residues on the protein kinase C (PKC) phosphorylation sites Ser42/44 in NxTnI exhibited a 0.9 nm-peak and completely stabilized alpha-helix, and the 23/27 on the PKA sites Ser23/24, narrowed the distribution at 1.4 nm and then stablized an extended conformation. We propose that these regions are the main determinants of the phosphorylation-dependent binding of NxTnI to cTnC and that the binding is quite dynamic. cTnT combines cTnI with Tm. We have determined the interspin distance between N-cTnT and Tm, and found that upon PKC phosphorylation of C-domain of cTnT (C-cTnT) in the thin filament, the residual mobility of spin label bound to the N-cTnT was markedly enhanced and the distance was markedly increased from less than 0.8 to 1.5-2.0 nm. This suggested that the loosening of N-cTnT-Tm binding upon PKC phosphorylation of C-cTnT reduces muscle force and ATP hydrolysis rate in the heart.

[1]Ueki, S. et al. *Biochemistry* **2005**, 44**,** 411. [2]Nakamura, M. et al. *JMB.* **2005**, 348, 127. [3]Abe, J. et al. *Appl. Mag. Reson.* **2012,** 42, 273. [4]Arata, T. *J. Mol.Biol.* **1990,** 214, 471. [5]Sugata, K. et al. *JMB.* **2009**;Yasuda et al. *BBRC* **2014**. [6]Ishii, K. et al. *GenesCells* **2014**. [7]Aihara, T. et al. *JBC.* **2010**, 285,10671 [8]Ueda, K. et al. *Biophys.J.* **2011**, 100; **2013**, 105.

Gliding Machinery of *Mycoplasma mobile* Visualized by High-speed Atomic Force Microscopy

Kohei KOBAYASHI[1], Noriyuki KODERA[2],
Yuhei O TAHARA[1,3], Takuma TOYONAGA[1],
Taishi KASAI[1], Toshio ANDO[2], Makoto MIYATA[1,3]

1. Graduate School of Science, Osaka City University, Japan
2. Bio-AFM Frontier Research Center, Kanazawa University, Japan
3. The OCU Advanced Research Institute for Natural Science and Technology (OCARINA), Osaka City University, Japan

Mycoplasma mobile, a fish pathogenic bacterium forms a protrusion at a cell pole and glides in the direction of the protrusion with a unique mechanism. In the mechanism, "legs" on a cell repeatedly catch, pull, and release sialylated oligosaccharides on substrate surfaces, driven by force generated through ATP hydrolysis on an internal novel motor[1].

In this study, we tried to visualize the alignment of gliding machinery in vivo by high-speed atomic force microscopy (high-speed AFM)[2].

Mycoplasma cells were fixed onto a glass slide by crosslinking with glutaraldehyde[3]. The cells were alive on the glass, because they restarted gliding after 2 hours incubation in a growth medium. The quick-freeze-replica electron microscopy showed that cells were fixed onto glass surfaces with keeping their shape tapered.

The structures of internal motor consistent with those reconstructed by cryo-electron microscopy were observed on the cells fixed onto a glass slide by the high-speed AFM, suggesting that we succeeded in visualizing the internal motors beneath the cell membrane. We found that the alignment of internal motors are tilted from cell axis, which may cause the bias direction of gliding[5].

[1] Miyata M.; Hamaguchi T. *Current Opinion in Microbiology* **2016**, 29, 15-21.
[2] Ando T. *Biophysical Review* **2017**, 9, 421–429
[3] Yamashita H.; Taoka A.; Uchihashi T.; Asano T.; Ando T.; Fukumori Y. *Journal of Molecular Biology*, **2012**, 422, 300-309
[4] Nishikawa MS.; Nakane D.; Toyonaga T.; Kawamoto A.; Kato T.; Namba K.; Miyata M. submitted
[5] Morio H.; Kasai T.; Miyata M. *Journal of Bacteriology* **2016**, 198, 283-290.

Structure and function of six cytoskeletal proteins in *Spiroplasma* swimming

Daichi TAKAHASHI[1], Aya KODAMA[1], Katsumi IMADA[2], Makoto MIYATA[1,3]

1. Dept. Bio., Grad. Sch. Sci., Osaka City Univ.

2. Dept. Macromol. Sci., Grad. Sch. Sci., Osaka Univ.

3. OCARINA, Osaka City Univ.

Abstract: *Spiroplasma eriocheiris* is a pathogenic bacterium that causes a serious disease to Chinese mitten crab [1]. *Spiroplasma eriocheiris* belongs to class *Mollicutes*, and lacks the peptidoglycan layer like *Mycoplasma* species [1]. It swims using a unique mechanism unrelated to flagella or pili, in which kinks propagate along its helical body [2]. The helical body is thought to be formed by six cytoskeletal proteins including Fibril, a *Spiroplasma* specific protein, and five MreB proteins (MreB1 ~ MreB5), bacterial actin homologs [3,4]. To elucidate the structure of these proteins, we individually expressed them as recombinant proteins with N-terminal His-tag in *Echerichia coli*. The cells expressing MreB1, MreB2 or MreB5 showed elongated cell morphology with a few times longer than the original strain, suggesting their ability to polymerize. Filamentous structures were observed in the cells lysed by sonication, under electron microscopy. To study the monomeric structures, the cells expressed for the proteins were lyzed and subjected to centrifugation. Fibril and MreB4 formed insoluble aggregates but others were soluble. MreB3 and MreB5 were successfully purified and crystallized. X-ray structural analysis of these proteins is underway.

References

[1] Wang W et al. *Int J Syst Evol Microbiol* **2011**, 61, 703.

[2] Schaevitz JW et al. *Cell* **2005**, 122, 941.

[3] Liu P et al. *Front Microbiol* **2017**, 8, 58.

[4] Kürner J et al. *Science* **2005**, 307, 436

Structure of P1 adhesin, the leg for infection of *Mycoplasma pneumoniae*, as novel sialic acid receptor

U MATSUMOTO[1], Akihiro KAWAMOTO[2,3], Takayuki KATO[2], Miki KINOSHITA[2], Yoshito KAWAKITA[1], Tsuyoshi KENRI[4], Shigetaro MORI[4], Keiichi NAMBA[2, 5] and Makoto MIYATA[1, 6]

[1]*Graduate School of Science, Osaka City University.*

[2]*Graduate School of Frontier Biosciences, Osaka University.*

[3]*Institute for Protein Research, Osaka University*

[4]*Department of Bacteriology II, National Institute of Infectious Diseases.*

[5]*Quantitative Biology Center, Riken.*

[6]*OCARINA, Osaka City University*

Mycoplasma pneumoniae, a human pathogenic bacterium, glides through repeated binding of sialylated oligosaccharides on host cells by P1 adhesin, a 170 kDa “leg” protein. P1 adhesin consists of three domains I, II and III, and recombinant P1 adhesins (rP1) consisting of domains I+II (rP1-short) and I+II+III (rP1-full) have been analyzed [1,2].

At the last annual meeting, we reported the binding activities between rP1-short and sialylated oligosacharide. In present study, we obtained a high resolution 3D image reconstructed from 190,022 particle images by cryo-electron microscopy, which revealed a novel shape as a sialic acid receptor (the first three authors contributed equally).

Structural and functional studies are underway on rP1-full and rP1 constructs mutated in the conserved region.

References

[1] Miyata M and Hamaguchi T. Frontiers in Microbiology. 2016, 7: 960.

[2] Nakane, D.; Adan-Kubo, J.; Kenri, T.; Miyata, M. Journal of Bacteriology. 2011, 193:715-22.

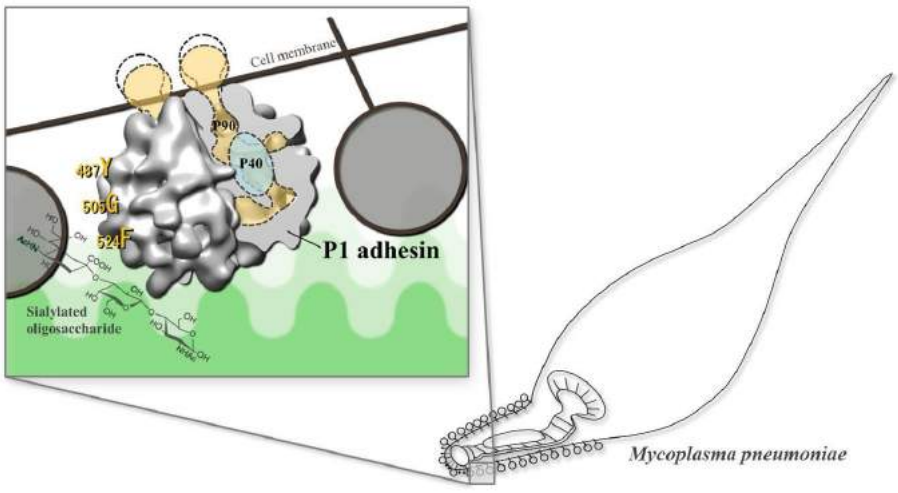

Template for the abstract

Effect of MreB Depolymerization on Helicity-Switching Swimming Motility in Crustacean pathogen, *Spiroplasma eriocheiris*

Yuya SASAJIMA[1], Isil TULUM[1,2], Makoto MIYATA[1,2]
1) Graduate School of Science, Osaka City University, Japan
2) OCARINA, Osaka City University, Japan

Spiroplasma eriocheiris, belonging to the class *Mollicutes* like *Mycoplasma* species, is a helical-shaped swimming bacterium without peptidoglycan layer, causing, trembling disease of crustacean [1,2,3]. This bacterium has a unique motility system in which kinks propagate along the cell body, based on its special internal structure involving five MreBs, a bacterial actin, and Fibril specific to genus *Spiroplasma* [3]. In this study, to elucidate the role of MreBs in the swimming, we observed the cells treated with A22, a MreB polymerization inhibitor. When the swimming cells were exposed to A22, they lost the helicity and kink propagation. However, the cells nonspecifically fixed on glass surface showed the translocation of the cell density to several spots on the cell, whose positional intervals increased with the A22 concentration used. The complete cytoskeletal structure were observed, consisting of a dumbbel and a helical ribbon, at the front and along the body, respectively, in the negative staining electron microscopy of the cell extracted by Triton X-100. The cell treated with A22 showed some bulges along the cell on EM grid, consistent with the observation by optical microscopy. The stacks of filaments were observed in the bulges by detergent treatment. No helicity was observed in the filaments left on the ribbon trace after A22 treatment. We isolated Fibril, known as another major component of the ribbon structure. It showed characteristic repeated structure but no helicity. These results suggest that MreBs interacting with Fibril form a helical ribbon as the cytoskelton, resulting in the helicity of cell.

[1] Miyata M and Hamaguchi T. Frontiers in Microbiology. 2016, 7, 960.
[2] Terahara N, Tulum I, and Miyata M. Biochemical and Biophysical Research Communication. 2017, 487, 488-93.
[3] Liu P, Zheng H, Meng Q, Terahara N, Gu W, Wang S, Zhao G, Nakane D, Wang W, and Miyata M. Frontiers in Microbiology**.** 2017, 8, 58.

Template for the abstract

Approach to biological specimens and material observation using Quick-Freeze and Deep-Etch (QFDE) replica microscopy

Yuhei O Tahara[1,2], Makoto Miyata[1,2]
1)Graduate School of Science, Osaka City University, Japan
2)OCARINA, Osaka City University, Japan

Quick-freeze and deep-etch replica is an electron microscopy method in which specimen is frozen and fixed in a moment by slamming on a cooled metal and observed with resolution of nanometer order and submillisecond time resolution. We adopt this technology in Grant-in-Aid for Scientific Research on Innovative Areas, Ministry of Education, Culture, Sports, Science and Technology in 2012 - 2016. Thirty two researchers and students from 19 research groups inside and outside Osaka City Universuty attempted various subjects listed below in four categories with related techniques, based on our helps for 226 days in the fiscal 2017.

(1) Motility machinery

Gliding machinery of *Mycoplasma*, Pili of *Termus thermophilus* Cytokinesis of slime mold and fission yeast, Flagella of thermophilic bacteria and *Escherichia coli*

(2) Infectious microorganisms

Peptidoglycan desruption of *Bacillus subtilis*, Pili of pathogenic *E. coli*, Surface structure of *Klebsiella pneumoniae* and *Ureaplasma*.

(3) Useful microorganisms

Membrane structures of *Saccharomyces cerevisiae* and *Schizosaccharomyces pombe* and spores.

(4) Soft Matter

Surface structure of antimicrobial material, Carbon nanoparticles, Carbocyanine, Lanthanide complex.

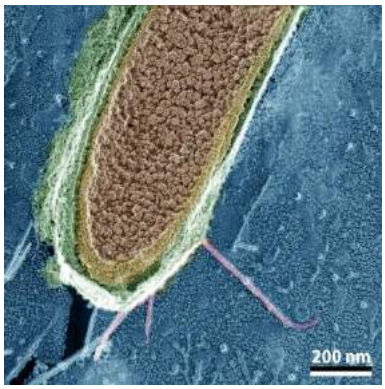

T. thermophilus

B. subtilis on moth-eye film

S. cerevisiae

Elucidation of the environmental factors influenced on the optical properties of fucoxanthin and chlorophyll *c* bound to the fucoxanthin chlorophyll *a/c* protein, FCP

Nami Yamano[1], Tadashi Mizoguchi[2], Ritsuko Fujii[1,3]

[1]Grad. Sch. Sci., Osaka City Univ., [2]Grad. Sch. Life Sci., Ritsumeikan Univ.,

[3]The OCU Advanced Res. Inst. for Natural Sci. and Tech., Osaka City Univ.

FCP (Fucoxanthin chlorophyll *a/c* binding protein) is the major light harvesting complex found in most-prospered aquatic-photosynthetic organisms such as diatoms and brown algae. Light-harvesting complexes in photosynthesis play the important role in regulating the light energy transferred to the photoreaction center: The decrease in luminal pH upon high irradiance of sunlight triggers structural changes of light-harvesting complexes to enhance quenching ability of excess excitation energy [1]. In the case of FCP, however, the molecular mechanism of the regulative function has not been clarified yet. Two kinds of characteristic-antenna pigments, chlorophyll *c* (Chl *c*) and fucoxanthin (Fx), absorb blue-green region of solar energy and transfer the excitation energy to chlorophyll *a* (Chl *a*) when bound to FCP. Chl *c* was reported to show the changes in optical properties upon changes in pH and/or ionic strengths of aqueous alcohols [2], as presumed from its chemical structure (see Fig. 1). Fx bound to FCP proteins shows a large bathochromic shift of absorption spectrum, but this shift is known to be labile during purification steps, suggesting that specific interactions around red-shifted Fx are easily modified by several environmental factors. Energetic heterogeneities of both Chl *c* and Fx, which is induced by the environmental factors, might allow FCP to possess flexible photosynthetic capacity in vivo.

In this study, we isolated FCP from the diatom, *C. calcitrans*, and measured its absorption, circular dichroism, and fluorescence-excitation spectra as the detergent micelle in a series of buffers with various pH values. We tried to evaluate the changes in the energy levels of Chl *c* and Fx bound to the FCP upon changing the solvent factors, such as pH, ionic strength, and viscosity.

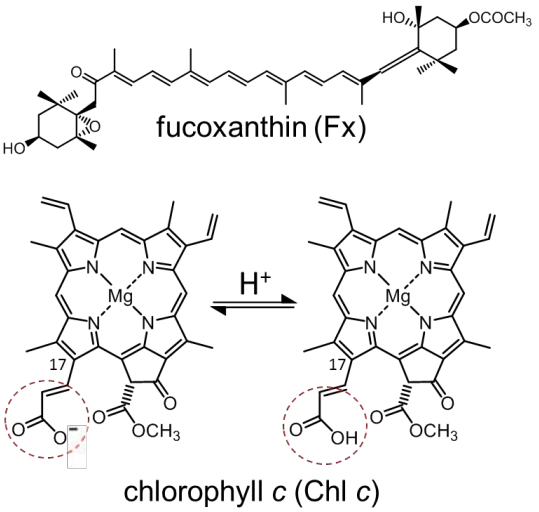

Fig.1 Chemical structures of pigments bound to FCP

[1] C. Büchel, J. Plant Physiol. 172 (2015) 62-75.

[2] S. W. Jeffrey, and K. Shibata, Biol. Bull.136 (1969) 54-62

Template for the abstract

Study on in vivo 3D Micro-Tomographic Visualization of Vascular Plexuses and Capillary Blood Flow Using Optical Coherence Doppler Velocigraphy

Daisuke FURUKAWA[1], Naoya KUSUMOTO[1], Souichi SAEKI[1], Masatsugu SHIBA[2]
Susumu AOKI[3], Takafumi ITO[3], Yoshiaki NISHINO[3], Yusuke HARA[1,4]
[1.] *Graduate School of Engineering, Mechanical & Physical Engineering, Osaka City University. 3-3-138, Sugimoto, Sumiyoshi-ku, Osaka, 558-8585*
[2] *Graduate School of Medicine, Department of Gastroenterology, Osaka City University*
[3] *TOKOTAKAOKA Co., Ltd, Hamamatsu, Japan*
[4] *SHISEIDO Research Center, Yokohama, Japan*

Abstract:
The skin aging process, e.g. wrinkles and saggings, caused by not only aging but also ultraviolet irradiation, could be related to the depression of metabolic function. The microcirculation system should be an important guideline of skin care for the anti/smart-aging. Rheological behavior of interstitial in epidermal and dermal tissue, including blood micro-circulation, can vary skin mechanics in micro scale, i.e. visco-elasticity. Therefore, an *in vivo* quantitative measurement of capillary blood flow velocity is crucial to clarify their properties. The purpose of this study is to visualize the tomographic flow velocity of red blood cell in capillaries below human epidermal skin using Optical Coherence Doppler Velocigraphy, i.e. OCDV [1]. This is constructed on a low coherence interferometer [2], which is based on Hilbert transform and adjacent auto-correlation. In order to validate OCDV system, this was *in vivo* applied to human cheek skin under the condition of control. As a result of skin tomography obtained by OCDV, *en face* cross-sectional imaging of doppler velocity was found to display networks of capillary blood vessels in upper dermal tissue around hair follicles, as well as morphological skin structure. It was confirmed that capillary vasculature and blood velocity can be visualized tomographically even in the upper subpapillary layer. In summary, OCDV system could be quite useful for a micro-tomographic imaging of blood flow velocity of capillary vessels inside skin.

References:
[1] Daisuke Furukawa, et al., “Accuracy Evaluation on Tomographic Micro-visualization of Flow Velocity using High Frequency Modulated Low Coherence Interferometer, J. JSEM, Vol.17, Issue 1, (2017), pp.52-56.
[2] Joseph M. Schmitt, “Optical Coherence Tomography (OCT): A Review”, IEEE Journal on Selected Topics in Quantum Electronics, Vol.5, No.4 (1999), pp.1134-1142.

Template for the abstract

Function of light-driven water-splitting device immobilizing photosystem II inside porous glass plate

Yusuke, Ikeda[1] Tomoyasu Noji[2], Keisuke, Kawakami [2] Tetsuro, Jin[3] Nobuo, Kamiya[2,1]

[1]Science, Osaka City University, [2]The OCU Advanced Research Institute for Natural Science & Technology (OCARINA), Osaka City University, [3]National Institute of Advanced Industrial Science and Technology, Osaka, Japan

Abstract: Researches to construct artificial photosynthesis utilizing photosystem II (PSII) have been attractive approaches because PSII obtains electrons from water via light-driven charge separation reactions of the quantum efficiency of 90%. In order to realize such kind of artificial photosynthesis, it is important to clarify a condition that PSII works efficiently and stably. We previously constructed a light-driven water-splitting device by immobilizing PSII and an electron acceptor 2,6-dichloroindophenol (DCIP) inside inner pores in porous glass plates (PGPs) with 50-nm pore-diameter.[1] Although the activity of PSII was maintained after immobilization, there was a problem that the excitation of PSII was inhibited by absorption of DCIP in the visible region. In this study, a quinone was used as an acceptor that has no absorption in the visible region. The oxygen evolved from PSII inside PGP was detected by an oxygen electrode. The activity of PSII was also measured by breaching rate of quinone after irradiation. The reducing rate of quinone was higher than that of DCIP. The turnover number (TON) of PSII-quinone/PGP50 system was 10^5 e^-/PSII that is 10 times higher than that of PSII-DCIP/PGP50 system. The external qutum eficnecty (EQE) of the PSII/PGP50 system was reahed to 11%, corresponding to a half of natural leaf (Figure 1). We will discuss a mechanism of the increasing efficiency.

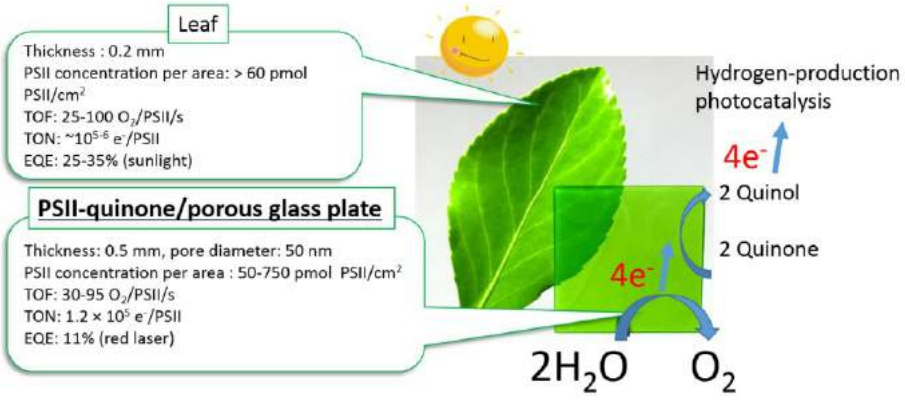

Figure 1. Water-oxidiation efficency of leaf vs PSII-quinone/porous glass plate.

References:

[1] Noji, T.; Kawakami, K.; Shen, J-R.; Dewa, T.; Nango, M.; Kamiya, N.; Itoh, S.; Jin, T. *Langmuir*, **2016**, 32, 7796

History of the Osaka City University Advanced Research Institute for Natural Science and Technology

2008	March	Founding Anniversary International Symposium held
	April	The OCU strategic key research project (2008-20 11) started
	December	International Workshop held on the efficient use of sunlight energy
2010	March	1st International symposium held
	April	Enforcement of official regulations(start of activities as an official bureau)
	October	Building 2 renovated for research floors of OCARINA
	November	Opening symposium for building 2 of OCARINA held
	December	2nd International symposium held
2011	March	3rd International symposium, "Kakuno memorial," held
2012	March	Annual meeting and the OCU strategic key research project (2008-20 11) debriefing held
	April	The OCU strategic key research project (20 12-20 14) started
	July	School of Science Building C completed, partial occupation
2013	March	4th International symposium held
	April	2 new full-time staff members appointed
	June	**Research Center of Artificial Photosynthesis opened**
2014	February	Partial occupation for the new School of Science Building
	February	One new full-time tenure track staff member appointed
	March	One new full-time tenure track staff member appointed
	March	5th International symposium held
	April	One new full-time tenure track staff member appointed
	April	The OCU strategic key research project (20 14-20 15) started
2015	March	6th International Symposium held
	April	One new full-time staff member appointed
	April	Three new projects started
2016	March	7th International Symposium held
	April	The OCU strategic key research project (20 16-20 17) started
	April	ReCAP authorized as a joint Usage/Research Center by Ministry of Education, Culture, Sports, Science and Technology (MEXT)
	April	One new project started
2017	March	8th International Symposium held
	April	Two new projects started

大阪市立大学
OSAKA CITY UNIVERSITY

Osaka City University Advanced Research Institute for Natural Science and Technology

3-3-138 Sugimoto, Sumiyoshi-ku,
Osaka 558-8585, Japan
http://www.ocarina.osaka-cu.ac.jp/